Summer 2013

Stabilizing circulating polyplexes through systematic modification of PEGylated polyacridine peptides in vivo

Koby Lynn Kizzire
University of Iowa

STABILIZING CIRCULATING POLYPLEXES THROUGH SYSTEMATIC MODIFICATION OF PEGYLATED POLYACRIDINE PEPTIDES IN VIVO

by

Koby Lynn Kizzire

A thesis submitted in partial fulfillment
of the requirements for the Doctor of
Philosophy degree in Pharmacy (Medicinal and Natural Products Chemistry)
in the Graduate College of
The University of Iowa

August 2013

Thesis Supervisor: Professor Kevin G. Rice

Graduate College
The University of Iowa
Iowa City, Iowa

CERTIFICATE OF APPROVAL

_____

PH.D. THESIS

_____

This is to certify that the Ph.D. thesis of

Koby Lynn Kizzire

has been approved by the Examining Committee
for the thesis requirement for the Doctor of Philosophy
degree in Pharmacy (Medicinal and Natural Products Chemistry) at the
August 2013 graduation.

Thesis Committee: _____
Kevin G. Rice, Thesis Supervisor

_____
Michael W. Duffel

_____
Michael D. Henry

_____
Robert J. Kerns

_____
Michael A. Spies

To the loving memory of Peggy Johnson and Harold Kizzire, Sr.

Pleasure to me is wonder—the unexplored, the unexpected, the thing that is hidden and the changeless thing that lurks behind superficial mutability. To trace the remote in the immediate; the eternal in the ephemeral; the past in the present; the infinite in the finite; these are to me the springs of delight and beauty.

H. P. Lovecraft
In Defence of Dagon

ACKNOWLEDGMENTS

I want to thank my wife for all the hard hours she put into this thesis by understandingly putting up with my frustrations. This was not possible without you, Jess. I would also like to thank Dr. Kevin Rice for his help in preparing me as a scientist. To Dr. Duffel, Dr. Henry, Dr. Kerns, and Dr. Spies, thank you for agreeing to take the time to serve on my thesis committee. I want to thank my lab mates for all of the help, support and friendship, especially Jason and Mark who have been with me from the beginning of my career here. I want to express my gratitude to Dr. Nicholas Baumhover and Dr. Christian Fernandez for laying the foundation that made my work possible and to Dr. Sanjib Khargharia for his invaluable collaboration. To all of my family and the friends I've made in this country and abroad over the years, thank you for preparing me for life. Finally, to mom, dad, Katie, and Kameron, tatenda.

ABSTRACT

The goal of non-viral gene delivery is to treat illnesses stemming from gene deficiencies or overexpression without the use of viruses, which can cause severe immunogenic response. Many barriers face the delivery of DNA both *in vivo* and *in vitro* and must be overcome by the development of a complex multi-component carrier designed to address each challenge. While it is intuitive to develop a carrier *in vitro*, the requirements for *in vivo* gene delivery differ greatly, and often a non-viral carrier optimized *in vitro* will fail in the bloodstream *in vivo* due to high surface charge, which encourages blood protein binding, or dissociation of the polyplex leaving the DNA vulnerable to nucleases.

It is evident that development of a non-viral gene delivery vector for use *in vivo* requires an easily amended platform to develop the carrier and a reproducible, calibrated assay to determine the expression of polyplexed DNA *in vivo*. Polyacridine peptides conjugated to polyethylene glycol (PEG) are a unique and characterizable set of carrier molecules that can be modified by peptide synthesis and various PEGylation strategies. Through the use of bioluminescence imaging and hydrodynamic stimulation (HS), a physical method that provides high levels of expression with small doses of DNA, it is possible to determine the state of polyplexed DNA in the bloodstream after various periods of circulation. The goal of this thesis was to overcome the first barrier of a systemically administered gene delivery system by developing a carrier molecule that reversibly binds to DNA and stabilizes it against metabolism in the bloodstream while avoiding undesirable biodistribution properties.

The PEGylated polyacridine peptides presented herein were modified in response to each polyplex's *in vivo* performance based on pharmacokinetics, biodistribution, and gene expression by HS in mice after intravenous dosing. Modifications to the DNA-binding motif of the peptide were addressed initially along with various formulation

strategies. Because PEG is installed to stealth polyplex surface properties, the effect of PEG attributes was also examined through optimization of PEG conjugation, size, and position. The results demonstrate the development of long circulating polyplexes that completely stabilize 1 μg of DNA in the bloodstream for five hours. This result provides a necessary prerequisite to allowing targeted accumulation of a polyplex at the site of action, which is the next step toward a fully-effective, systemically-administered non-viral gene delivery system.

TABLE OF CONTENTS

LIST OF TABLES

Table

LIST OF FIGURES

LIST OF ABBREVIATIONS

AFM.. .....atomic force microscopy

ASGPR .....asialoglycoprotein receptor

BLI.....bioluminescence imaging

Boc... .....t-butyloxycarbonyl

cir..... ..... circular

DIC..... diisopropylcarbodiimide

DIPEA.. .....diisopropylethylamine

DMEM..... Dulbecco's modified eagle medium

DMF.. .....*N,N*-dimethylformamide

DNA..... deoxyribonucleic acid

dp…… ..... degree of polymerization

DTT.. .....DL-dithiothreitol

EDTA.....ethylenediaminetetraacetic acid

EDT.. ..... 1,2-ethanedithiol

EPR.. ..... enhanced permeability and retention

ESI... .....electrospray ionization

FMOC.. .....9-fluorenylmethoxycarbonyl

HATU..O-(7-Azabenzo-triazol-1-yl)-N,N,N',N'-tetramethyluronium hexafluorophosphate

HBM.. .....Hepes buffered mannitol

HD .....hydrodynamic dose

HMW... .....high molecular weight

HOBt.. ..... 1-hydroxybenzotriazole

HPLC.. .....high performance liquid chromatography

HPMA.. .....*N*-(2-hydroxypropyl)methacrylamide

HS…… ..... hydrodynamic stimulation

i.p.… ..... intraperitoneal

ITC.. .....isothermal titration calorimetry

i.v.… .....intravenous

LC.... .....liquid chromatography

LMW .....low molecular weight

MALDI-TOF.. ..... matrix assited laser desorption ionization-time of flight

MS… .....mass spectrometry

mV… .....millivolt

NLS.....nuclear localization signal

NMP.. .....*N*-methylpyrrolidone

NMR.. ..... nuclear magnetic resonance

N:P.. ..... nitrogen to phosphorous ratio

PBS.. ..... phosphate buffered saline

PEG..... poly(ethylene)glycol

PEI... .....polyethyleneimine

PLL..... poly(L-lysine)

QELS... .....quasi-elastic light scattering

SAR..... structure-activity relationship

sc… ..... supercoiled

SPPS.....solid-phase peptide synthesis

RNA .....ribonucleic acid

RNAi .....ribonucleic acid interference

RP….....reverse phase

RT.....room temperature

siRNA ..... small interfering ribonucleic acid

TCEP.....tris(2-carboxyethyl)phosphine

TEM .....transmission electron microscopy

TFA... ..... trifluoroacetic acid

TIS... .....triisopropylsilane

Trt…..trityl

UV ..... ultraviolet

CHAPTER 1: LITERATURE REVIEW

Abstract

Chapter 1 presents a review of the current literature on non-viral gene delivery with special emphasis on peptide gene delivery carriers and the use of acridine. Barriers to systemically-administered non-viral gene delivery and remedies to overcome them individually will be discussed, and two physical methods of particular importance in examining circulating polyplexes (DNA and peptide carrier) *in vivo*, hydrodynamic dosing and hydrodynamic stimulation, will also be addressed. It is suggested herein that development of a gene delivery carrier requires careful tuning of parameters that influence polyplex attributes and needs to be conducted *in vivo* to ensure relevant optimizations are made.

Introduction

Successful gene delivery therapeutics would greatly enhance the current arsenal of modern medicine against diseases stemming from gene overexpression or deficiency. Efforts to accomplish successful and efficient gene delivery are divided into two categories – viral and non-viral. Viral gene therapy has seen greater success in efficacious, *in vivo* protein expression owing to the evolutionary advantage of viruses equipped to handle the many challenges presented by gene delivery in mammals. While engineered viruses are the most logical choice in accomplishing gene therapy at an initial glance, the use of viruses is hindered by issues of cost of production, irreproducibility, and limits in gene size [1]. These issues are overshadowed by the even greater problem of cytotoxicity and immunogenicity, which has already proven deadly in a clinical trial [1-3]. Non-viral approaches are under investigation as a means to circumvent problems facing viral gene therapy but face the hurdles to accomplishing *in vivo* gene delivery already overcome by viruses.

Though the concept of gene delivery was proposed over 40 years ago, clinical trials and approvals have only recently generated hope [4]. In July 2012, Glybera (alipogene tiparvovec by UniQure), a viral delivery vector for the treatment of lipoprotein lipase deficiency, was approved by the European Medicines Agency and is slated for European market release in 2013. Although Glybera was approved in part due to its treatment of a debilitating, ultra-orphan disease, this marks the first approval of a gene delivery therapeutic for use in Europe or the United States [5]. This formulation still poses inherent risks for reasons previously described.

Non-viral approaches have also seen recent progress with RNAi in Phase I trials. Davis *et al* were the first to report use of a nanoparticle siRNA formulation, CALAA-01, in clinical trials in 2010 [6]. Very recently, Tabernero *et al* reported some evidence of treatment of liver metastases by RNAi using a lipid nanoparticle formulation, ALN-VSP [7]. Despite these advances, siRNA and DNA delivery achieved via practical and systemic dosing still poses an incredible challenge for non-viral formulations.

Systemic administration of polyplexes (DNA bound by a polymeric or peptide carrier) meets a variety of barriers *in vivo* that need to be addressed by careful tuning of the carrier system. Barriers to gene delivery posed by intravenous (i.v.) administration of polyplexes will be discussed as will some of the methods used to overcome them, especially with regard to circulatory stability. *In vivo* parameters regarding peptides and some other polyamine carriers will also be presented with particular attention given to the use of acridine for DNA binding and the modifying agent polyethylene glycol (PEG). Because of the emphasis on circulatory stability and *in vivo* relevance of non-viral gene delivery systems, the physical methods hydrodynamic dosing (HD) and hydrodynamic stimulation (HS) will also be addressed.

Barriers to Non-Viral Gene Delivery

The directing of DNA to the nucleus of a target cell *in vivo* is challenged by many physiological barriers (Figure 1-1). Prior to administration of DNA via i.v. dosing of a non-viral system, the DNA is generally condensed with a synthetic polymer to form polyplexes or with a liposomal formulation to form lipoplexes. Condensation of the polynucleotide hinders accessibility to serum nucleases that would otherwise rapidly metabolize it [8, 9], and the bloodstream also harbors a high concentration of albumin, which binds non-specifically to cationic molecules [2]. Since most non-viral applications take advantage of cationic interaction with the anionic phosphodiester backbone of polynucleotides, the surface of most polyplexes is cationic, and ionic interactions of albumin and polyplexes have been shown to contribute to rapid clearance of a formulation or aggregation to form emboli that deposit in lung capillaries [10, 11].

Interestingly, this feature has one of the greater impacts in disjoining the outcomes of *in vitro* and *in vivo* gene transfection. *In vitro* conditions take advantage of the high cationic charge to associate with the anionic nature of the glycocalyx of the cell surface [12]. This association increases the chance of random uptake via macropinocytosis or endocytosis, and in some cases, further facilitates expression by endosomal escape resulting from endosomal buffering capacity by polyamine carriers [13, 14]. For reasons previously stated, cationic surface charge is not an advantage in the circulation *in vivo* and must be masked by polyethylene glycol (PEG) conjugation. It has also been more recently demonstrated that ionic interaction alone is inadequate at providing circulatory stability [15] presumably due to high salt concentrations in the bloodstream [16]. In order to prove reversibility of ionically-interacted, non-viral carriers, some have used increased titrations of NaCl and resolved DNA electrophoretically to demonstrate dissociation [17, 18].

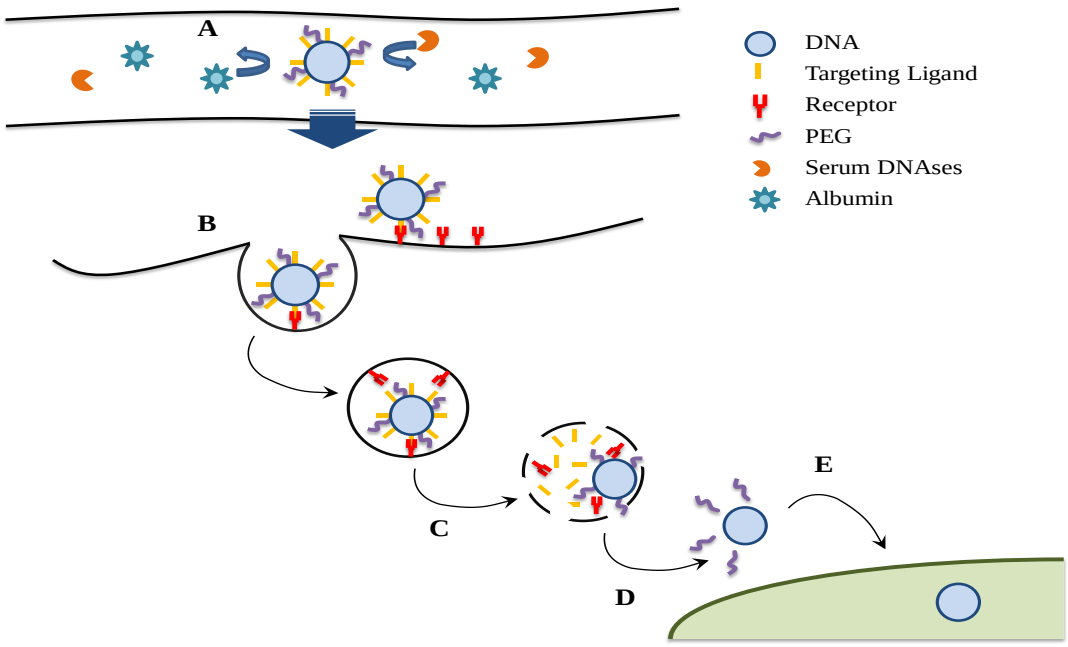

Figure 1-1. *Barriers to Non-Viral Gene Delivery*. The barriers to the non-viral gene delivery of a polyplex. (A) PEGylation makes polyplexes blood compatible so they can avoid protein binding and nuclease degradation. (B) Polyplexes must be small enough to allow passage from the circulation to the tissue, which can be targeted through use of a ligand recognized by a tissue-specific receptor that triggers endocytosis. (C) Endosomal escape must be facilitated to allow (D) localization in the cytoplasm. (E) The polyplex or DNA must achieve nuclear localization to be expressed, which also requires the reversibility of carrier binding

Assuming the polyplex is stable, it then faces the task of exiting the circulatory system through the endothelium of the vasculature. The liver is one tissue where large fenestrations in the endothelium are present, and the size of the fenestrae, though variable for different hepatic regions and physiological conditions, are approximately 100 nm in diameter in mice and humans [19, 20]. It is also well known that the vasculature of tumors is more permissive, or leaky, and allows larger particles (< 400 nm) to enter the

site more readily [21]. This phenomenon is known as the enhanced permeability and retention (EPR) effect [22]. Because polyplexes generally range in size above 30 nm, tumors and hepatic tissue present the most attractive *in vivo* targets for non-viral gene delivery.

The cells in the treated organism present the last set of hurdles. Cell-specific uptake *in vivo* via an i.v.-administered polyplex must be achieved via recognition and endocytosis by the targeted cell type. This is most commonly addressed by providing a ligand to a cell-specific receptor. Once inside the cell, the polyplex must have some means of entering the cytoplasm via endosomal escape, and two common methods include the use of fusogenic peptides or endosomal buffering capabilities inherent to polyamine carriers like PEI or PAMAM dendrimers [13, 14].

Nuclear localization and uptake of the polyplex or DNA are the final steps prior to expression of the gene. Uptake can be achieved passively during cell division when the nuclear membrane is compromised, which occurs frequently in immortalized cell lines [23]. Nuclear localization signals are peptide sequences that have been developed to address nuclear localization in primary cell lines but have met with moderate success *in vitro* [24]. Upon reaching the nucleus, it is also necessary for the carrier to be reversibly bound so the DNA can be properly transcribed.

In summary, *in vivo* non-viral gene delivery faces daunting challenges that must be met with careful tuning of the properties of a carrier and the polyplexes it forms. Two primary things are required to make progress in development of an efficient *in vivo* carrier: (1) a calibrated quantitative system to measure *in vivo* gene transfer, which directs carrier adjustment, and (2) the carrier platform, be it polymer, peptide, lipid, or otherwise, must be pliable and characterizable to allow incremental adjustment and reproducibility.

Hydrodynamic Dosing and Stimulation

In addition to the development of molecular conjugates to administer DNA for non-viral gene delivery, another way to address the challenges comes in the form of physical methods. Currently, many methods are under investigation for both *in vivo* and *in vitro* use including sonoporation, electroporation, or hydrodynamic dosing (HD) [25-30]. These methods rely on very different mechanisms of gene delivery, and HD has proven to be the most effective method to produce robust gene expression *in vivo*. HD is a rapid (~ 5 sec) dose of a large fluid volume containing the plasmid DNA or polyplex. In mice, this is 9% w/v administration (e.g. for a 20 g mouse, the volume is 1.8 ml), which is nearly equivalent to the original blood volume of a mouse (Figure 1-2A) [26, 31, 32]. Because of the of the elasticity of hepatic tissue, a majority of the volume of the bolus is localized in the liver leading to an expansion of the fenestrae to micron scale diameters and around 50% of hepatocytes being transfected with naked DNA [33]. Though the exact mechanism of transfection is unknown, the pressure of the fluid must lead to a transient poration of the cell membrane to allow hepatocyte uptake. This may also lead to a temporary compromise of the nuclear envelope, but this is not certain as subsequent cell division may allow nuclear localization. It is also known that transient liver toxicity is observed after use of HD [32, 34, 35]. Liver insult is known to lead to hepatocyte division, including partial hepatectomy or poisoning, which could be a less direct mechanism of nuclear localization of DNA under HD [36, 37].

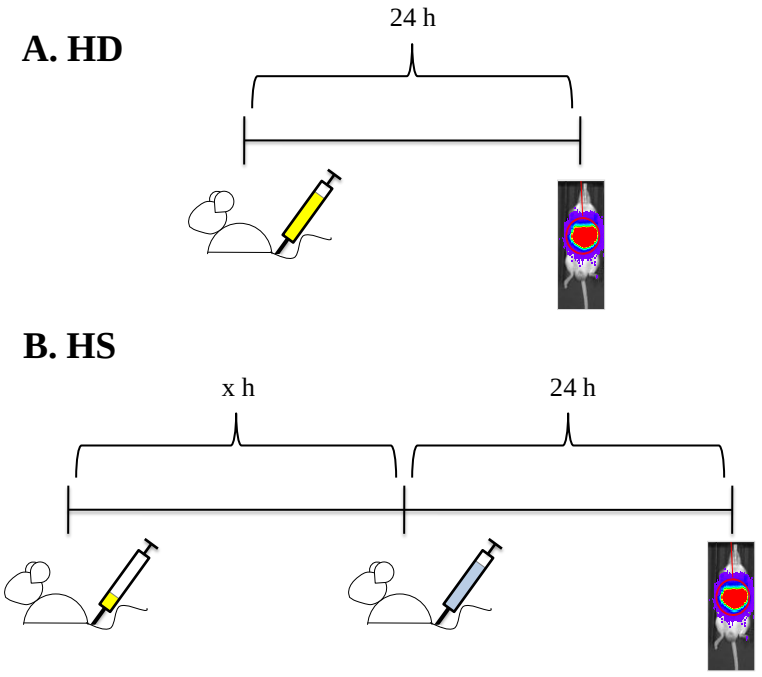

Figure 1-2. *Hydrodynamic Dosing (HD) and Stimulation (HS)*. The timelines presented illustrate (A) HD and (B) HS. (A) In HD, mice are rapidly dosed over 5 sec with 1 µg pGL3 or polyplex containing 1 µg pGL3 in a high volume of saline (1.8 ml for a 20 g mouse) via tail vein injection. At 24h, the mouse is anesthetized and dosed i.p. with luciferin to image expression by BLI. (B) A small volume (50 µl) is used to administer pGL3 polyplex at time 0h for HS. After some time 'X' has passed, the polyplex is stimulated to express by a large volume of saline (no pGL3) administered in the same manner as HD. Expression is similarly imaged by BLI at 24 h.

Bioluminescence imaging (BLI) provides a non-invasive approach to determining the amount of expression from HD. When mice undergo HD with pGL3, a luciferase plasmid with a SV40 promoter, expression is allowed to occur for 24 h, and the amount of expression can be determined by administering an i.p. dose of luciferin 5 min prior to imaging. Photons are emitted when the luciferin is oxidized by luciferase in a manner that corresponds to amount expressed. The expression detected by BLI was reported in a calibrated assay reported by Rettig et al. [38] (Figure 1-3).

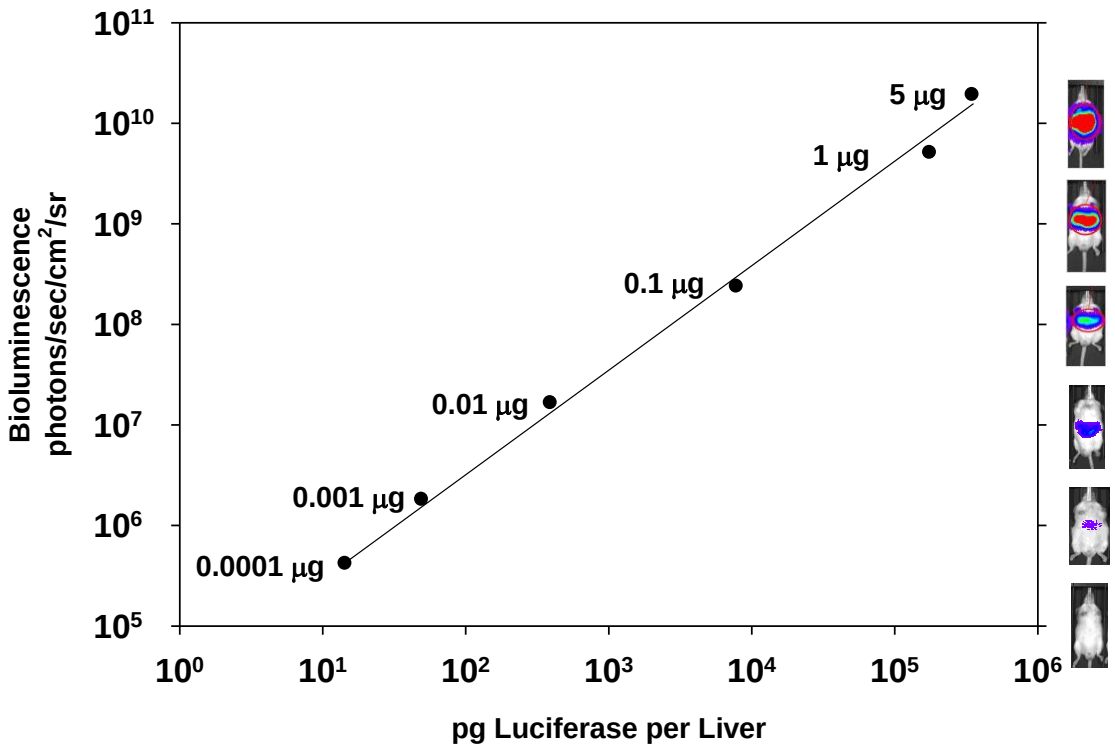

Figure 1-3. *Determination of Luciferase Expression by Bioluminescence Imaging (BLI).* The results of BLI are presented corresponding to varying amounts of pGL3 administered by HD in a calibrated assay. BLI is correlated with the amount of luciferase in pg expressed in the livers of mice. Mouse images representative of the orders of magnitude of BLI are illustrated at right. Adapted from Rettig et al. [38].

Regardless of mechanism of HD, it is apparent that many of the *in vivo* barriers of gene delivery are overcome because the DNA is expressed. The mechanism is also rapid enough to maintain DNA integrity in the face of DNases, but this may also be attributed to the dilution of nucleases by the volume administered. This discovery has called many of the primarily moderate successes in non-viral gene delivery into question because high volumes or amounts of DNA were administered, which may have led to unintended HD-like effects [2]. It has even been demonstrated that administering large amounts of DNA followed directly by a "liver massage" can produce measurable gene expression [39].

Currently, there are attempts to provide local administrations to other tissues types and this method has been translated to larger mammals including primates. Most advances have been focused on developing software-controlled, electronic- or gas-based pumps that can more reproducibly deliver the volume and limit the influence of human error [32, 35]. Obviously, the invasiveness of this technique still limits the possibility of clinical application, but its use as an *in vivo* tool for polyplex evaluation is still practical. For example, Chen *et al.* reported a modification of HD known as hydrodynamic stimulation (HS) (Figure 1-2B) [40]. This method of DNA administration relies on principles identical to HD to produce gene expression *in vivo*. The plasmid DNA or polyplex is administered using a small volume (50 µl) dosed i.v. via tail vein. The integrity of the DNA administered can be assayed after a circulation time by conducting a blank (saline only) HD. This is a powerful technique that provides an expression-based snapshot of the circulatory stability of polyplexed DNA. Using this method, Fernandez et al. modified PEGylated polyacridine peptides to develop greater circulatory stability of pGL3 polyplexed with these peptides [9].

Peptides and Other Polyamine Non-Viral Gene Delivery Carriers

DNA is a polyanionic molecule due to the phosphodiester backbone. One of the most investigated means of reversible binding with DNA for non-viral gene delivery vectors has been consequently ionic binding via a polycationic carrier. Cationic character of these carriers is most commonly accomplished through use of amines that are protonated at physiological pH. Most systems are alkyl amines arranged on various scaffolds and include polyethyleneimine (PEI), chitosan, and polylysine (PLL) (Figure 1-4) [13, 14]. Most commonly, polydisperse polymers like PEI and chitosan are formulated with DNA on the basis of an amine to phosphate (N:P) ratio (i.e. a charge-to-charge basis) and dry polymer weight. As previously stated, the association of polyamine

carriers with DNA results in a cationic surface charge that associates with the glycocalyx of cells and allows DNA uptake to occur non-specifically [12]. Expression is less difficult to achieve in cell culture because the cell lines transfected are generally non-quiescent [23].

PEI has been seen as the gold standard for *in vitro* transfection for decades since its discovery. Though many polyamine carriers exist that can effectively polyplex and condense DNA, PEI has the added feature of endosomal buffering [2, 13]. PEI possesses a large number of secondary and tertiary amines in addition to the primary amines responsible for DNA binding. These amines act as a "proton-sponge" by becoming protonated in later, more acidic stages of the endosome. The buffering of the endosome leads to an osmotic imbalance that causes the endosome to rupture and release the polyplex into the cytoplasm [13, 41]. High N:P ratios of PEI show efficient *in vitro* transfection as a result of excess PEI in the formulation to amplify this effect [42, 43]. Though PEI is an excellent *in vitro* transfection reagent, it displays high levels of toxicity both *in vitro* and *in vivo,* and most efforts attempting to utilize PEI currently focus on decreasing its cationic charge in an effort to decrease the related toxicity. Unfortunately, this research presents a significant challenge because reduction of the cationic character reduces the transfection competence of this carrier. The issue of toxicity is also exacerbated by the resistance of PEI to metabolism [36, 44, 45].

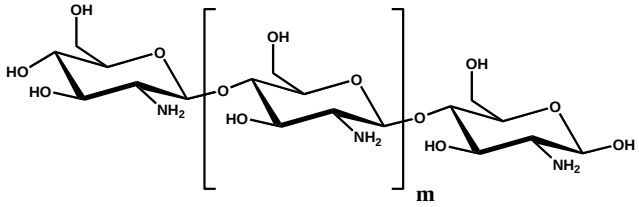

Chitosan

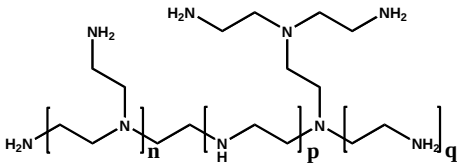

Branched Polyethyleneimine

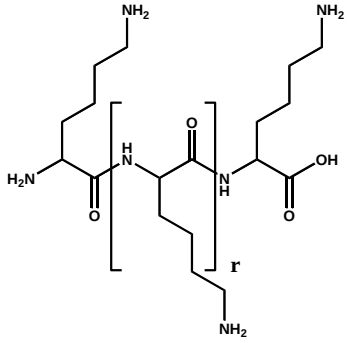

Polylysine

Figure 1-4. *The Structures of Polyamine Carriers for Non-Viral Gene Delivery*. Three common polyamine carriers are illustrated: Polyethyeneimine (PEI), Chitosan, and Polylysine (PLL). Polymer lettering (m, n, p, q, and r) have undefined values as these are polydisperse polymers.

Another approach to non-viral transfection is the use of polydisperse, high molecular weight (HMW) poly-L-lysine (PLL). This was one of the first peptide-based carriers for gene delivery. Early studies by the Wu group examined the use of HMW PLL in gene delivery using applications targeted to the hepatic asialoglycoprotein receptor [46, 47]. Although use of HMW PLL was thought to be a more favorable option than PEI because of its ability to be proteolytically degraded, use of the cationic polymer polyplexes still led to similar surface charge-based toxicities [18]. Efforts to decrease the toxicity were similar to PEI. Degree of polymerization (dp), or the number of lysines in

the polymer, was reduced and balanced stoichiometrically to create favorable polyplexes. PEG was also introduced for *in vivo* application, which simultaneously reduced the affinity for DNA. An added drawback was less *in vitro* transfection efficiency when compared to PEI because of the loss of endosomal buffering capability, although Midoux and Monsigny installed His residues conjugated to some of the Lys residues to introduce this feature to HMW PLL with improved *in vitro* transfection as a result [48, 49].

Other concerns were expressed about irreproducibility resulting from the polydispersity of HMW PLL, which some tried to address by purifications prior to modification. A ground-up approach, however, was presented with the development of low molecular weight (LMW) PLL. LMW PLLs were synthetic peptides that could be easily and reproducibly modified using well-developed peptide synthesis strategies, such as orthogonal protecting groups. The size of LMW PLLs was adjusted initially to discover that 13 Lys residues was a minimum length required for tight polyplexing of DNA [50]. Other modifications to the LMW PLL led to the development of the prototypical AlkCWK_{18} [16]. This peptide possessed excellent *ex vivo* properties. The 18 Lys residues provided adequate binding to DNA to form small (~ 80 nm) particles that were sonication shear and serum nuclease resistant, the Trp residue allowed for detection of the peptide via absorbance or fluorescence, and the alkylated Cys would later provide opportunities for the introduction of thiol-reactive moieties for specific modification. *In vivo*, however, Alk-CWK_{18} was inadequate as a gene delivery agent. Though the particles could resist dissociation in up to 0.4 M NaCl, dissociation was implicated as a major factor *in vivo* [17, 18].

Use of PEG-CWK_{18}, where a PEG is attached via maleimide linkage to the thiol of Cys, did not improve the *in vivo* efficacy of the polyplexes formed. Because of the implication of dissociation of the polyplex, ways to increase the affinity of LMW PLL carriers were investigated. The most common initial approach was crosslinking. PEG-CWK_{18} was applied again to form small polyplexes, and the amines were crosslinked

through reaction with glutaraldehyde. While this made stable particles with long circulatory half-lives, *in vivo* expression was not significantly improved because the polyplexes were too stable to allow efficient release of the DNA [8, 51].

Another crosslinking strategy using reducible disulfide conjugation met with greater success. The use of N- and C-terminal Cys residues in $CWK_{17}C$ was found to provide comparable stability to PLL_{1007}, and improved *in vitro* expression versus a non-crosslinked polyplex with Alk-CWK_{18} [48]. The crosslinking sequence could also be shortened to CK_8C without affecting *in vitro* transfection or *in vivo* pharmacokinetics. Further stability of this reducible series of peptides was investigated by the use of D-Lys residues to resist proteolytic degradation and the use of penicillamine (Pen) residues in place of the terminal Cys residues to form a sterically hindered disulfide bond [52]. Both changes were independently demonstrated to improve the pharmacokinetic half-life of polyplexes *in vivo*. The degree of crosslinking was also increased with the incorporation of an internal Cys. However, this led to increased particle sizes and a reduction of *in vitro* transfection possibly due to crosslinking of multiple particles within the same polyplex [17]. Of interesting note, PEI and cationic lipid carriers were similarly modified to be stabilized with the reducible crosslinker dimethyl-3,3'-dithiobispropionimidate leading to some moderate improvements *in vitro* [53-55].

The promising results of crosslinking peptides led to the formulation of more *in vivo* relevant particles through add-mixture of different Cys terminated moieties. Add-mixture is the combination of multiple, dissolved gene carrier elements (condensing agent, targeting moiety, fusogen, etc.) prior to the addition of DNA to incorporate them on DNA in a definable manner that allows stoichiometric changes of each component. The different portions of a complete carrier can be incorporated predictably during add-mixture provided that the DNA-binding motif is not disrupted [56]. While this approach and pre-synthesis of a PEGylated glycoprotein (PGP) eventually led to a carrier that included PEG, fusogenic peptide (melittin), and a targeting moiety (triantennary), these

peptides were only found to have low expression using a 5 min HS, which indicated marginal circulatory stability. These particles were very large (220-300 nm) but maintained only slight electropositive zeta potential (~ + 5 mV) [40].

It became apparent that condensing DNA solely using cationic residues may not provide the greatest stability *in vivo*. The Nielsen and Szoka groups had investigated the use of polyacridine polymers in conjunction with a nuclear localizing sequence and neoglycopeptides but had little success *in vitro* [57, 58]. Ueyama et al. investigated the use of acridine peptides as fluorescent intercalators for reversible labeling of DNA and reported a high affinity peptide series that bound DNA reversibly through intercalative and cationic interaction [59-61] (Figure 1-5). Adopting this strategy, the 9 position of acridine was conjugated to the ε-amine of Lys and incorporated into peptides using FMOC-based chemistry [61-63]. Acridine not only adds intercalation to polyacridine peptides but also allows simple determination of peptide concentrations because of its unique absorbance properties at visible wavelengths.

Using polyacridine peptides, it was discovered that the spacing amino acid changes led to substantial changes in affinity for DNA with use of Lys > Arg > Leu > Glu. Also, using the general motif $(Acr\text{-}Lys)_n$ with repeats of n = 2, 4, or 6, it was found that increasing the length of these peptides also coincidentally increased the affinity for DNA. The optimal peptide of this study was $(Acr\text{-}Lys)_6$-Cys-mal-PEG_{5kDa} (Figure 1-6), which allowed maximal expression of 1 µg pGL3 under a 1 hour HS after polyplexing with 0.2 nmol peptide [9]. This result illustrated that stable and reversible binding of a non-viral carrier with DNA could be achieved to allow circulation of an i.v.-dosed polyplex for an extended period of time.

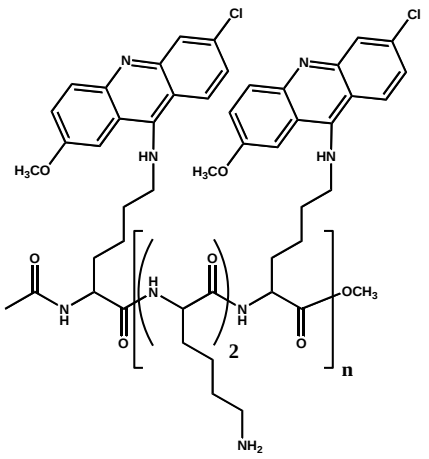

Figure 1-5. *Polyacridine Peptides Reported by Ueyama et al [60]*. The structure of the polyacridine peptide reported by Ueyama et al., where n=1-4, is illustrated above.

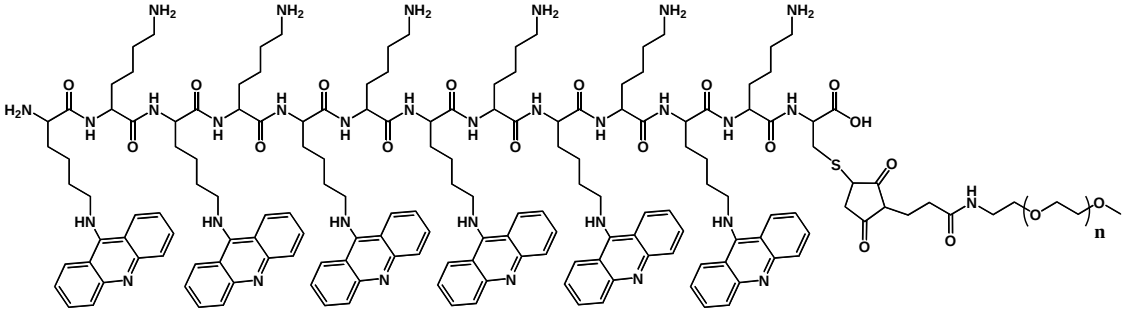

Figure 1-6. *Polyacridine Peptide Reported by Fernandez et al* [9]. The polyacridine peptide, $(Acr\text{-}Lys)_6$-Cys-mal-PEG_{5kDa}, is illustrated above.

Physical Characterization Techniques of DNA Particles and Carriers

Carrier molecules are analyzed primarily for their affinity for DNA or other polynucleotides. Most measurements of affinity and polyplex formation are relative and semi-quantitative in nature although more quantitative methods such as isothermal titration calorimetry (ITC) have been employed [64]. In general, polyplex formation is evaluated by varying stoichiometry of the carrier to DNA and measuring by

electrophoresis or fluorescent dye displacement. The electrophoretic assay is known as a band-shift or –retardation assay and indicates positive polyplexing via decreasing migration of the detected DNA band as more carrier is added [16, 65]. Fluorescent dyes such as ethidium bromide and thiazole orange have been used in the dye displacement assay [66, 67]. This technique relies on fluorescence unique to each dye while intercalating DNA base pairs. As increasing carrier is added, a graded condensation of DNA is observed through the decrease in fluorescence observed when compared with the absence of carrier (Figure 1-7). Full displacement is indicated by the fluorescence at a minimum value, which is correlated to the stoichiometry of peptide required to achieve it. Achieving full displacement at a lower stoichiometry indicates higher affinity of the carrier relative to other compounds evaluated under the same conditions. Some carriers with lower affinities may also exhibit an asymptote that does not achieve full displacement indicating the highest association with DNA but an inability to fully condense it. The point at which this equilibrium at full or partial dye displacement is established is sometimes referred to as the equivalence point [15].

Polyplexes are analyzed for various characteristics prior to their administration *in vitro* or *in vivo.* Most commonly, particle size and zeta potential are taken into consideration. One of the more broadly used techniques to address these measurements is quasi-elastic light scattering (QELS). QELS, also referred to as dynamic light scattering or photon-correlation spectroscopy, is used to obtain a measurement of fluctuations in light caused by the Brownian motion of particles in a solution, and algorithms are applied to these measurements to obtain particle diameters, which are most often reported in nm [68, 69]. QELS principles may also be applied to perform a zeta potential (often represented by ζ) analysis of polyplexes. To measure a zeta potential, a voltage is applied to particles in a solution. Particles possessing surface charge will migrate between the electrodes, and the velocity and direction of these particles is detected by light scattering. Correlation of the light scattering data with the voltage field applied and the previously

determined particle diameter is used to obtain the zeta potential [70], which is usually reported in + or - mV. While QELS can be used to quantify particle size and zeta potential and report distributions of these measurements, the algorithms used to report particle size require an assumption of uniform shape. Because the effective diameter is often assumed for a spherical particle, high biases towards larger diameters are observed for particles that possess non-spherical, rough, or multi-faceted surfaces. Also, the most accurate of the ways to report an effective diameter via QELS, the light intensity-based measurement, weights the particle size toward larger sizes because larger particles will cause higher intensity disruptions [69].

Other methods are employed to measure particle size are atomic force microscopy (AFM) and transmission electron microscopy (TEM), but these are more limited in their ability to provide comprehensive distribution data of particle size. Most often, TEM and AFM are applied as confirmative measurements of QELS data. TEM has questionable application to polyplex size determination due to sample preparation and fixing in an ethanol solution [71]. While AFM can be performed in dry and aqueous solutions to simulate more relevant polyplexing conditions [72], the measurement is somewhat invasive as it requires “gentle tapping” of a cantilever on the surface of polyplexes, which can lead to flattening of particles (larger perceived size) or dragging when portions of the polyplex or water molecules become affixed to the cantilever tip (author’s personal observation). In spite of these drawbacks, TEM and AFM can corroborate well with data obtained from QELS and provide important information regarding polyplex shape.

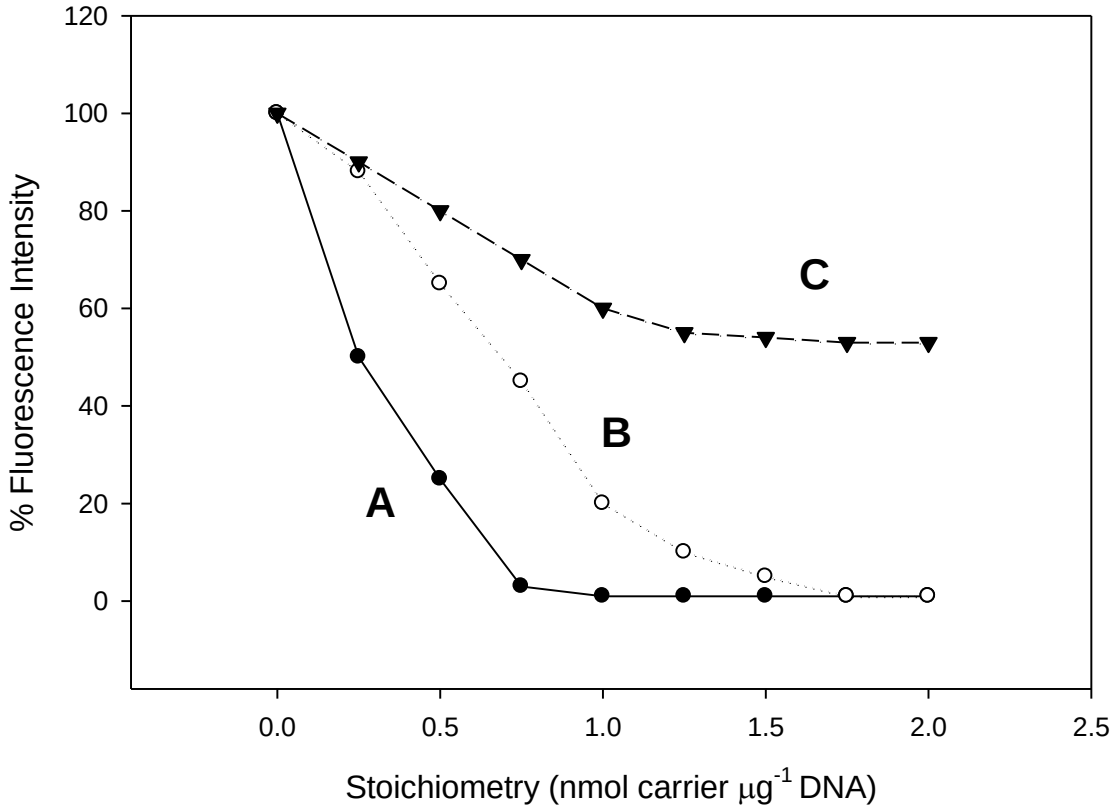

Figure 1-7. *Determining Relative DNA Affinity of Non-viral Carriers via Fluorescent Dye Displacement.* The binding of three different non-viral gene delivery carriers to DNA is illustrated using a fluorescent dye displacement assay. Carrier A is a high affinity carrier that can fully displace the dye to achieve background with low amounts of carrier. Carrier B has moderate affinity compared to A because it fully displaces the dye at a higher stoichiometry, and carrier C is a low affinity compound showing incomplete displacement of the dye at the asymptote, which indicates the saturation or equivalence point.

Polyethylene Glycol (PEG) in Non-Viral Gene Delivery

PEG conjugation, or PEGylation, is a now common technique that was originally conducted on model proteins in the late 1970s [73]. Since then, its use both chemically and therapeutically has increased dramatically. PEG has the attribute of being far more hydrophilic than similar polymers including polymethylene oxide [74], and its conjugation to proteins leads to reduction in immunogenicity and increases in half-life *in*

vivo [75]. Because of these desirable properties, PEG has seen over 20 years of clinical use as a protein conjugate with the earliest approval of PEG-adenosine deaminase (Adagen) in 1990 [75], and, currently, there are many pharmaceutical and chemical suppliers that provide a variety of PEG sizes, branching states, and reactive moieties of both mono- and multifunctionality.

Many studies have addressed PEG-nanoparticle biodistribution *in vivo* and have reported that increases in PEG length and loading density decreases serum protein binding and lung localization [10, 11, 76, 77]. PEG conjugation does not appear to adequately stealth nanoparticles against Kupffer cell recognition in the liver, where a majority of the dose is biodistributed after i.v. administration [78, 79].

In addition to protein and drug nanoparticle formulations, PEG has been extensively applied in gene delivery applications. Surface charge of polyplexes can be masked via conjugation of PEG with the carrier molecule, which makes the cationic polyplex blood-compatible for reasons described above [14]. PEGylation is also vital to anionic polyplexes, which are removed by Kupffer cells in the liver via scavenger receptor in the absence of PEG [8]. While PEG loading density can be increased on polyamine gene delivery carriers like PEI [45, 80], polylysine, and chitosan [36], a corresponding reduction in the capacity to polyplex DNA is observed. This is due to the conjugation of PEG to primary amines, which are the primary source of cationic charge. Thus, reduction in affinity for DNA leads to higher dissociation in the bloodstream [44]. Many other commercially available PEGs, however, provide possible routes to circumvent this issue via reactive moieties for thiol (e.g. vinyl sulfone, maleimide, S-2-sulfanylpyridine) and carbonyl functional groups (e.g. amine, aminoxy, hydrazide) as well as the more recently marketed alkyne- and azide-PEGs for click chemistry.

The Use of Acridine for DNA Binding

Named for its ‘acrid’ odor, acridine was first discovered after isolation from the anthracene fraction of coal tar by Graebe and Caro in 1870 (Figure 1-8) [81]. Though unsubstituted acridine possesses many interesting spectral properties, its use synthetically is limited, and since its discovery, many have undertaken the syntheses of a wide variety of substituted derivatives. Several derivatives possessing a chlorine moiety at the C9 position are of particular interest because nucleophilic activation of the position with a more labile leaving group allows for further derivatization [82]. One leaving group is phenol to form 9-phenoxyacridine, which allows for nucleophilic substitution of C9 by a primary amine, and it is via this reaction that Fmoc (or Boc)-Lys-OH can be conjugated at the ε-amine to acridine and incorporated into solid phase peptide synthesis to create mono- or polyintercalative peptides [60-63] (Figure 1-9).

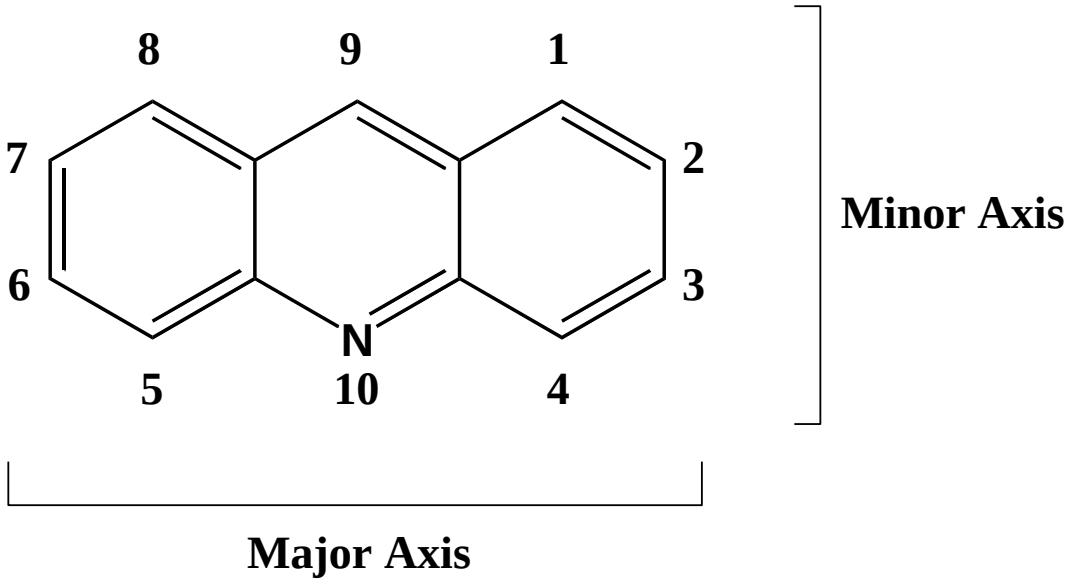

Figure 1-8. *The Structure of Acridine*. The structure of acridine is illustrated. The numbering system still in use is included [83] as is the indication of the major and minor axis described by Wakelin [84].

9-Aminoacridines have been shown to bind preferentially to B-form DNA [85]. The structure of B-form DNA is the model proposed by Watson and Crick in 1953 and has been further supported by subsequent structural studies. B-form DNA is the most common form of DNA under physiological conditions. In this form, double-stranded DNA forms a right-handed helix with ten nucleotide basepairs per full turn, and a 3.4 Å distance separates each base pair [86]. Though many other models for DNA structure have been proposed or observed with the most notable being A- and Z-form [86], the B-form is most widely accepted and was used to develop 'classical' and 'non-classical' models of DNA intercalation.

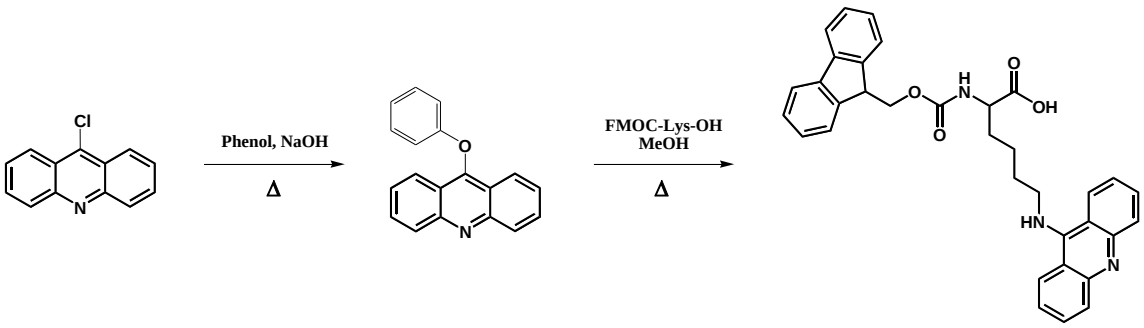

Figure 1-9. *The Synthesis of Fmoc-Lys(acridine)-OH*. 9-Chloroacridine is first converted to 9-Phenoxyacridine by dissolving it in molten phenol in the presence of sodium hydroxide and reacting for 3 h at ~100˚C [87]. Reaction of FMOC-Lys-OH with 9-phenoxyacridine is achieved by heating at 50-60˚C in methanol [62] or phenol [63].

Acridine has been studied extensively for its DNA-binding properties, which were initially observed by Peacocke and Skerrett in 1956 using proflavine and UV spectrophotometry. The dye appeared to have two primary modes of binding with the strongest of the associations providing a ratio of 1 dye molecule bound per 5 nucleotides [88]. Based on this observation and further work by Lerman, the 'classical' model of intercalation was proposed in 1961 [89]. Utilizing equilibrium dialysis and X-ray

crystallography, Lerman identified that acridine was intercalating DNA. He observed that intercalation caused DNA to become more rigid but proposed that it maintained the 3.4 Å spacing during the intercalation process. This model was modified later to accommodate findings throughout the 1960s which formed the 'non-classical' intercalation theory [90]. Cohen and Eisenberg developed the quantitative viscosimetric assay to evaluate DNA lengthening and helix unwinding as it relates to solution viscosity. Further use of this assay uncovered that some unsubstituted intercalators (e.g. phenanthroline, acridine) and their symmetrically substituted counterparts adhered to the 'classical' model by exhibiting expected viscosities. However, symmetrical substitutions of these intercalators led to smaller viscosities than expected indicating DNA bending, which was confirmed in 1973 by X-ray crystallography of actinomycin with a complimentary dinucleotide mixture [91]. This DNA bending and widening of the intercalative space to accommodate bulky or asymmetrical intercalators is the central idea to the 'non-classical' model of intercalation.

Several models of DNA binding by various ligands including intercalators have been proposed. One model, which incorporates the 'classical' intercalation model and is still in use today, is the 'nearest-neighbor exclusion' model developed by McGhee and von Hippel in 1974 [84, 92, 93]. Their approach treated DNA as an extremely long, one-dimensional lattice that can be bound by mono- or polyinteractive ligands. Using a Scatchard-like approach to DNA binding data in previous studies, McGhee and von Hippel noted that intercalator interactions with DNA typically generated an intercalator:intercalation site of 1:2 [92]. This implied that any site on DNA could be occupied, but once occupied, the intercalation site directly adjacent could no longer be occupied. Thus, two intercalators bound by a single, flexible linker would have to be distanced 10.2 Å to accomplish bisintercalation [94] (Figure 1-10).

Many attempts were made to examine the 'nearest-neighbor' exclusion model experimentally in its relation to polyintercalating molecules [84], but these studies often

resulted in conflicting outcomes. For example, the most simplified molecules included alkyl-linked bisintercalators which incorporated unsubstituted acridine (alkyl substitution at C9 via amine moiety) or 6-chloro-2-methoxyacridine, the intercalator found in the antimalarial compound quinacrine (Atebrin) [95]. Viscosimetric and equilibrium dialysis studies indicated bisintercalation of di-6-chloro-2-methoxyacridine tethered via a -$(CH_2)_8$- having a length of 11.3 Å, but when the intercalators were bound via -$(CH_2)_6$- (8.8 Å) or smaller, only monointercalation was observed supporting the exclusion model [96]. This was a confirmation of earlier work by Le Pecq and colleagues who utilized alkylamino spacing in the same fashion and also found a requirement of a minimum eight atom separation between intercalators allowed for bisintercalation [94]. However, in studies using unsubstituted diacridine or diacridine possessing an ethyl group at C4 separated by -$(CH_2)_6$-, bisintercalation was evident by the same procedures leading to the hypothesis that substitutions of the major axis of acridine alone strictly followed the exclusion model. While the 'one base pair sandwich' of unsubstituted and minor-axis substituted acridine may exist, it is unlikely to be the primary mode of intercalation due to the steric demands on DNA [84].

Acridine derivatives have a rich history in use as topical and local antimicrobial agents since the widespread use of proflavine and acriflavine to combat wound infection during World War I. In 1930, quinacrine was discovered and became a widely used antimalarial and a treatment for many other parasitic infections such as giardiasis [97]. It was also found to have prophylactic benefit against malaria and was used heavily by the United States in the Pacific theater of World War II. Though considered safe at the time, quinacrine was found to cause reversible psychosis at high doses and was eventually replaced by chloroquine [98].

Since the reported discovery of chemical-induced mutation by Auerbach and Robson in 1947 [99], various derivatives of acridine have been studied for mutagenic and clastogenic potential. DNA intercalators are prone to cause frameshift mutagenesis, and

this is the most well documented source of mutagenicity for simple acridine derivatives like 9-aminoacridine [100].

The general consensus concerning 9-aminoacridine and related, non-alkylating derivatives in terms of toxicity are as follows: (1) These compounds are known frameshift mutagens simply by the nature of intercalation as evidenced by numerous *in vitro* assays in prokaryotes [97, 98, 101]. (2) Conflicting evidence of genotoxicity is presented in *in vitro* studies involving mammalian cells although positive indications show weak mutagenic effect [97, 100]. (3) There is little evidence *in vivo* that indicates 9-aminoacridine is genotoxic or carcinogenic [98, 100, 101].

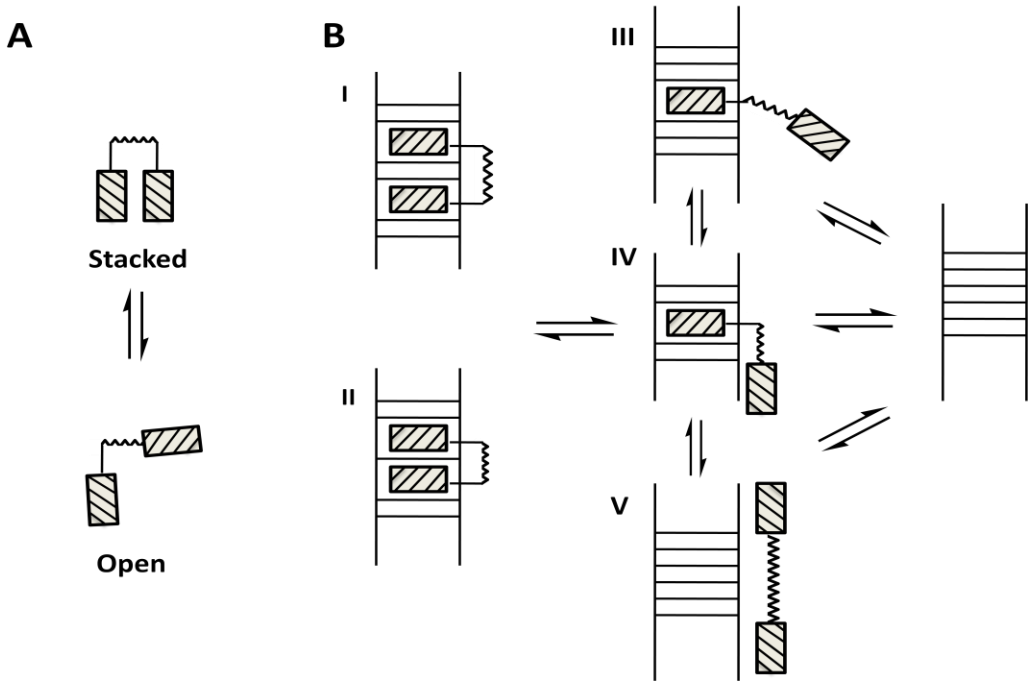

Figure 1-10. *Possible Modes of Binding of a Di-Intercaltor with DNA.* The drawing illustrates the ways in which DNA and a diacridine might bind. Panel A shows that the intercalators may exist in solution intramolecularly stacked or open. Panel B shows DNA interaction possibilities for the diacridine system. Binding can occur by (III) single intercalation, (IV) single intercalation and non-intercalative interaction of the other moiety, (V) non-intercalative interaction, and either adhere (I) or not adhere (II) to the nearest-neighbor exclusion principle. Adapted from Le Pecq *et al*. [94].

While use of 9-aminoacridine intercalators is relatively safe in the case of polyacridine peptides, its ability to cause frameshift mutagenesis in prokaryotes and the stigma associated with acridines because of the DNA modifying derivatives, such as acridine mustards, make its clinical use in current times unlikely [98]. However, acridine in polyacridine peptides serves as a valuable investigative tool. It is possible that acridine could later be substituted for other intercalators currently approved for clinical use, and it has been shown that some natural amino acids (Tyr, Trp, and Phe) possess some ability to intercalate DNA [102-106].

Research Objectives

To date, no non-viral gene delivery carrier achieves efficient *in vivo* transfection under systemic delivery due to the careful balance of affinity and polyplex properties required to overcome all of the issues presented by the bloodstream, vascular penetration, and cell uptake and expression. Polyacridine peptides were developed to begin addressing circulatory issues, namely the dissociation of polyamine carriers in the presence of high salt concentrations of the blood. While progress was made leading to a carrier that exhibited completely transfection-competent polyplexes in the bloodstream for 1 hour with a pharmacokinetic half-life of 2 hours [9], polyplexes with more favorable half-lives *in vivo* will allow accumulation at tissues targeted by specific receptors [15].

Development of non-viral carriers that function well *in vitro* rarely results in a carrier that is suited for *in vivo* use. However, until recently, a method by which circulating polyplexes could be evaluated for their ability to preserve the integrity of the DNA was not readily available. Hydrodynamic stimulation (HS) and analysis of pGL3 expression by bioluminescence imaging (BLI) to determine luciferase expression provides clear evidence of the stability of polyplexed DNA *in vivo*. In conjunction with characterization of the physical properties of polyplexes and pharmacokinetic and biodistribution analyses, HS will provide a platform for the *in vivo* evaluation and

structure-activity relationship of PEGylated polyacridine peptides in this thesis. Though the initial development of PEGylated polyacridine peptides to arrive at $(Acr\text{-}Lys)_6$-Cys-mal-PEG_{5kDa} represents a critical first step toward polyplexes with greater *in vivo* stability, much remains to be explored about these peptides.

The neighbor-exclusion principle presents a requirement of a 10.2 Å separation to allow intercalation of 2 bound moieties as previously mentioned [92]. Though inclusion of the side chains on polyacridine peptides as part of the linear distance between acridines more than meets this separation, the branching of polyintercalator peptides does not allow a direct comparison of this principle [84]. When distance between α-carbons of each amino acid (branching points) bearing acridine was considered, 6.8 Å separated the side chains in the $(Acr\text{-}Lys)_n$ motif versus 10.3 Å when considering the $(Acr\text{-}Lys_2)_n$ motif (Figure 1-11). A single Lys residue spacing two acridines could thus allow for intramolecular stacking of acridine, which has been observed in fluorometric analyses of acridine and other bound intercalators [59, 60, 84]. Takenaka's group developed similar polyacridine peptides possessing two spacing Lys residues between each Acr(CM), where the intercalator was 6-chloro-2-methoxyacridine (Figure 1-5). This spacing was reported to allow simultaneous intercalation of all acridines in the peptide based on viscosimetric analyses of helix unwinding and circular dichroism analyses [59]. On the basis of these findings, the development of a polyacridine peptide series that varies the number of spacing Lys residues was investigated to increase reversible binding affinity for DNA through more favored polyintercalation and additional ionic interaction.

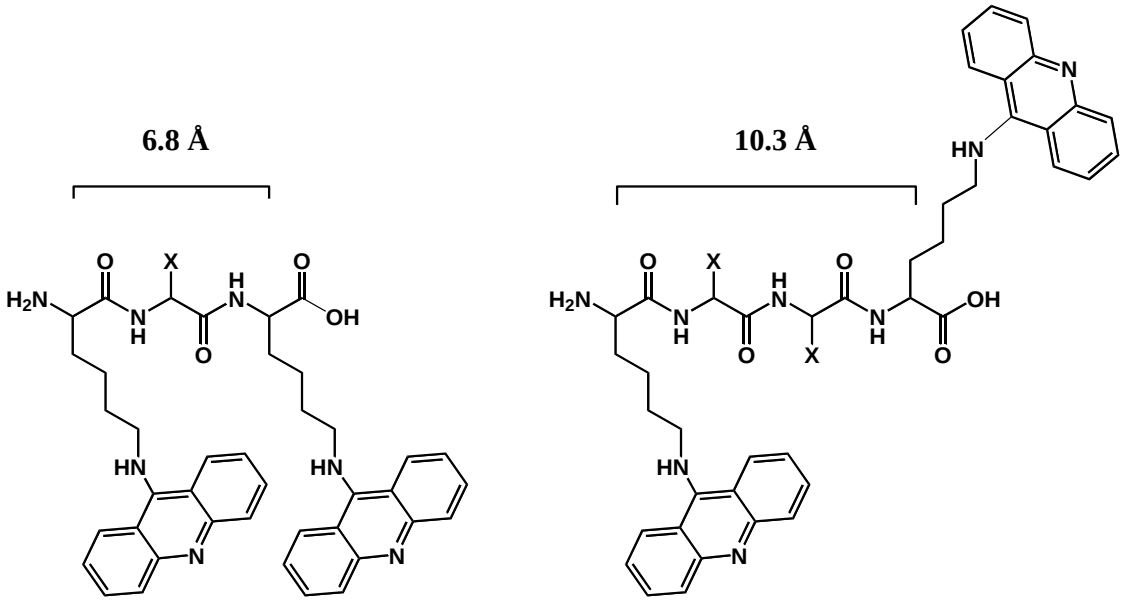

Figure 1-11. *The Spacing of Acridine in Polyacridine Peptides.* Two simplified motifs of polyacridine peptides are presented: Acr-Lys-Acr (left) and Acr-Lys-Lys-Acr (right), where X is the side chain of Lys. The measurements indicate the linear distance between the branching points of the side chains of Acr residues.

Because of the well-established importance of PEG in providing favorable polyplex characteristics for systemic delivery of nanoparticles and proteins [75], several parameters regarding this moiety were investigated. The type of linkage binding PEG to the Cys thiol of polyacridine peptides was examined to determine if premature release of PEG could be controlled to improve circulatory stability. Additionally the position of PEG attachment within the peptide and PEG length were investigated.

This thesis aims to improve PEGylated polyacridine peptides to provide further circulatory stability through the modification of the unexplored features mentioned above. The approach reported herein will demonstrate a ground-up approach to the *in vivo* optimization of a non-viral gene delivery vector, specifically addressing the requirements for the circulation of polyplexed DNA. The ability of a synthetic carrier to reversibly bind and protect DNA in the circulatory system to allow accumulation at a

tissue site through ligand-mediated targeting is of vital importance to the development of any systemically-delivered, non-viral gene delivery system.

CHAPTER 2: POLYACRIDINE PEPTIDE MODIFICATION AND FORMULATION ACHIEVES LONGER CIRCULATORY STABILITY OF POLYPLEXED DNA *IN VIVO*

Abstract

Polyethylene glycol (PEG)ylated polyacridine peptides present a unique non-viral gene delivery system that incorporates acridine modified Lys residues (Acr) to polyplex DNA through polyintercalative and ionic interaction. Previously, $(Acr\text{-}Lys)_6$-Cys-PEG_{5kDa} was shown to mediate hydrodynamically-stimulated (HS) (saline only) gene expression of 1 µg of polyplexed pGL3 in mice. The level of expression was equivalent in magnitude to hydrodynamic dosing (HD) of 1 µg pGL3 and demonstrated that polyplexed pGL3 was fully stabilized in the circulation for 1 h. A structure-activity relationship that improves circulatory stability mediated by polyacridine polyplexes is reported herein. The results demonstrate that increasing spacing of four Acr residues by four or five Lys residues allows fully-stabilized, polyplexed pGL3 to circulate for up to 5 h and mediate maximal HS expression. Maximal HS expression is further maintained for 9 h using a polyplex containing 1 µg pGL3 and 9 µg of a decoy, non-expressing plasmid. This study presents a rationale for the *in vivo* requirements of a non-viral gene delivery carrier that allow it to bind to and maintain transfection-competent DNA in the circulation. This parameter is vital to allow accumulation of polyplexes at the site of therapeutic action.

Introduction

The development of highly-efficient nonviral gene delivery systems that mediate expression in animals following intravenous (i.v.) dosing remains a substantial challenge [2]. Delivery systems optimized *in vitro* often fail to mediate expression *in vivo* due to a combination of aberrant pharmacokinetics or biodistribution [107], inadequate

intracellular trafficking or DNA release [80, 108, 109], or the inability to achieve nuclear localization [110].

To systematically overcome the barriers associated with hepatic non-viral gene delivery, we have adopted a strategy of administering a 1 µg dose of pGL3 polyplex (non-viral delivery system bound to DNA) via a small volume (50 µl) tail vein injection in mice. Following a delay time of 5 min to 9 h, a hydrodynamic stimulation (HS) (1.8-2.25 ml depending on body weight) of saline is delivered via tail vein and the resulting luciferase expression of the liver is measured by quantitative bioluminescence imaging (BLI) at 24h. This approach circumvents optimization of parameters toward efficient *in vitro* gene transfer by instead allowing direct optimization of parameters key to successful *in vivo* gene delivery. To be fully transfection-competent in HS delivery, DNA polyplexes must be sufficiently stable in the circulation to survive DNase metabolism, avoid protein binding and biodistribution to the lung, and release DNA intracellularly following HS [9, 40].

Polyethylenimine (PEI, **P**) or Lipofectamine (Invitrogen, Carlsbad, CA, USA) (**L**) mediated gene transfer have emerged as benchmark delivery agents for comparison with developmental *in vitro* gene transfer agents [111, 112]. Similarly, hydrodynamic dosing (HD) is the most efficient benchmark delivery method to calibrate the development of *in vivo* gene transfer agents. HD delivery of 10 ng to 5 µg of pGL3 in mice produces a linear BLI calibration curve covering a dynamic range of 5 orders of magnitude (10^5–10^{10} photons sec^{-1} cm^{-2} sr^{-1}) [38, 113]. Although *in vitro* transfer of naked plasmid DNA fails to mediate significant levels of gene expression, likewise tail vein administration of 1–5 µg of pGL3 in 50 µl, followed by a 5-min delay before an HS dose of saline, results in no detectable luciferase expression, due to the rapid metabolism of DNA in the blood [8, 9]. Polyethylene glycol (PEG)ylated glycoproteins were the first gene delivery systems that produced measurable luciferase expression following HS [40]. However, the level of expression was very low (10^6 photons sec^{-1} cm^{-2} ser^{-1}) and was only detectable at an

escalated 5 μg dose of pGL3 polyplex and at a short HS delay time of 5 min post DNA delivery. Without applying HS, these delivery systems fail to produce measurable luciferase expression in the liver.

To overcome the very limited efficacy of gene delivery systems to produce expression by HS, PEGylated polyacridine peptides were developed [9]. Modification of the ε-amine of Fmoc-Lys with acridine affords an amino acid (Acr) that is incorporated into a peptide during solid phase synthesis [60, 63]. It was previously reported that increasing the number of Acr residues from 2 to 6 greatly increases the binding affinity of polyacridine peptides for DNA [9]. The identity of a spacing amino acid separating Acr residues also greatly influences DNA-binding affinity with Lys > Arg > Leu > Glu. Even with a time delay of up to 1 h post-DNA delivery, $(Acr\text{-}Lys)_6$-Cys-PEG_{5kDa}/pGL3 (1 μg) polyplexes mediated luciferase expression equivalent in magnitude to direct-HD dosing of 1 μg of naked pGL3 [9].

Fluorescence investigations of polyintercalators in general have revealed a tendency towards intramolecular stacking in aqueous solutions, which leads to a decrease in affinity for dsDNA [59, 84]. Takenaka's group developed similar polyacridine peptides possessing two spacing Lys residues between each Acr(CM), where the intercalator was 6-chloro-2-methoxyacridine. This spacing was reported to allow simultaneous intercalation of all acridines in the peptide based on viscosimetric analyses of helix unwinding and circular dichroism analyses [60]. In a peptide with one Lys residue spacing each Acr, the intercalator branching points are spaced by 6.8 Å versus 10.3 Å when two Lys residues are between, the latter of which would support the nearest-neighbor exclusion priniciple requiring 10.2 Å to achieve occupancy of non-adjacent intercalation sites.

It was hypothesized that spacing Acr residues by at least two Lys residues would reduce the possible intramolecular stacking of acridines to increase intercalation and simultaneously increase cationic charge to increase ionic interaction. The resultant

increase in affinity would lead to improved circulatory stability. Based on this hypothesis and the promising results of our prior study, we explored the relationship between the number of Lys residues spacing Acr residues within PEGylated polyacridine peptides and its effects on HS expression. The results of this structure–activity relationship study report novel PEGylated polyacridine peptides that stabilize polyplexes containing 1 μg pGL3 in the circulation for up to 5 h. The contents of this chapter were originally reported by Kizzire et al [15].

Materials and Methods

Unsubstituted Wang resin, 9-hydroxybenzotriazole, Fmoc-protected amino acids, O-(7-Azabenzo-triazol-1-yl)-*N,N,N′,N′*-tetramethyluronium hexafluorophosphate (HATU), Fmoc-Lysine-OH, and *N*-methyl-2-pyrrolidone were obtained from AAPPTec (Louisville, KY, USA). *N*,*N*-dimethylformamide, trifluoroacetic acid (TFA) and acetonitrile were purchased from Fisher Scientific (Pittsburgh, PA, USA). Diisopropylethylamine, piperidine, acetic anhydride, Tris(2-carboxyethyl)-phosphine hydrochloride, 9-chloroacridine and thiazole orange were obtained from Sigma Chemical Co. (St Louis, MO, USA). Agarose was obtained from Gibco-BRL (Carlsbad, CA, USA). mPEG-maleimide (5000 Da) was purchased from Laysan Bio (Arab, AL, USA). d-Luciferin and luciferase from *Photinus pyralis* were obtained from Roche Applied Science (Indianapolis, IN, USA). pGL3 control vector, a 5.3-kbp luciferase plasmid containing a SV40 promoter and enhancer, was obtained from Promega (Madison, WI, USA). pGL3 was amplified in a DH5α strain of *Escherichia coli* and purified according to the manufacturer's instructions.

Synthesis and Characterization of Polyacridine Peptides

9-Phenoxyacridine and Fmoc-Lysine(Acr)-OH were prepared as recently reported [114, 115]. Polyacridine peptides were prepared by solid phase peptide synthesis on a 30 μmol scale using an APEX 396 synthesizer (Advanced ChemTech, Louisville, KY, USA)

with standard Fmoc procedures. The reaction yields were improved by activating amino acids with 9-hydroxybenzotriazole and HATU while using double coupling of Fmoc-Lys(Acr)-OH and triple coupling for the spacing amino acid, using a fivefold excess of amino acid over resin. Peptides were removed from resin and deprotected using a cleavage cocktail of TFA/ethanedithiol/water (93:4:3 v/v/v) for 3 h followed by precipitation in cold ether. Precipitates were centrifuged at 5000 × *g* and 4 °C for 10 min and the supernatant decanted. Peptides were then reconstituted with 0.1 v/v % TFA and purified to homogeneity on reversed phase-high pressure liquid chromatography (RP-HPLC) by injecting 0.5–2 μmol onto a Vydac C18 (Grace Davison Discovery Sciences, Deerfield, IL, USA) semi-preparative column (2 × 25 cm) eluted at 10 ml min^{-1} with 0.1 v/v % TFA with an acetonitrile gradient of 15–25 v/v % over 30 min while monitoring acridine at 409 nm. The major peak was collected and pooled from multiple runs, concentrated by rotary evaporation, lyophilized and stored at −20 °C. Purified peptides were reconstituted in 0.1 v/v % TFA and quantified by absorbance (acridine $\varepsilon_{409\,nm}$=9266 M^{-1} cm^{-1} assuming additivity of ε for multiple acridines) to determine isolated yield. Purified peptides were characterized by liquid chromatography–mass spectrometry (LC-MS) by injecting 2 nmol onto a Vydac C18 analytical column (0.47 × 25 cm) eluted at 1 ml min^{-1} with 0.1 v/v % TFA and an acetonitrile gradient of 15–45 v/v % over 30 min while acquiring electrospray ionization mass spectrometry (ESI-MS) in the positive mode.

Synthesis and Characterization of PEGylated Polyacridine Peptides

PEGylation of the Cys residue on $(Acr\text{-}Lys_n)_3$-Acr-Lys-Cys (where n = 1–6) was achieved by reacting 1 μmol of peptide with 1.1 μmol of PEG_{5kDa}-maleimide in 4 ml of 100 mM 4-(2-hydroxyethyl)-1-piperazineethanesulfonic acid (HEPES) buffer pH 7 for 12 h at room temperature. PEGylated peptides were purified by semi-preparative RP-

HPLC eluted with 0.1 v/v % TFA with an acetonitrile gradient of 20–60 v/v % acetonitrile while monitoring acridine at 409 nm. The major peak was collected and pooled from multiple runs, concentrated by rotary evaporation, lyophilized and stored at −20 °C. The counter ion was exchanged by chromatography on a G-25 column (2.5 × 50 cm) equilibrated with 0.1 v/v % acetic acid to obtain the peptide in an acetate salt form. The major peak corresponding to the PEG peptide eluted in the void volume (100 ml) was pooled, concentrated by rotary evaporation and freeze dried. PEG peptides were reconstituted in water and quantified by Abs_{409nm} (each acridine $\varepsilon_{409\,nm}$=9266 M^{-1} cm^{-1}) to determine isolated yield. PEG peptides were characterized by matrix-assisted laser desorption/ionization-time of flight mass (MALDI-TOF) spectrometry by combining 1 nmol with 10 µl of 2 mg ml^{-1} α-cyano-4-hydroxycinnamic acid in 50 v/v % acetonitrile and 0.1 v/v % TFA. Samples were spotted onto the target and ionized on a Bruker Biflex III Mass Spectrometer (Bruker Daltonics Inc., Billerica, MA, USA) operated in the positive ion mode.

Formulation and Characterization of PEGylated Polyacridine Peptide Polyplexes

The relative binding affinity of PEGylated polyacridine peptides for pGL3 was determined by a fluorophore exclusion assay [18]. pGL3 (200 µl of 5 µg ml^{-1} in 5 mM HEPES pH 7.5 containing 0.1 µM thiazole orange) was combined with 0, 0.05, 0.1, 0.13, 0.15, 0.18, 0.2, 0.25, 0.3, 0.4 0.5 or 1 nmol of PEGylated polyacridine peptide in 300 µl of HEPES and allowed to bind at room temperature for 30 min. Thiazole orange fluorescence was measured using an LS50B fluorometer (Perkin-Elmer, Cambridge, UK) by exciting at 498 nm while monitoring emission at 546 nm with the slit widths set at 10 nm. A fluorescence blank of thiazole orange in the absence of pGL3 was subtracted from all values before data analysis.

The particle size and zeta potential were determined by preparing 2 ml of polyplex in 5 mM HEPES pH 7.5 at a pGL3 concentration of 30 μg ml^{-1} and a PEGylated polyacridine peptide stoichiometry of 0.8 nmol μg^{-1} of pGL3. The particle size was measured by quasi-elastic light scattering at a scatter angle of 90° on a Brookhaven ZetaPlus Particle Sizer (Brookhaven Instruments Corporation, Holtsville, NY, USA). The zeta potential was determined as the mean of 10 measurements immediately following acquisition of the particle size.

Pharmacokinetic Analysis of PEGylated Polyacridine Polyplexes (In collaboration with Sanjib Khargharia)

Radioiodinated pGL3 was prepared as previously described [116]. Triplicate mice were anesthetized by intraperitoneal injection of ketamine hydrochloride (100 mg kg^{-1}) and xylazine hydrochloride (10 mg kg^{-1}) and underwent a dual cannulation of the right and left jugular veins. An i.v. dose of ^{125}I-pGL3 (3 μg, 1.2 μCi in 50 μl of HEPES-buffered mannitol (5 mM HEPES, 0.27 M mannitol pH 7.4) or ^{125}I-pGL3 polyplex (3 μg) was administered via the left catheter. Blood samples (10 μl) were drawn from the right catheter at 1, 3, 6, 10, 20, 30, 60, 90 and 120 min and immediately frozen. The volumes withdrawn were replaced with 10 μl of normal saline. The amount of radioactivity in each blood sample was quantified by direct γ-counting. Blood samples were digested with proteinase K for 12 h and polyplexes were extracted with 500 μl of phenol/chloroform/isoamyl alcohol (24:25:1) to remove PEGylated peptides followed by precipitation of DNA with the addition of 1 ml of ethanol [8, 9]. The precipitate was collected by centrifugation at 13,000 × *g* for 10 min, and the DNA pellet was dried and dissolved in 5 mM HEPES buffer pH 7.4. DNA samples were combined with 2 μl of loading buffer and applied to a 1% agarose gel (50 ml) and electrophoresed in Tris-borate-EDTA buffer at 70 V for 60 min [51]. The gel was dried on a zeta probe

membrane and autoradiographed on a Phosphor Imager (Molecular Devices, Sunnyvale, CA, USA) following a 15 h exposure.

Biodistribution Analysis of PEGylated Polyacridine Polyplexes (In collaboration with Sanjib Khargharia)

^{125}I-pGL3 (1.5 μg in 50 μl of HEPES-buffered mannitol, 0.6 μCi) or ^{125}I-pGL3 polyplexes (1.5 μg) were dosed in triplicate mice via tail vein. At times ranging from 5 min to 6 h, mice were anesthetized by intraperitoneal injection of ketamine (100 mg kg^{-1}) and xylazine (10 mg kg^{-1}) and then killed by cervical dislocation. The major organs (liver, lung, spleen, stomach, kidney, heart, large intestine and small intestine) were harvested, rinsed with saline, and the radioactivity in each organ was determined by direct γ-counting and expressed as the percentage of the dose in the organ.

Hydrodynamic Dosing and Hydrodynamic Stimulation (In collaboration with Sanjib Khargharia)

pGL3 (1 μg), pGL3-PEGylated polyacridine polyplexes (0.8 nmol μg^{-1} of pGL3), pGL3- PEI (N:P of 5) or -chitosan (N:P of 20) polyplexes, or pGL3-Lipofectamine (2:1 Lipid:pGL3 wt ratio) lipoplexes were prepared in a volume of normal saline corresponding to 9 w/v % of the mouse's body weight (1.8–2.25 ml based on 20–25 g mice). Hydrodynamic dosing (HD) of pGL3, polyplexes or lipoplex was achieved by administering the 1.8–2.25 ml volume to the tail vein of triplicate mice in 5 s according to a published procedure [26, 117]. Hydrodynamic stimulation (HS) was performed by tail vein dosing triplicate mice with 1 μg of pGL3, PEGylated polyacridine polyplexes, PEI polyplex, chitosan polyplex or Lipofectamine lipoplex in 50 μl of HEPES-buffered mannitol. At times ranging from 5 min to 9 h, a HS dose of normal saline (9 w/v% of the body weight) was administered over 5 s.

At 24 h post-HS or -HD, mice were anesthetized by 3% isofluorane, and an intraperitoneal dose of 80 μl (2.4 mg) of D-luciferin (30 μg μl^{-1} in phosphate-buffered

saline) was administered. At 5 min following the D-luciferin dose, mice were analyzed by bioluminescence imaging (BLI) on an IVIS Imaging 200 Series (Xenogen, Hopkins, MA, USA). BLI was performed in a light-tight chamber on a temperature-controlled, adjustable stage while isofluorane was administered by a gas manifold at a flow rate of 3%. Images were acquired at a 'medium' binning level and a 24.6-cm field of view with 10 s acquisition time. The Xenogen system reported bioluminescence as photons s^{-1} cm^{-2} sr^{-1} in a 2.86-cm diameter region of interest covering the liver. The integration area was transformed to pmols of luciferase in the liver using a previously reported standard curve [38]. Results were determined to be statistically significant ($p \leq 0.05$) based on a two-tailed unpaired t-test.

Results

To advance the development of i.v. dosed non-viral gene delivery systems that mediate expression in the liver, we designed a series of PEGylated polyacridine peptides, each with four Acr residues and an increasing number of Lys residues (ranging from 1 to 6) separating Acr residues (Figure 2-1, peptides **1–6**). Based on the nearest-neighbor exclusion principle and previously reported observations of the full intercalation of four acridine moieties using a motif of Acr residues spaced by two Lys residues [60, 92], we hypothesized that increasing the spacing of Acr with at least two Lys residues (Figure 2-1, peptide **2**) would increase binding affinity to DNA by allowing less hindered intercalation and additional ionic interaction, and this would potentially increase the *in vivo* stability and gene transfer efficacy of DNA polyplexes. The six Acr motif of PEGylated polyacridine peptide, which demonstrated high hydrodynamically stimulated (HS) gene transfer, was used as an optimal reference from a prior study (Figure 2-1, peptide **R2**) [9].

R1. PEG_{5kDa}-mal-Cys-Trp-Lys_{18}

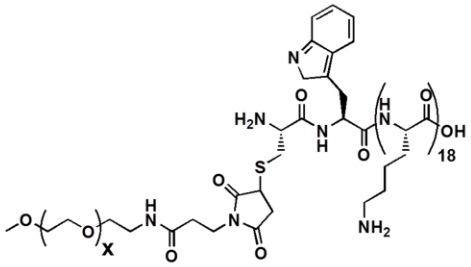

R2. $(Acr\text{-}Lys)_6$-Cys-mal-PEG_{5kDa}

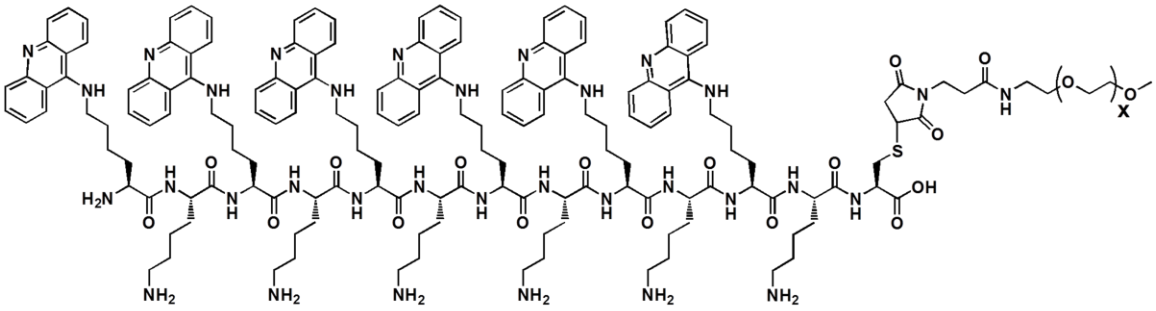

1-6. $(Acr\text{-}Lys_n)_3$-Acr-Lys-Cys-mal-PEG_{5kDa}

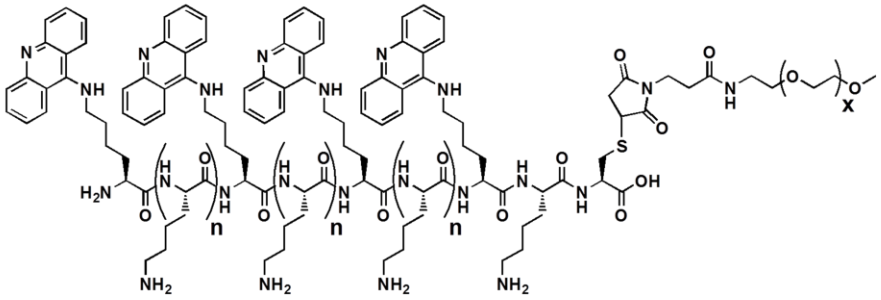

Figure 2-1. *PEGylated Polyacridine and Reference Peptide Structures.* The two reference peptides (**R1** and **R2**) are used as comparisons in the current study. Peptides **1-6** correspond with the number of spacing Lys residues, where n=1-6. Peptides **1D**, **4D**, and **6D** are peptides in which D-Lys was substituted for the unsubstituted L-Lys in peptides **1, 4,** and **6** (not shown, see Table 2-1). **R1D** is similar to **R1** where all L-Lys were substituted with D-Lys, and peptide **4** was altered by incorporation Lys(acetyl)-OH as spacing residues to make **4Ac** (not shown, see Table 2-1). All peptides were conjugated to mal-PEG_{5kDa}, and 'x' is an average of 130 due to the polydispersity of PEG.

Table 2-1. *Polyacridine Peptide Sequences, Yields, and Masses.*

Polyacridine Peptide Sequence	**Synthetic Yield (%)**	**Mass[a] (calc/obs)**	**PEGylated Polyacridine Peptide Sequence**	**Synthetic Yield (%)**	**Mass[b] (calc/obs)**
(Acr-Lys)$_3$-Acr-Lys-Cys	26	1855.3/1855.6	**(Acr-Lys)$_3$-Acr-Lys-Cys-PEG (Peptide 1)**	55	7355/7218
(Acr-DLys)$_3$-Acr-DLys-Cys	26	1855.3/1855.8	**(Acr-DLys)$_3$-Acr-DLys-Cys-PEG (Peptide 1D)**	61	7755/7500
(Acr-Lys$_2$)$_3$-Acr-Lys-Cys	10	2239.9/2239.6	**(Acr-Lys$_2$)$_3$-Acr-Lys-Cys-PEG (Peptide 2)**	42	7740/7684
(Acr-Lys$_3$)$_3$-Acr-Lys-Cys	19	2624.4/2624.6	**(Acr-Lys$_3$)$_3$-Acr-Lys-Cys-PEG (Peptide 3)**	69	8524/8316
(Acr-Lys$_4$)$_3$-Acr-Lys-Cys	20	3008.9/3008.8	**(Acr-Lys$_4$)$_3$-Acr-Lys-Cys-PEG (Peptide 4)**	77	8909/8697
(Acr-DLys$_4$)$_3$-Acr-DLys-Cys	26	3008.9/3008.6	**(Acr-DLys$_4$)$_3$-Acr-DLys-Cys-PEG (Peptide 4D)**	56	8909/8787
(Acr-Lys(ac)$_4$)$_3$-Acr-Lys-Cys	4	3513.3/3512.8	**(Acr-Lys(ac)$_4$)$_3$-Acr-Lys-Cys-PEG (Peptide 4Ac)**	29	9413/9131
(Acr-Lys$_5$)$_3$-Acr-Lys-Cys	19	3393.4/3393.4	**(Acr-Lys$_5$)$_3$-Acr-Lys-Cys-PEG (Peptide 5)**	73	9293/9202
(Acr-Lys$_6$)$_3$-Acr-Lys-Cys	18	3777.9/3777.6	**(Acr-Lys$_6$)$_3$-Acr-Lys-Cys-PEG (Peptide 6)**	56	9678/9332
(Acr-DLys$_6$)$_3$-Acr-DLys-Cys	13	3777.9/3777.4	**(Acr-DLys$_6$)$_3$-Acr-DLys-Cys-PEG (Peptide 2)**	47	9678/9482

[a]Mass determined by ESI-MS.

[b]Mass determined by MALDI-TOF

In an effort to increase DNA-binding affinity while simultaneously decreasing the number of Acr residues, a polyacridine peptide series of $(Acr\text{-}Lys_n)_3$-Acr-Lys-Cys-PEG was prepared where n = 1–6 (Figure 2-1). By incorporating only four evenly spaced Acr residues the overall size of the polyacridine peptide series was decreased, and ranged from 9 to 24 residues. In addition to L-Lys polyacridine peptides, several D-Lys peptides were prepared (**1D, 4D** and **6D**) using Fmoc-D-Lys(Boc) (Table 2-1). Likewise, an ε-acetyl Lys polyacridine control peptide (**4Ac**) was prepared using Fmoc-Lys(Ac) (Table 2-1). Peptides were purified by preparative RP-HPLC and characterized by LC-MS to establish their mass (Table 2-1).

Each peptide possessed a C-terminal Cys residue that was modified with a commercially available PEG_{5kDa}-maleimide. High molecular weight (≥ 2kDa), derivatized PEGs are purchased as polydisperse mixtures. An average mass of the resulting PEG-Peptide was calculated based on the average mass of PEG_{5kDa}-maleimide assessed by MALDI-TOF (Figure 2-2). Following PEGylation and purification by RP-HPLC, PEGylated polyacridine peptides were characterized by MALDI-TOF mass spectrometry to confirm this mass (Table 2-1, Figure 2-3). Based on our previous findings, the counter ions on PEGylated polyacridine peptides were converted from trifluoroacetic acid (TFA) to acetate to improve *in vivo* activity [9].

Properties and hydrodynamic dosing of PEGylated polyacridine peptide polyplexes

It is important to saturate DNA polyplexes with carrier material to prohibit nuclease access. In atomic force microscopy (AFM) images produced using **R2** polyplexes, two different forms of polyplexes were observed (Figure 2-4) [9]. At 0.2 nmol peptide μg^{-1} DNA, PEGylated **R2** produced open polyplexes (Figure 2-4B), and at a higher stoichiometry (0.8 nmol peptide μg^{-1} DNA), closed, spherical polyplexes were

observed indicating a greater degree of DNA compaction (Figure 2-4C). The polyplexes in this study were characterized at a saturating stoichiometry of 0.8 nmol μg^{-1} DNA.

PEGylated peptides **1–6** are comparable in size (9–24 amino acids) to PEGylated peptide **R1** (20 amino acids) and peptide **R2** (13 amino acids) (Figure 1). PEGylated-Cys-Trp-Lys_{18} (**R1**) lacks Acr and thereby binds to DNA exclusively through ionic interaction [56]. Although peptide **R1** has 18 Lys residues and forms polyplexes that remain stable during *in vitro* transfection [51, 56], peptide R1 polyplexes rapidly dissociate in the circulation when dosed i.v., leading to the immediate metabolism of the plasmid by serum DNase [8, 40, 118]. In contrast, peptide **R2**, possessing six Acr and only six Lys residues, binds DNA with a much higher affinity than **R1** due to its combined polyintercalation and ionic interaction [9]. Consequently, peptide **R2** polyplexes are stable in the circulation for up to 2 h, and thereby mediate maximal luciferase expression upon HS for up to 1 h post DNA delivery [9].

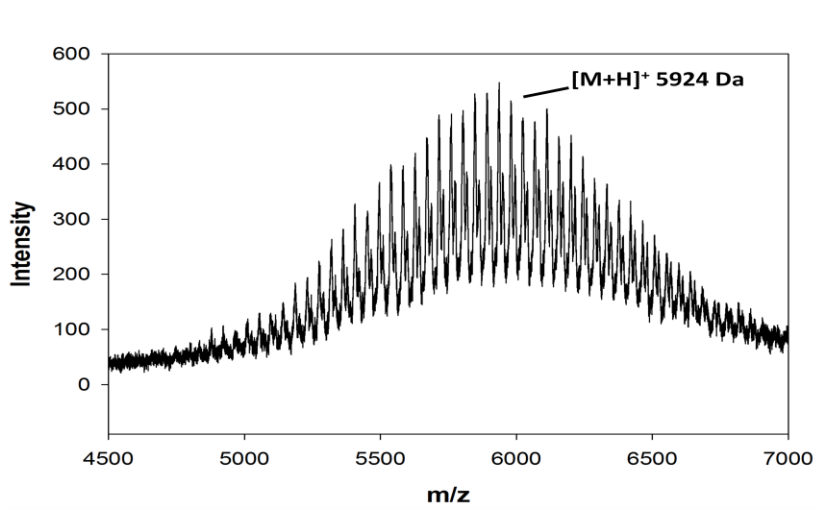

Figure 2-2. *MALDI-TOF Analysis of PEG_{5kDa}-maleimide.* The average molecular weight of PEG_{5kDa}-maleimide was determined by MALDI-TOF mass spectrometry to illustrate the polydispersity of commercially available PEGs.

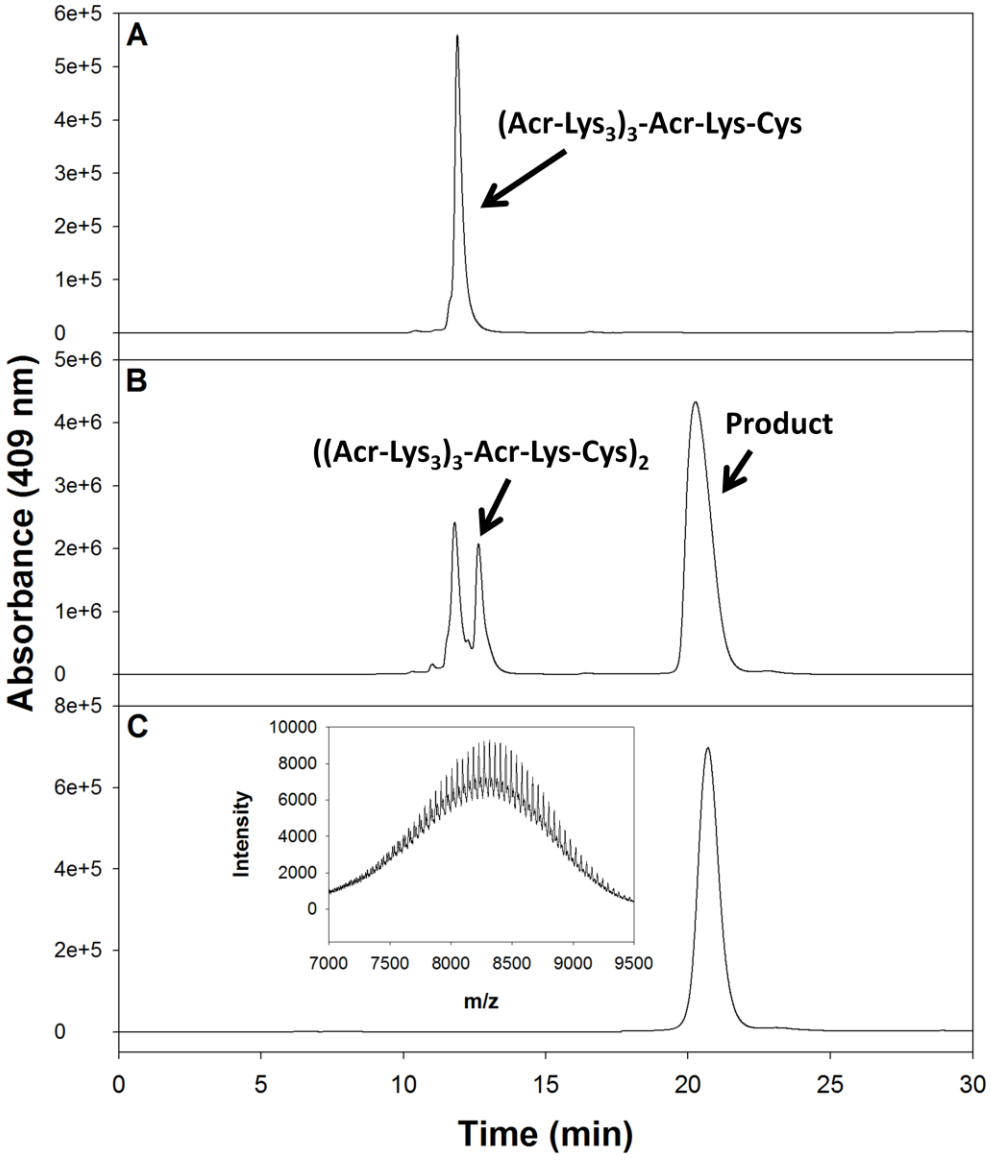

Figure 2-3. *PEGylation of Polyacridine Peptides.* Panels A-C illustrate the PEGylation of $(Acr\text{-}Lys_3)_3$-Acr-Lys-Cys with PEG_{5kDa}-maleimide using RP-HPLC while detecting acridine absorbance at 409 nm. The chromatograms were acquired using 0.1 v/v % TFA and an acectonitrile gradient of 10-55 v/v % over 30 min. Purified peptide (without PEG) is represented in panel A eluting at 11.8 min. Panel B is an analysis of the PEGylation reaction mixture prior to purification, which shows the formation of PEG-peptide (peptide **3**, 20.3 min) and the disulfide-bound byproduct, $((Acr\text{-}Lys_3)_3\text{-}Acr\text{-}Lys\text{-}Cys)_2$ (12.6 min). Panel C is an analysis of the purified product after semi-preparative purification with the inset displaying the MALDI-TOF analysis.

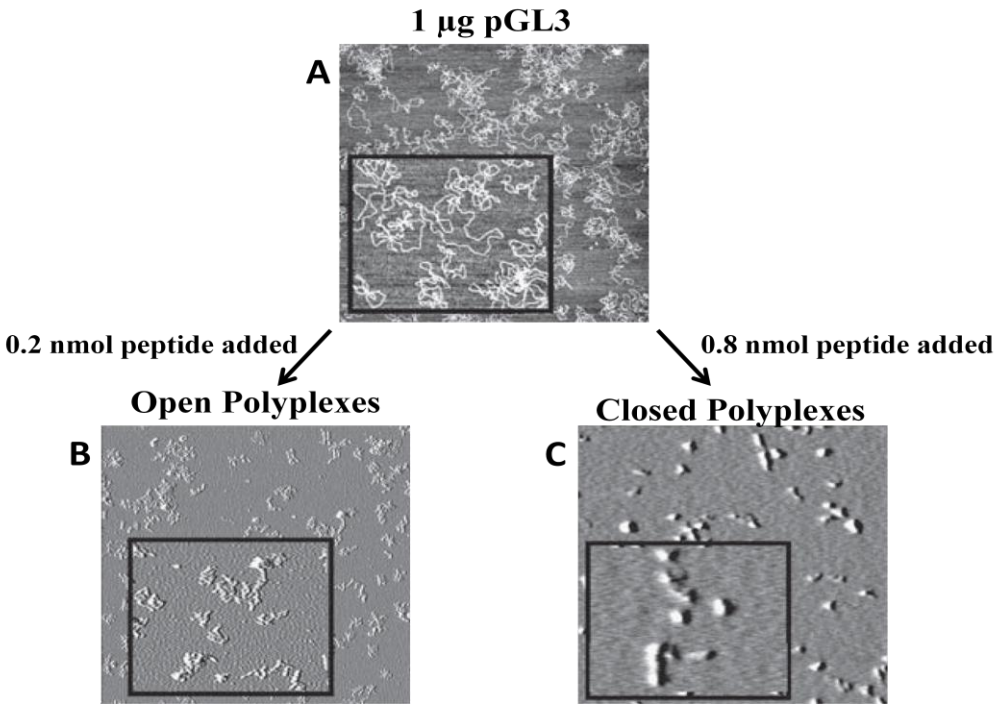

Figure 2-4. *Polyacridine Peptide Polyplex Morphology*. AFM images of pGL3 (panel A) and peptide **R2** polyplexes at 0.2 (panel B) and 0.8 nmol μg^{-1} pGL3 (panel C) are displayed. Lower stoichiometries of peptide where DNA is unsaturated lead to the formation of open, rod-like polyplexes, and high stoichiometries form closed, spherical polyplexes that are more resistant to metabolism by DNase. Images are 5 μm^2 with magnified insets of 1 μm^2. Adapted from Fernandez *et al* [9].

PEGylated peptides **1–6** were evaluated for relative binding affinities using a thiazole orange dye displacement assay. Each was able to bind to pGL3 and displace a thiazole orange fluorescent dye at a binding equivalent ranging from 0.13 to 0.4 nmol of peptide per µg of pGL3 (Figure 2-5). Peptide **1** and **1D** both possessed equivalent low affinity for binding DNA, but a noticeable increase in affinity was observed when comparing these peptides to peptide **2**, which supported the hypothesis of increasing Lys spacing to two. However, a modest affinity increase was revealed with the addition of spacing Lys residues for peptides **2–6**, which exhibit similar binding affinity when compared to previously reported results for peptide **R2**. Unexpectedly, D-Lys peptides

4D and **6D** were found to bind pGL3 with lower affinity compared with **4** and **6**. As anticipated, Lys-acetyl control peptide (**4Ac**) that possessed four Acr residues, each spaced by four acetylated Lys residues, possessed a lower apparent affinity when compared with its counterpart, peptide **4**.

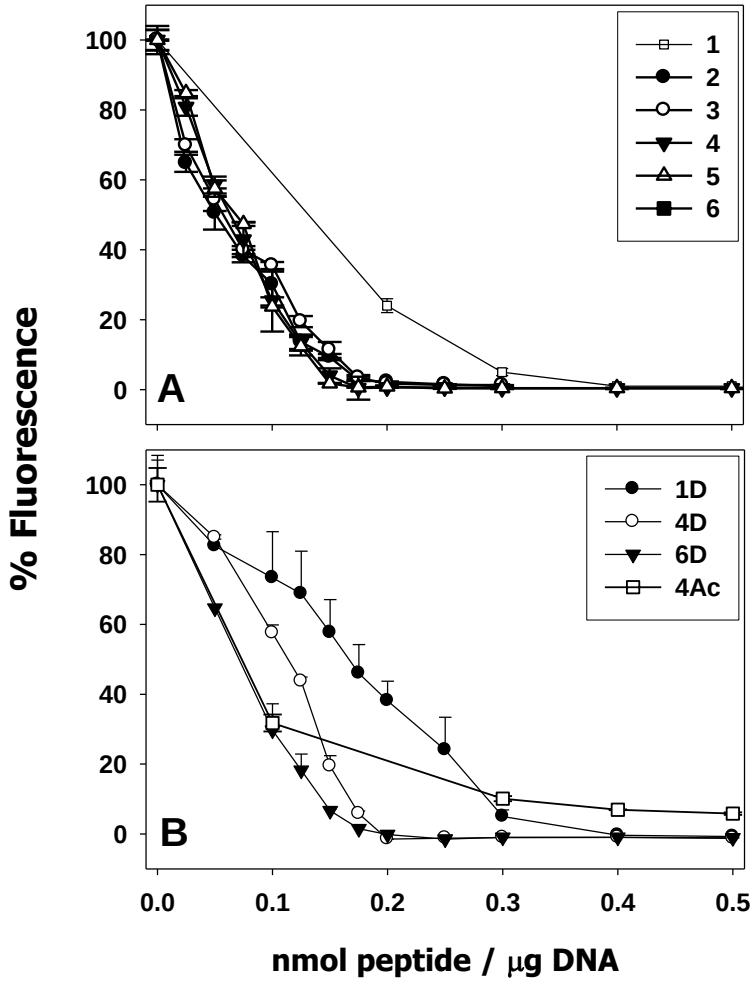

Figure 2-5. *Relative DNA-Binding Affinity of PEGylated Polyacridine Peptides*. Thiazole orange fluorescent dye displacement assay was used to determine the relative binding affinities of peptides **1-6** (panel A) and **1D, 4D, 6D,** and **4Ac** (panel B) for pGL3. The results indicate a strong gain in affinity as spacing Lys residues were increased from 1 to 2 (peptide **1** vs. **2**). The mean and standard deviation of each point were obtained from three determinations.

We previously analyzed the quasi-elastic light scattering particle size and zeta potential of peptide **R2** and **1** pGL3 polyplexes as a function of peptide to DNA stoichiometry to establish an asymptote at 0.8 nmols of peptide per µg of DNA or less [9]. Based on this result, the closed polyplex morphology (Figure 2-4), and the binding equivalence determined by thiazole orange displacement (Figure 2-5), the peptide to DNA stoichiometry was kept constant at 0.8 nmol of peptide per µg of pGL3 to allow direct comparison of the physical and biological properties of each peptide polyplex. The size and charge of pGL3 polyplexes prepared with peptides **R1, R2** and **1–6** established a mean diameter that ranged from 140 to 180 nm (Figure 2-6A) and a zeta potential ranging from -3 to +21 mV (Figure 2-6B). Peptides **R1** and **R2** both produced electro-positive polyplexes of ~ 150 nm diameter. As polyplex surface charge depends on the Lys to PEG ratio, peptide **R1** polyplexes possessed a higher zeta potential of +18 mV compared with peptide **R2** polyplexes with a zeta potential of +8 mV (Figure 2-6B). We previously observed that at a lower stoichiometry of 0.2 nmol of peptide per µg of pGL3, peptide **R2** forms metabolically stable open polyplexes that are -5 mV in charge [9]. Similarly, even at full saturation of pGL3, peptide **1** forms 160 nm polyplexes with a charge of -3 mV (Figure 2-6B). By comparison, peptides **2–6** polyplexes are of similar size (140–180 nm in diameter), but increase in charge incrementally from +5 to +21 mV, directly correlated with the Lys to PEG ratio (Figure 2-6A and B).

Peptide **4Ac** control polyplex possessed a similar particle size of 160 nm and a negative charge of -6 mV due to the lack of Lys ε-primary amine groups (Figure 2-6C and D). Compared with L-Lys peptides, D-Lys peptides **1D**, **4D** and **6D** each produced larger polyplexes of 200–250 nm diameter (Figure 2-6C). Polyplexes prepared with **1D** and **4D** also possessed a much higher zeta potential (Figure 2-6D). The difference in polyplex physical properties resulted from weaker binding affinity and contributed to lower gene expression for D-Lys peptide polyplexes as discussed below.

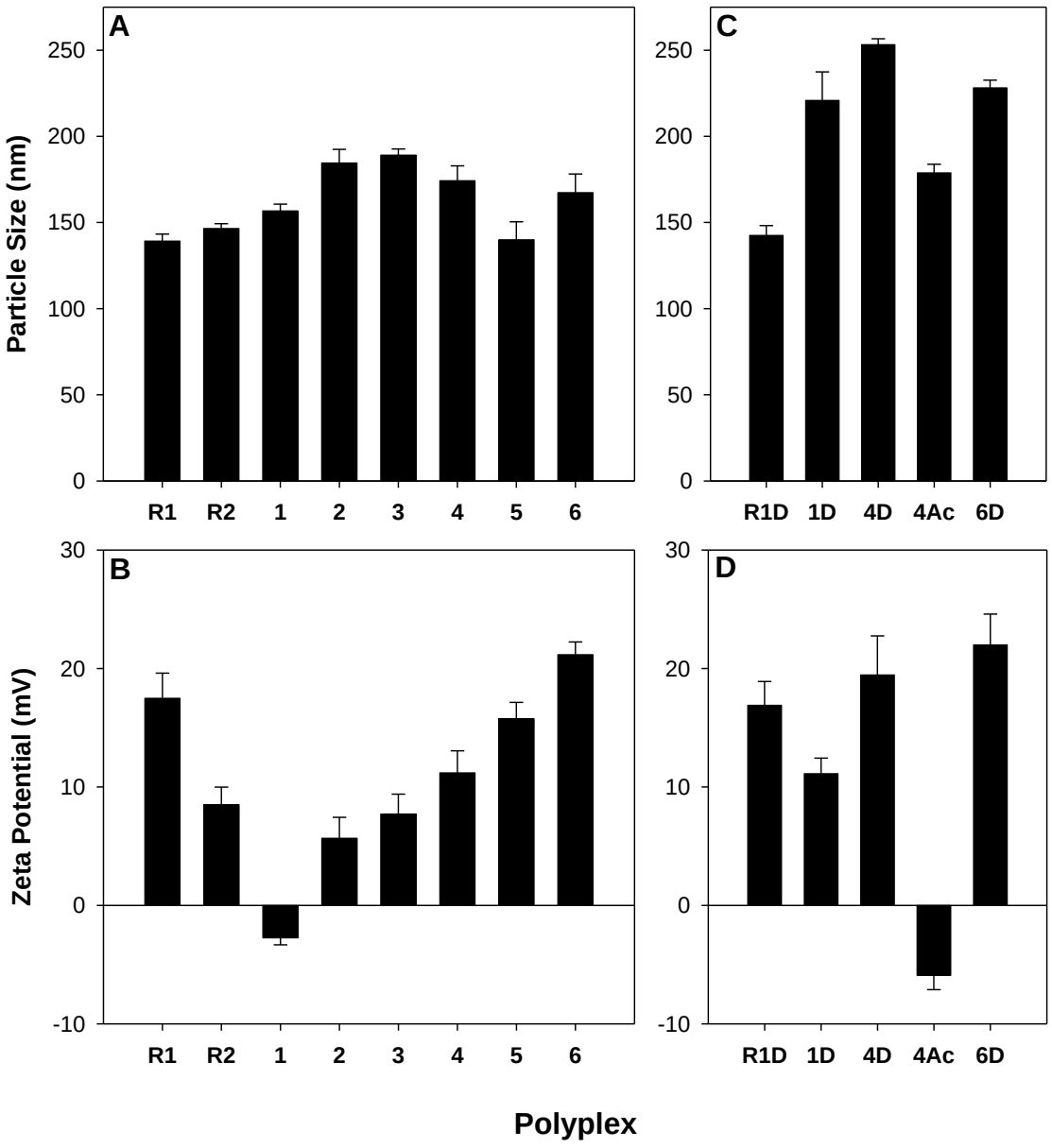

Figure 2-6. *Size and Charge of PEGylated Polyacridine Peptide Polyplexes.* Polyacridine peptide polyplexes were prepared at 0.8 nmol peptide μg^{-1} pGL3 and a concentration of 30 µg pGL3 ml^{-1}. Panels A and B compare the particle sizes and zeta potentials of peptide **R1, R2,** and **1-6** polyplexes. Panels C and D make the same comparisons for **R1D, 1D, 4D, 4Ac,** and **6D** polylexes. The data are plotted as the mean and standard deviation of multiple determinations.

Hydrodynamic dosing (HD) (1 μg) of pGL3, polyplexes and lipoplex, followed by bioluminescence imaging (BLI) measurement of luciferase in the liver at 24 h, was used to compare gene transfer efficiency (Figure 2-7). The level of expression mediated by peptide **R1** or **4Ac** polyplexes was indistinguishable from pGL3 (Figure 2-7A and B). Conversely, polyplexes prepared with peptides **R2** and **1–6** increased gene transfer during HD (Figure 2-7A). A five-fold statistically significant increase in HD-mediated gene transfer efficiency over pGL3 was realized when using peptide **3** polyplexes (Figure 2-7A). These results suggest that short peptides that bind DNA by ionic binding (**R1**), polyintercalation (**4Ac**), or a combination thereof are bound reversibly to DNA resulting in a level of expression coincident to the HD delivery of free pGL3. Unlike Lipofectamine (**L**) lipoplexes, PEI (**P**) and chitosan (**C**) polyplexes suppress HD gene transfer efficiency by 10–100-fold relative to HD of pGL3, indicating an inability to release DNA intracellularly (Figure 2-7A versus C).

In contrast to HD, HS with a short 5-min delay separating the primary dose and secondary stimulatory dose revealed that pGL3, peptide **R1, R1D, P** and **C** polyplexes, and **L** lipoplexes were all inactive in mediating gene transfer (Figures 2-7, Panels D-F). Not surprisingly, peptide **R1** and **R1D** polyplexes perform identically to naked pGL3 during direct HD and HD stimulation due to rapid dissociation of peptide **R1** and **R1D** in the blood, followed by rapid DNAse-mediated metabolism. **L** lipoplexes also perform identically as naked DNA, producing a high level of gene expression under HD and no expression under 5-min delayed HS, suggesting they also rapidly dissociate in the blood, leaving DNA susceptible to DNAse as has been reported previously [16]. Although inefficient transfer under HD may indicate greater polyplex stability for **P** and **C** polyplexes (Figure 2-7C), the complete loss of gene transfer activity by these polyplexes under a short 5-min HS (Figure 2-7F) is consistent with their rapid removal from the circulation due to protein aggregation and filtration in the lung [76].

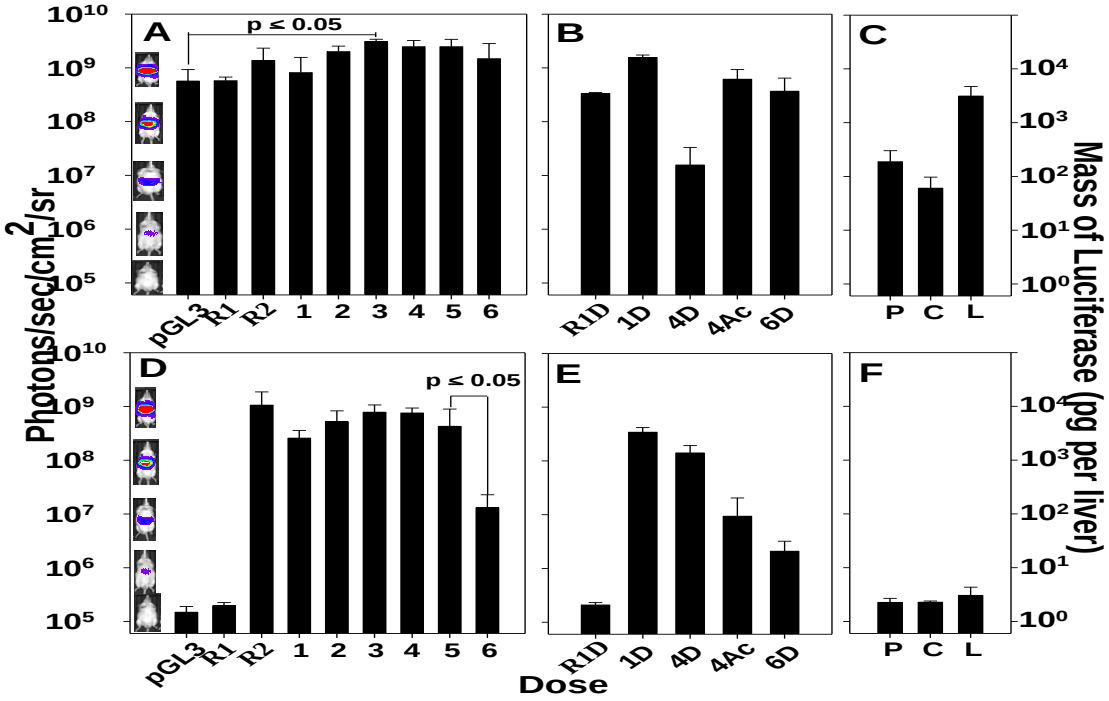

Figure 2-7. *Hydrodynamic dosing (HD) and hydrodynamic stimulation (HS) of PEGylated polyacridine polyplexes.* A comparison of the gene expression of 1 µg pGL3 different formulations under HD (Panels A-C) and 5-min HS (Panels D-F) is presented with representative mouse images corresponding to the BLI scale. Panels A and D correspond to BLI from HD and HS performed on naked DNA (pGL3) and polyplexes with reference peptides (**R1** and **R2**) and peptides **1-6**. BLI is shown in panel B and E for peptide **R1D, 1D, 4D, 4Ac,** and **6D** and panels C and F for polyethyleneimine (**P** at 5:1 N:P), chitosan (**C** at 20:1 N:P), and lipofectamine (**L** at weight ratio 2:1 **L**:pGL3). Peptides were used in polyplexes at 0.8 nmol μg^{-1} pGL3. Mean and standard deviations determined from triplicate mice.

By comparison, polyplexes composed of PEGylated peptides **1–5** all produced a high level of gene expression under 5-min delay HS (Figure 2-7D). The high level of gene expression confirms that peptide **1–5** polyplexes are stable in the circulation. However, peptide **6** polyplexes were 15-fold less efficient at mediating gene transfer relative to peptide **5** polyplexes (Figure 2-7D). This could be due to either premature dissociation of the polyplex, protein binding followed by removal from the circulation, Kupffer cell uptake, or incomplete intracellular DNA release. However, premature dissociation appears unlikely given the apparent high affinity of peptide **6** for pGL3 (Figure 2-5A).

Peptide **4D** polyplexes resulted in a five-fold lower gene transfer efficiency compared with peptide **4** polyplexes, and peptide **6D** polyplexes were 10-fold less efficient than peptide **6** polyplexes (Figures 2-7D and E). However, peptide **1** and **1D** polyplexes were equivalent in gene transfer. Although there is apparently no enhancement in gene transfer realized by stabilizing polyacridine peptides to the action of proteases using D-Lys, the loss of gene transfer efficiency of **4D** and **6D** can be partially rationalized by considering their lower apparent binding affinity for DNA, resulting in polyplexes with larger particle sizes and higher zeta potentials (Figure 2-6C and D), which could negatively influence biodistribution. It is speculated that the lower DNA-binding affinity of **4D** and **6D** is influenced by the misalignment of Acr residues due to the reversed chirality of D-Lys residues.

Under HD, control peptide **4Ac** polyplexes were ~100-fold less active in gene transfer relative to peptide **4** polyplexes (Figures 2-7D and E). This loss of activity is attributed to polyplex dissociation, as **4Ac** binds DNA exclusively through polyintercalation with much less affinity than **4** (Figure 2-5A versus B) and forms electronegative polyplexes (Figure 2-6D) that are less likely to experience altered biodistribution. This hypothesis is supported by the results of HS with extended time delay as discussed below.

Pharmacokinetics and biodistribution of PEGylated polyacridine peptide polyplexes

Following i.v. dosing, naked ^{125}I-pGL3 is rapidly metabolized into fragments and eliminated from the blood (Figure 2-8A and C) [8, 9]. The lack of DNA stability in blood accounts for the complete loss of HS expression at 5 min post DNA delivery (Figure 2-7D). PEGylated peptide **1** formed a more stable pGL3 polyplex with a longer α-half-life and a delayed DNA metabolism in the circulation as demonstrated by gel electrophoresis and autoradiography of blood time points (Figure 2-8A and D). The improved stability of peptide **5** polyplexes in the circulation is evident by gel electrophoresis and autoradiography analysis of blood time points out to 2 h. Pharmacokinetic analysis of polyplexes prepared with peptides **2–6** established a correlation between the β-half-life and mean residence time with increased protection of DNA from metabolism (Figure 2-8A, Table 2-2). The longest half-lives were determined for polyplexes prepared with peptides **4** and **6** (Figure 2-8A, Table 2-2), which are comparable to that achieved with DNA encapsulated in stealthed liposomes [119].

Biodistribution analysis established that each of the polyplexes produced a significant percent of dose associated with the liver at 5 min post-DNA administration, ranging from 49 to 66% (Figure 2-8B, Table 2-3). Naked DNA is metabolized and eliminated from the liver such that only 6% of the ^{125}I-pGL3 dose is recovered in the liver at 2 h (Figure 2-8B). Increasing the number of Lys residues in PEGylated peptides **1–6** closely correlates with an increasing percentage of the dose remaining in the liver at 2 h (Figure 2-8B). The liver and blood accounted for the majority of the ^{125}I-pGL3 over time (Table 2-3). However, a slightly higher percentage of the dose was recovered in lung for peptide **3** polyplexes, in the spleen for peptide **1, 2, 3** and **4,** and in the stomach for all polyplexes at 2 h as a result of the liver metabolism. The total recovery was determined by addition of results from two separate experiments (pharmacokinetics and biodistribution) and sometimes exceeded 100% (Table 2-3).

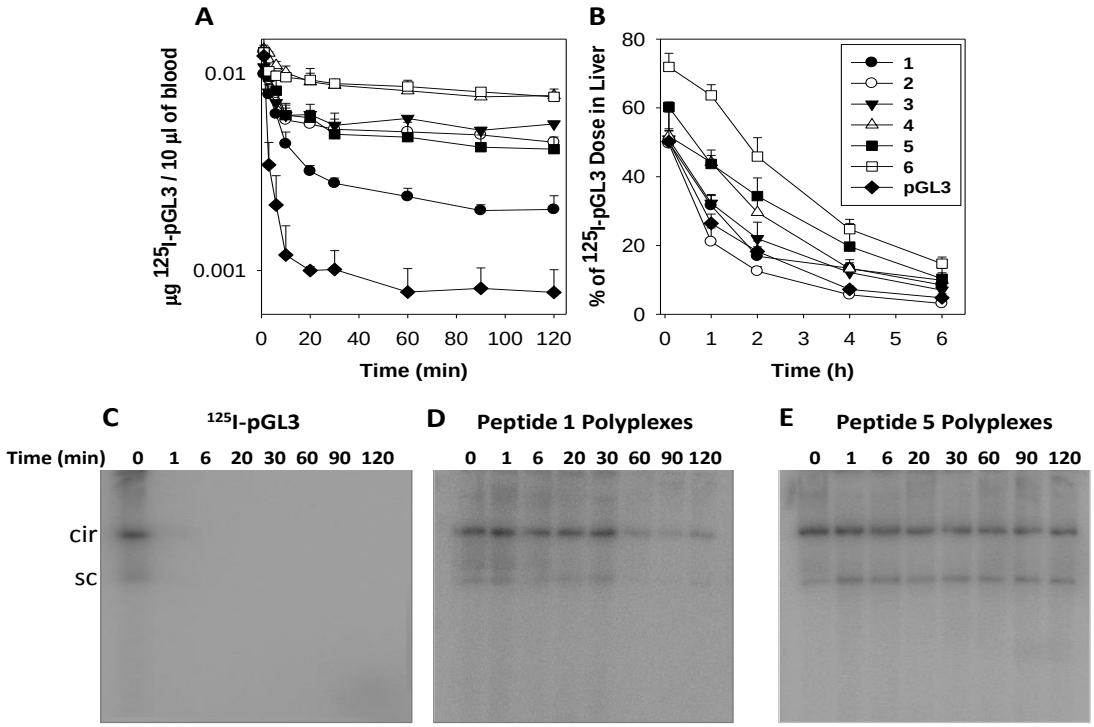

Figure 2-8. *Pharmacokinetics (PK) and Liver Biodistribution (BD) of PEGylated Polyacridine Peptides.* The PK and BD of peptide 1-6 polyplexes were evaluated using ^{125}I-pGL3 at 0.8 nmol µg^{-1} pGL3 (Panels A and B). Blood samples collected for ^{125}I-pGL3 (Panel C), peptide 1 polyplexes (Panel D), and peptide 5 polyplexes (Panel E) were extracted to isolate DNA, which was resolved by agarose gel electrophoresis and imaged via autoradiography. DNA is presented in two states indicated by two bands in each lane – circular (*cir*) and supercoiled (*sc*). Results are the mean and standard deviation of three determinations.

Table 2-2. *Pharmacokinetics of PEGylated Polyacridine Peptide Polyplexes*[a]

Polyplex	$t_{1/2}\alpha$[b] (min^{-1})	$t_{1/2}\beta$[c] (min^{-1})	V_d[d] (ml)	Cl[e] (ml min^{-1})	MRT[f] (min)	AUC[g] (µg*min ml^{-1})
1. $(Acr\text{-}Lys)_3$-Acr-Lys-Cys-PEG/^{125}I-DNA	3.4 ± 0.6	112.1 ± 28.3	357.1 ± 41.3	2.3 ± 0.4	162.5 ± 34.6	67.2 ± 10.3
2. $(Acr\text{-}Lys_2)_3$-Acr-Lys-Cys-PEG/^{125}I-DNA	2.1 ± 0.7	231.6 ± 53.9	289.5 ± 3.8	0.9 ± 0.2	326.3 ± 79.1	172.3 ± 38.1
3. $(Acr\text{-}Lys_3)_3$-Acr-Lys-Cys-PEG/^{125}I-DNA	2.1 ± 0.4	375.4 ± 91.2	221.1 ± 17.3	0.4 ± 0.1	545.8 ± 128	365.3 ± 65.4
4. $(Acr\text{-}Lys_4)_3$-Acr-Lys-Cys-PEG/^{125}I-DNA	4.1 ± 2.2	373.6 ± 44.3	159.1 ± 9.4	0.3 ± 0.1	540.3 ± 62.3	507.7 ± 43.2
5. $(Acr\text{-}Lys_5)_3$-Acr-Lys-Cys-PEG/^{125}I-DNA	3.2 ± 1.7	260.5 ± 87.7	333.6 ± 16.8	0.9 ± 0.4	371.6 ± 134	169.3 ± 57.1
6. $(Acr\text{-}Lys_6)_3$-Acr-Lys-Cys-PEG/^{125}I-DNA	3.8 ± 1.6	291.1 ± 97.4	178.3 ± 32.3	0.5 ± 0.1	420.6 ± 140	352.8 ± 92.1

[a]Calculated using blood cpm values over 120 min and assuming complete DNA stability.

[b]Calculated α-half-life.

[c]Calculated β-half-life.

[d]Volume of distribution.

[e]Total body clearance rate.

[f]Mean residence time.

[g]Area under the curve.

Table 2-3. *Biodistribution of PEGylated Polyacridine Peptide Polyplexes*

	Time (min)	Blood	Liver	Lung	Spleen	Stomach	Kidney	Heart	Large Intestine	Small Intestine	Total
^{125}I-pGL3	5	10.8 ± 4.3	65.7 ± 2.5	6.1 ± 2.2	2.8 ± 0.3	0.2 ± 0.0	0.9 ± 0.2	0.1 ± 0.0	0.2 ± 0.1	0.4 ± 0.1	81.1 ± 9.7
	60	3.9 ± 1.2	12.7 ± 2.0	0.9 ± 0.2	1.3 ± 0.2	4.5 ± 1.0	3.5 ± 0.6	0.2 ± 0.0	1.1 ± 0.2	2.1 ± 0.3	30.2 ± 5.8
	120	3.9 ± 1.5	6.1 ± 1.5	0.5 ± 0.2	0.8 ± 0.2	9.4 ± 3.2	1.6 ± 0.9	0.1 ± 0.1	1.9 ± 0.8	2.6 ± 0.5	26.9 ± 8.4
Peptide 1/^{125}I-pGL3	5	30.0 ± 3.6	49.9 ± 3.3	2.2 ± 0.6	8.5 ± 4.3	0.5 ± 0.1	0.5 ± 0.2	0.3 ± 0.1	0.6 ± 0.1	0.6 ± 0.3	93.0 ± 10.7
	60	11.4 ± 2.1	31.6 ± 2.9	1.3 ± 0.1	9.1 ± 3.4	4.4 ± 1.6	1.2 ± 0.1	0.2 ± 0.1	1.8 ± 0.5	0.6 ± 0.2	61.6 ± 10.4
	120	9.9 ± 1.3	16.9 ± 2.7	0.8 ± 0.2	8.3 ± 5.1	7.9 ± 3.4	1.6 ± 0.2	0.1 ± 0.0	2.3 ± 0.6	0.8 ± 0.2	48.6 ± 13.7
Peptide 2/^{125}I-pGL3	5	42.4 ± 3.8	49.6 ± 4.3	1.2 ± 0.2	11.6 ± 2.0	0.5 ± 0.2	1.6 ± 0.1	0.3 ± 0.1	0.8 ± 0.1	0.3 ± 0.1	108.0 ± 10.9
	60	32.6 ± 4.4	21.1 ± 4.0	1.2 ± 0.2	10.1 ± 2.5	5.6 ± 3.7	2.0 ± 0.4	0.2 ± 0.0	2.4 ± 0.2	1.0 ± 0.3	76.3 ± 15.9
	120	29.7 ± 2.4	12.5 ± 1.3	0.9 ± 0.2	11.6 ± 6.3	7.4 ± 3.4	1.7 ± 0.1	0.2 ± 0.1	2.5 ± 0.3	1.2 ± 0.2	67.9 ± 14.3
Peptide 3/^{125}I-pGL3	5	41.1 ± 4.3	50.9 ± 7.8	5.8 ± 1.8	7.2 ± 2.1	0.5 ± 0.2	0.9 ± 0.5	0.2 ± 0.1	0.6 ± 0.2	0.5 ± 0.4	107.6 ± 17.6
	60	34.2 ± 2.8	32.3 ± 2.5	6.1 ± 0.2	9.2 ± 2.1	3.3 ± 1.1	2.1 ± 0.4	0.2 ± 0.0	2.5 ± 0.8	0.8 ± 0.4	90.7 ± 10.3
	120	32.1 ± 3.7	22.0 ± 4.8	5.6 ± 1.5	10.5 ± 3.1	4.5 ± 1.1	1.9 ± 0.4	0.2 ± 0.0	2.4 ± 0.5	1.6 ± 0.3	80.6 ± 15.4
Peptide 4/^{125}I-pGL3	5	47.9 ± 5.3	51.8 ± 7.5	2.6 ± 1.8	4.3 ± 0.8	0.4 ± 0.2	1.0 ± 0.5	0.3 ± 0.1	0.4 ± 0.1	0.2 ± 0.1	108.3 ± 16.6
	60	35.9 ± 3.5	44.1 ± 2.0	0.8 ± 0.2	8.6 ± 0.8	2.4 ± 1.1	1.2 ± 0.1	0.2 ± 0.0	1.2 ± 0.2	0.4 ± 0.1	94.9 ± 8.1
	120	32.0 ± 2.8	29.6 ± 4.8	0.8 ± 0.1	6.5 ± 0.6	4.3 ± 0.8	1.7 ± 0.6	0.2 ± 0.1	1.6 ± 0.6	0.9 ± 0.1	77.5 ± 10.5
Peptide 5/^{125}I-pGL3	5	41.3 ± 3.4	60.2 ± 2.5	2.3 ± 0.0	3.0 ± 0.8	0.8 ± 0.1	1.3 ± 0.3	0.5 ± 0.1	0.5 ± 0.1	0.2 ± 0.0	110.2 ± 7.5
	60	24.1 ± 3.5	43.7 ± 4.0	1.4 ± 0.7	6.3 ± 1.5	3.0 ± 1.7	2.1 ± 0.5	0.2 ± 0.0	2.0 ± 0.6	0.5 ± 0.1	83.3 ± 12.6
	120	20.9 ± 3.0	34.7 ± 5.3	1.0 ± 0.2	3.0 ± 1.3	5.9 ± 0.8	1.9 ± 0.9	0.2 ± 0.0	2.8 ± 0.8	0.8 ± 0.0	78.1 ± 12.1
Peptide 6/^{125}I-pGL3	5	40.7 ± 3.6	66.2 ± 3.3	4.4 ± 0.9	1.4 ± 0.7	0.3 ± 0.1	1.4 ± 0.1	0.5 ± 0.2	0.7 ± 0.1	0.3 ± 0.1	115.9 ± 9.1
	60	37.4 ± 3.7	57.8 ± 4.1	2.9 ± 0.2	5.3 ± 0.4	3.5 ± 0.7	1.2 ± 0.1	0.4 ± 0.0	1.1 ± 0.2	0.7 ± 0.0	110.5 ± 9.6
	120	31.5 ± 2.9	47.8 ± 5.2	2.1 ± 1.1	3.1 ± 0.6	8.1 ± 0.2	0.8 ± 0.1	0.2 ± 0.1	1.3 ± 0.3	0.6 ± 0.1	96.6 ± 10.5

Values reported are % of dose assessed from cpm observed in biodistribution or pharmacokinetics analyses.

Hydrodynamically Stimulated Expression of PEGylated Polyacridine Peptide Polyplexes

A distinguishing feature of PEGylated polyacridine peptide polyplexes is their ability to mediate gene expression when dosed i.v. followed by an extended time delay before HS. In a previous study, PEGylated peptide **R2** was used to form electronegative open polyplexes at 0.2 nmol μg^{-1} of DNA and shown to mediate 10^8 photon sec^{-1} cm^{-2} ser^{-1} upon HS at a 1-h stimulation time, followed by a 100-fold decline at 2 h (Figure 2-9A) [9]. Anticipating that at DNA saturation (0.8 nmol peptide to 1 µg pGL3) peptide **R2** polyplexes may be more protected from metabolism and mediate expression at prolonged stimulation times, we compared the level of luciferase expression at 0.2 and 0.8 nmols as a function of stimulation time. The results establish that 0.8 nmol of peptide maintained full expression when applying HS at times up to 3 h, followed by a steady decline to near zero expression when applying HS at 7 h (Figure 2-9A).

Comparison of the HS expression of pGL3 (1 µg) polyplexes mediated by 0.8 nmol of peptides **1–6** revealed a strong dependence on the number of Lys residues spacing Acr and the level of expression at extended delay times (Figure 2-9B). A single Lys in peptide **1** resulted in polyplexes that only produce 10^7 photons sec^{-1} cm^{-2} ser^{-1} at a 1 h stimulation time, which decreases to zero by 3 h (Figure 2-9B). Two Lys residues in **2** improved the level of expression to 10^8 at a 1 h HS time, but still led to rapid loss of expression reaching zero by 3 h (Figure 2-9B). The addition of a third spacing Lys residue in **3** markedly improved the stability of HS expression maintaining nearly 10^8 photons sec^{-1} cm^{-2} ser^{-1} at a 3 h stimulation time, followed by a similar decrease to zero over 4 h. PEGylated polyacridine peptides **4** and **5** both mediated maximal HS gene expression at delay times of 4–5 h, followed by a decrease in the level of HS expression over 4 h. HS of pGL3 polyplexes prepared with **6** resulted in ~ 10-fold lower expression compared with **4** and **5**, however, the level of HS expression remained stable for 5 h

before declining over 4 h (Figure 2-9B). The decreased level of HS gene expression mediated with peptide **6** polyplexes under extended time delay is consistent with the results of HS at 5-min delay (Figure 2-7D).

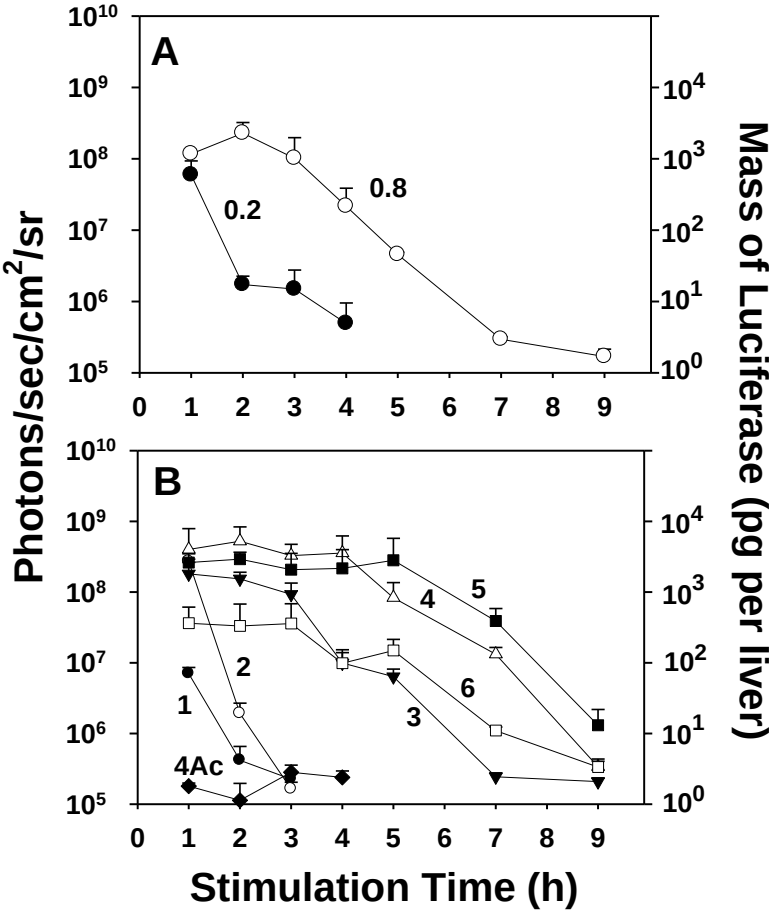

Figure 2-9. *Extended Hydrodynamically Stimulated Gene Expression of PEGylated Polyacridine Peptide Polyplexes*. Panel A illustrates the use of differing amounts of peptide **R2** (0.2 and 0.8 nmol) to polyplex 1 µg pGL3 for HS gene expression at stimulation times of 1 to 9 h. Saturation of pGL3 with **R2** leads to polyplexes that maintain maximal expression levels for 3 h. At 0.8 nmol, peptides **1-6** and **4Ac** were used to polyplex 1 µg pGL3 for HS with a stimulation delay of 1 to 9 h as shown in panel B. All polyplexes were dosed i.v. via tail vein in a small volume (50 µl), and stimulations were performed with 1.8-2.25 ml saline at times indicated followed by BLI at 24 h. The results are the mean and standard deviation of triplicate mice.

There are several important conclusions that can be made from analysis of the results presented in Figure 2-9. The addition of spacing Lys residues results in maintenance of maximal expression for longer HS delay times. Although the addition of multiple Lys residues increases the peptide affinity for DNA through increased ionic binding, it is also clear that the combination of both polyintercalation and ionic binding is essential, and neither mode is individually sufficient. Polyplexes prepared with the weakly binding polyintercalating peptide **4Ac** show no expression at delay times of 1 h. Intermediate affinity peptides such as **1** or **2** produce a stimulation profile that rapidly declines to zero at 3-h delay times. Higher affinity peptides **3, 4** and **5** have stimulation profiles with sustained maximal expression for 3–5 h before declining steadily to zero over 4 h. In conjunction with the notable trend of increased liver accumulation as polyplex charge increases (Figure 2-8B), the stimulation profile produced by peptide **6** polyplexes suggests its lower level of sustained expression is the result of Kupffer cell uptake. This also explains the observation that peptide **6** can fully release pGL3 under HD to maintain the same maximal expression as naked pGL3 (Figure 2-7A).

To investigate if the steady decline in HS expression for peptide **4** polyplexes after 4 h was due to DNA metabolism in the blood, peptide **4** polyplexes were incubated for 24 h in heparinized whole mouse blood at 37 ˚C followed by i.v. dosing and HS after 1 h (Figure 2-10A). Comparison of polyplexes dosed immediately with those incubated in blood for 24 h established a 10-fold loss in HS gene expression, suggesting that peptide **4** polyplexes were only partially digested by DNase in the blood (Figure 2-10A).

A contributing factor to the steady decline of HS expression over 4 h for peptides **3–6** polyplexes could also be the shedding of the reversibly-bound PEGylated peptide in the circulation, thereby exposing pGL3 to metabolism by DNase. To test this hypothesis, a decoy dose of plasmid expressing secreted alkaline phosphatase (pSEAP) (1.5, 4 and 9 μg) was used to form peptide **4** polyplexes that were co-administered with pGL3 (1 μg) peptide **4** polyplexes.

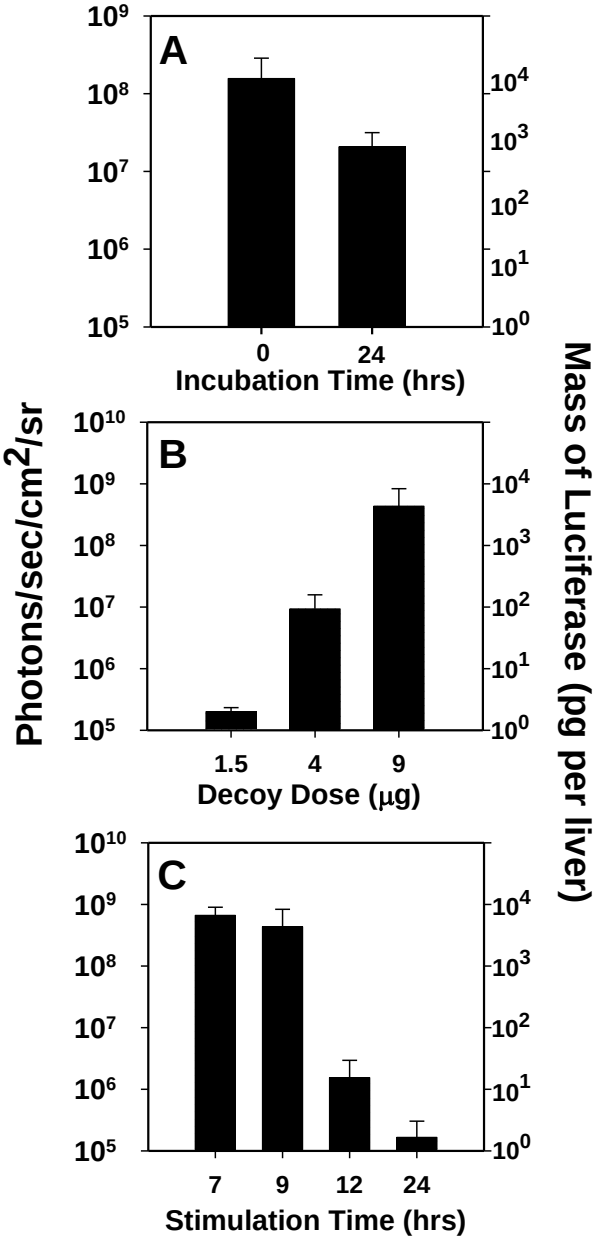

Figure 2-10. *Blood Stability and Decoy-Enhanced HS Gene Expression.* In panel A, 1 μg pGL3 was polyplexed with 0.8 nmol peptide **4** and incubated in 70 μl heparinized mouse blood for 0 or 24 h at 37 ˚C. Polyplex was dosed and HS gene expression determined at 1h analyzed by BLI 24 h post-stimulation. Panel B illustrates the co-administration of 1 μg pGL3 polyplex with increasing amounts of polyplexed pSEAP (decoy polyplex). All polyplexes were made with peptide **4** at 0.8 nmol μg^{-1} DNA and administered by HS at a stimulation time of 9 h. Panel C illustrates HS expression at various times using co-administered 1 μg pGL3 and 9 μg pSEAP polyplexes formed with peptide **4** at 0.8 nmol μg^{-1} DNA.

HS at 9 h established a dose–response relationship in which maximal expression was restored at 9 µg of pSEAP polyplex (Figure 2-10B). Extending the HS time delay from 7 to 24 h established that a decoy dose of 9 µg of polyplex restored maximal expression at 7 and 9 h, which declined nearly 1000-fold by 12 h and diminished to zero at a HS delay time of 24 h (Figure 2-10C). It is likely that this result stems from an inhibition of Kupffer cell uptake and metabolism. This would serve to explain why a small increase in polyplex dose leads to such a dramatic increase in the duration of pGL3 polyplexes because Kupffer cells make up a much smaller portion of the liver than hepatocytes and are presumably responsible for a majority of the hepatic uptake of polyplex observed (Figure 2-8B). These results may also support a hypothesis that shedding of PEGylated polyacridine peptides during circulation results in exposure of DNA to DNase. The decoy dose should also shed peptide and could serve as a substrate to occupy DNase in the circulation, delaying the metabolism of pGL3 polyplexes. HS of peptide **R2** polyplexes prepared at 0.2 and 0.8 nmol of peptide per µg of pGL3 models this effect, with 0.2 nmol peptide **R2** polyplexes resembling partially shed polyplexes that have HS profiles shifted to the left relative to 0.8 nmol peptide **R2** polyplexes (Figure 2-9A).

Discussion

The development of non-viral gene delivery systems that mediate expression in the liver following a conventional small volume i.v. dose of 1 µg of plasmid DNA polyplex is hampered by the lack of measurable expression for all delivery platforms studied to date. This has caused researchers to increase the DNA dose to 10–50 µg in mice, allowing the detection of measurable, but low levels of luciferase in the liver [76, 118, 120-122]. Generally, the expression levels have been difficult to compare due to the use of many different plasmids with different promoters and the lack of dose-matched comparison with HD delivery. Furthermore, as has been noted previously [107], a 25 µg

polyplex dose in mice equates to a 100 mg dose in humans, strongly suggesting that non-viral delivery systems possessing greatly improved efficiency need to be developed.

A standardized protocol was previously developed to compare the level of expression mediated by i.v.-dosed pGL3 polyplexes with dose-matched HD delivery of pGL3 [40]. The use of a calibrated BLI measurement for quantifying luciferase in the liver of albino ICR mice following a 1 μg dose of pGL3 or pGL3 polyplex, allows for a direct efficiency comparison.

The protocol described was developed to optimize *in vivo* delivery of DNA polyplexes. Although PEGylated polyacridine polyplexes can be stimulated to express *in vivo*, they do not transfect cells in culture under standard *in vitro* gene transfer protocols. This is primarily the result of stealthing of the polyplex by PEG, which blocks it from binding to cells [56]. Following the i.v. administration of PEGylated polyacridine pGL3 polyplexes, there is also no detectable expression without application of HS. However, with the application of HS at time delays of 5 min or longer, certain pGL3 polyplexes express luciferase as efficiently as HD administration of pGL3. The results suggest that HS transports pGL3 polyplexes in the blood or liver into the nuclei of hepatocytes leading to the observed gene expression. The magnitude of expression following a variable delay-time between pGL3 polyplex dose and HD stimulation is a parameter used to estimate polyplex stability. Polyplexes with minimal stability mediate relatively low levels of expression at very short HS delay times of 5 min due to metabolism of DNA in the blood [40]. Conversely, polyplexes that are optimally stabilized result in maximal expression for prolonged HS delay times of 4 to 5 h. Polyplexes that exceed optimal stability fail to release DNA and produce lower levels of expression for prolonged HS delay times. This delicate balance between polyplex stability and release has been noted as a key barrier to achieving efficient non-viral delivery [76, 109].

PEGylated polyacridine peptide polyplexes are unique in mediating efficient HS gene expression at extended delay times because of the ability to tune the affinity for

DNA by changing the number of Acr and Lys residues. A significant finding of this study is that spacing Acr with additional Lys residues significantly extends the delay times that achieve maximal gene expression under HS. PEGylated polyacridine peptides with four Acr and either four or five spacing Lys residues (peptides **4** and **5**) form polyplexes that circulate and maintain HS expression for up to 4–5 h (Figure 2-9B). By comparison, peptide **R2** possessing 6 Acr, each spaced by a single Lys residue, resulted in a maximal expression for up to 3 h in the circulation (Figure 2-9A). It is also clear, by comparison of HS expression using polyplexes prepared with peptide **R1**, **4Ac** and **4**, that a combination of intercalator and ionic binding to DNA is necessary to achieve sufficient polyplex stability to mediate HS expression (Figure 2-7D and E). This is further supported by the observation that polyplexes or lipoplexes prepared with PEI, Lipofectamine, or chitosan all fail to mediate HS expression even at 5 min (Figure 2-7D and F). These results are consistent with prior studies that examined the stability of lipoplexes in the blood and the pharmacokinetics and biodistribution of PEI and chitosan polyplexes [36, 107, 123-127].

An unexpected finding was the difference between L-Lys and D-Lys peptide polyplexes. Peptides **4D** and **6D** polyplexes resulted in at least a 10-fold loss in expression relative to peptides **4** and **6** polyplexes when delivered by HD (Figures 2-7A and B) or HS (Figure 2-7D and E). This result correlates with the apparent lower affinity of peptides **4D** and **6D** for binding DNA relative to **4** and **6** (Figure 2-5A and B), a larger particle size for **1D, 4D** and **6D** relative to **1, 4** and **6** (Figure 2-6A and C) and a higher zeta potential for **1D** and **4D** relative to **1** and **4** (Figures 2-6B and D). Therefore, the differences in DNA binding between L and D peptides, leading to both larger size and higher charge, likely result in changes in biodistribution to Kupffer cells that decreases the amount of DNA polyplex available for HS expression. Loss in expression under HD may indicate that D peptides have a lessened ability to release DNA as well (Figure 2-7B).

Extending the time delay by which HS expression leads to maximal expression is important toward achieving targeted delivery of polyplexes and expression in tissues outside the liver. The shedding of PEGylated peptides from pGL3 polyplexes results in rapid deactivation of the DNA due to the action of DNase in the blood and liver. This is evident with PEGylated Cys-Trp-Lys_{18} (**R1**), which rapidly dissociates in the circulation. The ability to dramatically extend maximal HS expression to 9 h by administering a decoy dose of pSEAP polyplex (Figures 2-10B and C) provides another important clue as how to improve nonviral gene delivery systems. This may be the result of saturating DNase in the blood [107] or by blocking uptake of the scavenger receptor as has been reported previously [78]. The result also hints that dose-dependency of these polyplexes could improve HS expression profiles and that dramatic changes in pharmacokinetic and biodistribution expression profiles will be obtained by modest increases in pGL3 polyplex dose above 1 μg. It is likely that this is what contributes to a total percentage of dose exceeding 100% when they are added from pharmacokinetic and biodistribution assays because they are performed using different dosages of 3.0 μg and 1.5 μg pGL3, respectively (Table 2-3). Interestingly, the DNase protection afforded to pGL3 by PEGylated polyacridine peptides in blood is not as critical as when dosing polyplexes via local administration, such as intramuscular electroporation [128].

In conclusion, the design of PEGylated polyacridine peptides was significantly improved by increasing the spacing between Acr residues resulting in more efficient gene delivery. Simultaneously, we have demonstrated a process by which non-viral gene delivery systems can be systematically optimized to provide greater circulatory stability *in vivo*. PEGylated polyacridine peptides present a broad template of chemical space, which provides many possible routes for further improvement.

CHAPTER 3: PEG LINKAGE AFFECTS *IN VIVO* STABILITY OF DNA POLYPLEXED WITH PEGYLATED POLYACRIDINE PEPTIDES

Abstract

Polyethylene glycol (PEG) plays an integral role in stabilizing therapeutic particles in the bloodstream by masking surface charge and preventing protein binding and aggregation. In Chapter 2, polyacridine peptide structure was modified to create $(Acr\text{-}Lys_4)_3$-Acr-Lys-Cys-PEG, where a 5 kDa PEG was conjugated to the Cys thiol via maleimide (**SM**). **SM** formed polyplexes with 1 µg pGL3 that stably circulated for up to 5 h as demonstrated by maximal hydrodynamically-stimulated (HS) gene expression *in vivo*. In an effort to further improve circulatory stability of this peptide, the influence of the type of PEG linkage to polyacridine peptides on circulatory stability of PEGylated polyacridine peptide polyplexes was examined and is reported here in Chapter 3. In addition to **SM,** 5 kDa PEG was conjugated to $(Acr\text{-}Lys_4)_3$-Acr-Lys-Cys via disulfide (**SS**), vinyl sulfone (**SV**), and acetamide (**SA**). $(Acr\text{-}Lys_4)_3$-Acr-Lys-Pen was also synthesized and conjugated to 5kDa PEG via disulfide (**PS**) and maleimide (**PM**). Pharmacokinetics established that there was rapid metabolism of **SV** and **SA** polyplexes, which coincidentally resulted in complete loss of HS expression by 5 h. Polyplexes formed with **PS**, **PM,** and **SM** were found to be the most stable in this series with maximal HS expression profiles up to 5 h. The results presented indicate the importance of PEG linkage chemistry in the development of PEGylated gene delivery carriers for systemic administration *in vivo*.

Introduction

The addition of polyethylene glycol (PEG) to a non-viral gene delivery system is considered essential in order to improve blood compatibility of DNA polyplexes [76, 77]. Without PEGylation, upon i.v. administration the cationic surface of most polyplexes

binds albumin and other serum proteins causing a rapid increase in particle size and entrapment in the capillary bed of the lung [10, 11]. In the absence of PEGylation, anionic polyplexes and plasmid DNA are rapidly removed from the circulation by liver Kupffer cells via the scavenger receptor [78, 79].

The cross-linking of residual amines with glutaraldehyde was previously used to stabilize PEGylated DNA polyplexes from dissociation in the circulation [8]. Likewise, *N*-(2-hydroxypropyl)methacrylamide (HPMA) was used previously to cross-link amines on the surface of polyplexes resulting in laterally stabilized DNA nanoparticles that possessed a long circulatory half-life [129]. However, both of these approaches resulted in polyplexes that failed to mediate appreciable gene expression *in vivo*, presumably due in part to their inability to release DNA inside the cell [130, 131].

As described in Chapter 2, we have previously reported on the unique attributes of PEGylated polyacridine peptides that bind to DNA to form polyplexes, overcoming the limitations of other strategies by providing a long circulatory half-life, and demonstrate *in vivo* activity. In prior studies, the properties of the peptide portion of PEGylated polyacridine peptides were first optimized to achieve efficient *in vivo* gene expression following a delayed hydrodynamically stimulated (HS) dose of saline after i.v. administration of the polyplex [9]. Short PEGylated polyacridine peptides of the general structure $(\text{Acr-Lys})_{n=2,4,6}$-Cys, where Acr is a Lys residue modified on its ε-amine with acridine, were found to bind pGL3 with high affinity through a combination of polyintercalation and ionic interaction. PEGylation of the C-terminal Cys residue resulted in PEGylated polyacridine peptides that bind to pGL3 to form polyplexes that are fully stable in the circulation for up to 1 h [9]. Further optimization of the peptide sequence revealed that four Acr residues spaced by four Lys residues, $(\text{Acr-Lys}_4)_3$-Acr-Lys-Cys-PEG, dramatically increased the stability of a 1 μg i.v. dose of pGL3 polyplex in the circulation for 5 h [15].

These studies used one reliable form of thiol modification – a thioether conjugation via Michael addition to a maleimide. While it is well-documented that maleimides and the resulting thiol-bound succinimide can undergo hydrolysis at physiological pH, this decreases the efficiency of the conjugation and would not sever the moiety bound to the thiol [132]. However, recent literature suggests that maleimide conjugation is reversible in the presence of reducing equivalents like glutathione (GSH), which are present in hepatocytes and to a lesser extent in the bloodstream [132, 133]. As PEG is a vital component that endows *in vivo* suitability to polyacridine polyplexes, it was important to determine if stability of the linkage that bound PEG to polyacridine peptides was unstable *in vivo*. Simultaneously, it was desirable to investigate if another route for thiol modification could improve the ability of PEGylated polyacridine peptides to stabilize circulating, polyplexed DNA *in vivo*.

The influence of PEG linkage on DNA polyplex pharmacokinetics (PK), biodistribution, and gene expression *in vivo* is examined herein. Using the optimal peptide, $(Acr\text{-}Lys_4)_3$-Acr-Lys-Cys, from a previous study reported in Chapter 2 [15], a 5 kDa PEG was linked to the C-terminal Cys using four different chemical linkages which included thiol-maleimide (**SM**), thiol-thiol (**SS**), thiol-acetamide (**SA**), and thiol-vinyl sulfone (**SV**). $(Acr\text{-}Lys_4)_3$-Acr-Lys-Pen was also synthesized to conjugate PEG via penicillamine-thiol-thiol (**PS**) and penicillamine-thiol-maleimide (**PM)**.

The results were surprising in that linkages anticipated to be most stable (**SA, SV**) were found to result in short PK half-lives and rapid loss of HS gene expression. Interestingly, linkages expected to be metabolically less stable (**SS, PS**) proved to be more stable than **SA** and **SV**, resulting in longer PK half-lives and extended HS expression profiles. The results address the importance of parameters regarding the attachment of PEG to DNA polyplexes that improve the performance of i.v. dosed non-viral gene delivery systems in mice. The contents of this chapter are previously reported by Khargharia et al [134].

Materials and Methods

Unsubstituted Wang resin, 9-hydroxybenzotriazole, Fmoc-protected amino acids, O-(7-Azabenzo-triazol-1-yl)-*N,N,N′,N′*-tetramethyluronium hexafluorophosphate (HATU), Fmoc-Lysine-OH, *N*-methyl-2-pyrrolidone (NMP), FMOC-Penicillamine(trityl)-Wang (FMOC-Pen) were obtained from AAPPTec (Louisville, KY, USA). *N,N*-dimethylformamide (DMF), trifluoroacetic acid (TFA) and acetonitrile were purchased from Fisher Scientific (Pittsburgh, PA, USA). Diisopropylethylamine, piperidine, acetic anhydride, Tris(2-carboxyethyl)-phosphine hydrochloride (TCEP), 9-chloroacridine, thiazole orange, *N*-hydroxysuccinimide (NHS), iodoacetic acid and dicyclocarbodiimide (DCC) were obtained from Sigma Chemical Co. (St Louis, MO, USA). Agarose was obtained from Gibco-BRL (Carlsbad, CA, USA). $mPEG_{5kDa}$-maleimide, $mPEG_{5kDa}$-amine, $mPEG_{5kDa}$-S-2-sulfanylpyridine were purchased from Laysan Bio (Arab, AL, USA), and $mPEG_{5kDa}$-vinylsulfone was acquired from Jenkem Technologies (Beijing, China). D-Luciferin and luciferase from *Photinus pyralis* were obtained from Roche Applied Science (Indianapolis, IN, USA). pGL3 control vector, a 5.3-kbp luciferase plasmid containing a SV40 promoter and enhancer, was obtained from Promega (Madison, WI, USA). pGL3 was amplified in a DH5α strain of Escherichia coli and purified according to the manufacturer's instructions.

Synthesis and Characterization of Polyacridine Peptides

9-Phenoxyacridine and Fmoc-Lysine(Acr)-OH were prepared as recently reported [114, 115]. Polyacridine peptides were prepared by solid phase peptide synthesis on a 30 μmol scale using an APEX 396 synthesizer (Advanced ChemTech, Louisville, KY, USA) with standard Fmoc procedures. The reaction yields were improved by activating amino acids with 9-hydroxybenzotriazole and HATU while using double coupling of Fmoc-Lys(Acr)-OH and triple coupling for the spacing amino acid, using a five-fold excess of amino acid over resin. Peptides were removed from resin and deprotected using a

cleavage cocktail of TFA/ethanedithiol/water (93:4:3 v/v/v) for 3 h followed by precipitation in cold ether. Precipitates were centrifuged at 5000 × *g* and 4 °C for 10 min and the supernatant decanted. Peptides were then reconstituted with 0.1 v/v % TFA and purified to homogeneity on reversed phase-high pressure liquid chromatography (RP-HPLC) by injecting 0.5–2 μmol onto a Vydac C18 (Grace Davison Discovery Sciences, Deerfield, IL, USA) semi-preparative column (2 × 25 cm) eluted at 10 ml min^{-1} with 0.1 v/v % TFA with an acetonitrile gradient of 15–25 v/v % over 30 min while monitoring acridine at 409 nm. The major peak was collected and pooled from multiple runs, concentrated by rotary evaporation, lyophilized and stored at −20 °C. Purified peptides were reconstituted in 0.1 v/v % TFA and quantified by absorbance (acridine $\varepsilon_{409\,nm}$=9266 M^{-1} cm^{-1} assuming additivity of ε for multiple acridines) to determine isolated yield. Purified peptides were characterized by LC-MS by injecting 2 nmol onto a Vydac C18 analytical column (0.47 × 25 cm) eluted at 1 ml min^{-1} with 0.1 v/v % TFA and an acetonitrile gradient of 15–45 v/v % over 30 min while acquiring electrospray ionization mass spectrometry (ESI-MS) in the positive mode.

Synthesis and Characterization of PEGylated Polyacridine Peptides

PEGylation of the Cys/Pen residue on $(Acr\text{-}Lys_4)_3$-Acr-Lys-Cys/Pen was achieved by reacting 1 μmol of peptide with 1.1 μmol of PEG_{5kDa}-maleimide in 4 ml of 100 mM 4-(2-hydroxyethyl)-1-piperazineethanesulfonic acid (HEPES) buffer pH 7 for 12 h at room temperature. The same conditions were applied to reactions of $(Acr\text{-}Lys_4)_3$-Acr-Lys-Cys/Pen with $mPEG_{5kDa}$-S-2-sulfanylpyridine to form $(Acr\text{-}Lys_4)_3$-Acr-Lys-Cys-SS-PEG_{5kDa} and $(Acr\text{-}Lys_4)_3$-Acr-Lys-Pen-SS-PEG_{5kDa}. Reaction of 1 μmol $(Acr\text{-}Lys_4)_3$-Acr-Lys-Cys with 10 μmol PEG_{5kDa}-vinylsulfone in 100 mM HEPES pH 7.5 generated $(Acr\text{-}Lys_4)_3$-Acr-Lys-Cys-SV-PEG_{5kDa}.

PEG_{5kDa}-iodoacetamide was synthesized by derivatization of PEG_{5kDa}-amine with NHS-iodoacetic acid. PEG_{5kDa}-amine (5 µmol) was reacted with 50 µmol NHS-iodoacetic acid in 5ml 100 mM ammonium bicarbonate pH 8.0 for 5 hrs. The product was isolated by size exclusion chromatography using Sephadex G10 (2.5 x 50 cm) eluted with 0.1% v/v TFA by collecting the peak eluting at 100 ml, which was concentrated by rotary evaporation, freeze dried, reconstituted in water and quantified by absorbance of iodoacetamide ($\varepsilon_{280nm} = 370\ M^{-1}\ cm^{-1}$) [135]. The product was analyzed by RP-HPLC with 0.1% v/v TFA and an acetonitrile gradient of 15-65% v/v monitoring Abs_{280nm}. Reaction of 5 µmol PEG_{5kDa}-iodoacetamide with 1 µmol $(Acr\text{-}Lys_4)_3$-Acr-Lys-Cys in 100 mM ammonium bicarbonate pH 8.0 resulted in formation of $(Acr\text{-}Lys_4)_3$-Acr-Lys-Cys-SA-PEG_{5kDa}.

PEGylated peptides were purified by semi-preparative RP-HPLC eluted with 0.1% v/v TFA with an acetonitrile gradient of 20–60% v/v acetonitrile while monitoring acridine at 409 nm. The major peak was collected and pooled from multiple runs, concentrated by rotary evaporation, lyophilized and stored at −20 °C. The counter ion was exchanged by chromatography on a G-25 column (2.5 × 50 cm) equilibrated with 0.1 v/v % acetic acid to obtain the peptide in an acetate salt form. The major peak corresponding to the PEG peptide eluted in the void volume (100 ml) was pooled, concentrated by rotary evaporation and lyophilized. PEG peptides were reconstituted in water and quantified by Abs_{409nm} (each acridine $\varepsilon_{409\,nm}=9266\ M^{-1}\ cm^{-1}$) to determine isolated yield. PEG peptides were characterized by matrix-assisted laser desorption/ionization-time of flight (MALDI-TOF) mass spectrometry by combining 1 nmol with 10 µl of 2 mg ml^{-1} α-cyano-4-hydroxycinnamic acid in 50% v/v acetonitrile and 0.1% v/v TFA. Samples were spotted onto the target and ionized on a Bruker Biflex III Mass Spectrometer (Bruker Daltonics Inc., Billerica, MA, USA) operated in the positive ion mode.

Formulation and Characterization of PEGylated Polyacridine Peptide Polyplexes

The relative binding affinity of PEGylated polyacridine peptides for pGL3 was determined by a fluorophore exclusion assay [18]. pGL3 (200 µl of 5 µg ml^{-1} in 5 mM HEPES pH 7.5 containing 0.1 µM thiazole orange) was combined with 0, 0.05, 0.1, 0.13, 0.15, 0.18, 0.2, 0.25, 0.3, 0.4, or 0.5 nmol of PEGylated polyacridine peptide in 300 µl of HEPES and allowed to bind at room temperature for 30 min. Thiazole orange fluorescence was measured using an LS50B fluorometer (Perkin-Elmer, Cambridge, UK) by exciting at 498 nm while monitoring emission at 546 nm with the slit widths set at 10 nm. A fluorescence blank of thiazole orange in the absence of pGL3 was subtracted from all values before data analysis.

The particle size and zeta potential were determined by preparing 2 ml of polyplex in 5 mM HEPES pH 7.5 at a pGL3 concentration of 30 µg ml^{-1} and a PEGylated polyacridine peptide stoichiometry of 0.8 nmol μg^{-1} of pGL3. The particle size was measured by quasi-elastic light scattering at a scatter angle of 90° on a Brookhaven ZetaPlus Particle Sizer (Brookhaven Instruments Corporation, Holtsville, NY, USA). The zeta potential was determined as the mean of 10 measurements immediately following acquisition of the particle size.

Pharmacokinetic Analysis of PEGylated Polyacridine Polyplexes (In collaboration with Sanjib Khargharia)

Radioiodinated pGL3 was prepared as previously described [116]. Triplicate mice were anesthetized by intraperitoneal injection of ketamine hydrochloride (100 mg kg^{-1}) and xylazine hydrochloride (10 mg kg^{-1}) and underwent a dual cannulation of the right and left jugular veins. An i.v. dose of ^{125}I-pGL3 (3 µg, 1.2 µCi in 50 µl of HEPES-buffered mannitol (5 mM HEPES, 0.27 M mannitol pH 7.4)) or ^{125}I-pGL3 polyplex (3 µg) was administered via the left catheter. Blood samples (10 µl) were drawn from the right

catheter at 1, 3, 6, 10, 20, 30, 60, 90 and 120 min and immediately frozen. The volumes withdrawn were replaced with 10 µl of normal saline. The amount of radioactivity in the blood samples at each time point was quantified by direct γ-counting. Blood samples were digested with proteinase K for 12 h and polyplexes were extracted with 500 µl of phenol/chloroform/isoamyl alcohol (24:25:1) to remove PEGylated peptides followed by precipitation of DNA with the addition of 1 ml of ethanol [8, 9]. The precipitate was collected by centrifugation at 13 000 × *g* for 10 min, and the DNA pellet was dried and dissolved in 5 mM HEPES buffer pH 7.4. DNA samples were combined with 2 µl of loading buffer and applied to a 1% agarose gel (50 ml) and electrophoresed in Tris-borate-EDTA buffer at 70 V for 60 min [51]. The gel was dried on a zeta probe membrane and autoradiographed on a Phosphor Imager (Molecular Devices, Sunnyvale, CA, USA) following a 15 h exposure.

Biodistribution Analysis of PEGylated Polyacridine Polyplexes (In collaboration with Sanjib Khargharia)

^{125}I-pGL3 (1.5 µg in 50 µl of HEPES-buffered mannitol, 0.6 µCi) or ^{125}I-pGL3 polyplexes (1.5 µg) were dosed in triplicate mice via tail vein. At times ranging from 5 min to 6 h, mice were anesthetized by intraperitoneal injection of ketamine (100 mg kg^{-1}) and xylazine (10 mg kg^{-1}) and then killed by cervical dislocation. The major organs (liver, lung, spleen, stomach, kidney, heart, large intestine and small intestine) were harvested, rinsed with saline, and the radioactivity in each organ was determined by direct γ-counting and expressed as the percentage of the dose in the organ.

Metabolic Stability of PEGylated Polyacridine Peptides (In collaboration with Sanjib Khargharia)

PEGylated peptides (10 nmols) were incubated with 500 µl of either whole mouse blood containing 2 mg ml^{-1} EDTA, freshly prepared mouse liver or spleen homogenate prepared in 0.25M sucrose [136]. After incubation at 37 ˚C for 4 h, the blood, liver

homogenate and spleen homogenate samples were precipitated by addition of 125 µl 20% v/v TFA/ddH_2O, followed by incubation at 4 ˚C for 30 min and centrifugation at 10,000 x *g* for 30 min. The supernatants containing the PEGylated peptides were analyzed by RP-HPLC eluted at 1 ml min^{-1} with 0.1% v/v TFA and a gradient of 15-60% v/v acetonitrile while detecting Abs_{409nm}. The retention time of PEG-peptide digests were compared to untreated peptide standards and non-PEGylated peptide to determine metabolic status. Esterase activity in spleen and liver homogenates was confirmed by *p*-nitrophenyl acetate (pNPA) assay [137]. Briefly, protein concentrations of freshly prepared homogenates were determined by BCA assay. Solutions of 0.1 M Tris buffer pH 8.0 containing 1.6 mM pNPA were monitored for absorbance of the hydrolysis product, *p*-nitrophenol (ε_{405nm} = 16,240 M^{-1} cm^{-1}) at 20 ˚C for 3 min in 30-sec intervals prior to (non-enzymatic blank) and after addition of 0.1-1 µg ml^{-1} homogenate protein. Activity measurements were corrected using the non-enzymatic blank.

Hydrodynamically Stimulated Expression (In collaboration with Sanjib Khargharia)

Hydrodynamically stimulated (HS) expression was performed by tail vein dosing triplicate mice with 1 µg of pGL3 polyplexes, prepared with 0.8 nmol PEG-peptide per µg pGL3, in 50 µl of HBM. At times ranging from 5 min to 9 h, a HS dose of normal saline (9 wt/v% of the body weight) was administered over 5 sec. At 24 h post-HS, mice were anesthetized by 3% isofluorane, and an intraperitoneal dose of 80 µl (2.4 mg) of D-luciferin (30 µg $µl^{-1}$ in phosphate-buffered saline) was administered. At 5 min following the D-luciferin dose, bioluminescence imaging (BLI) was performed on mice using an IVIS Imaging 200 Series (Xenogen, Hopkins, MA, USA). BLI was performed in a light-tight chamber on a temperature-controlled, adjustable stage while isofluorane was administered by a gas manifold at a flow rate of 3%. Images were acquired at a ‘medium’ binning level and a 24.6-cm field of view with 10 sec acquisition time. The Xenogen

system reported bioluminescence as photons sec^{-1} cm^{-2} sr^{-1} in a 2.86-cm diameter region of interest covering the liver. The integration area was transformed to pmols of luciferase in the liver using a previously reported standard curve [38]. Results were determined to be statistically significant ($p \leq 0.05$) based on a two-tailed unpaired t-test (Dunnett T3 using SPSS 19.0 analysis of variance software).

Results

The development of nonviral gene delivery systems that function *in vivo* requires careful optimization using realistic doses in animal models with reliable gene expression readouts. Optimization of PEGylated polyacridine peptide delivery systems is achieved herein using a standardized tail vein dose of 1 µg of pGL3 in 50 µl in 15-20 g male ICR mice. pGL3 is a standard commercially available 5.3 kbp plasmid expressing luciferase under the control of an SV40 promoter. It has been previously demonstrated that pGL3 is rapidly metabolized by endogenous DNase in the blood resulting in no detectable luciferase expression when delivered i.v. to mice [8, 9, 15]. Alternatively, a rapid (5 sec) hydrodynamic dose (HD) of 1 µg of pGL3 in approximately 1.8 ml of saline via the tail vein in a 20 g mouse results in the bioluminescence imaging (BLI) detection of 10^8 photons $sec^{-1}cm^{-2}steradian^{-1}$ for luciferase in the liver after 24 h [9, 26].

As demonstrated in Chapter 2, the delivery of 1 µg of pGL3 PEGylated polyacridine polyplex to mice via the tail vein in 50 µl also leads to no detectable expression in the liver. However, following polyplex delivery, the administration of a blank (saline only) hydrodynamically-stimulated (HS) dose at times ranging from 5 min to 9 h post-DNA delivery, results in appreciable luciferase expression in the liver. Both the magnitude of expression and the length of the stimulation time window are influenced by the structure of the PEGylated polyacridine peptide [9, 15]. Increasing the affinity of PEGylated polyacridine peptides for DNA results in polyplexes with greater stability in the circulation and a longer stimulation time window [9, 15]. Using an optimized

PEGylated polyacridine peptide polyplex, the magnitude of expression mediated by HS is equivalent to that of HD dosing of 1 µg of pGL3 [9].

In the present study, we examined the influence of PEG linkage by attaching PEG_{5kDa} to $(Acr\text{-}Lys_4)_3$-Acr-Lys-Cys/Pen (Peptides **1** and **2**, Table 3-1) using six unique linkages which included thiol-maleimide (**SM**), thiol-thiol (**SS**), thiol-acetamide (**SA**), thiol-vinyl sulfone (**SV**), penicillamine-thiol-maleimide (**PM**), and penicillamine-thiol-thiol (**PS**) (Figure 3-1, Table 3-1). Note that the thiol in **SV** is covalently bound to an ethylene sulfone linker but was produced via conjugation to a vinyl sulfone moiety. PEGylated polyacridine peptides were prepared by first synthesizing peptides **1** and **2,** which were RP-HPLC purified in approximately 20 % isolated yield and characterized by LC-ESI/MS prior to derivatization with PEG (Table 3-1). Note that **SM** is the same as "peptide **4**" from Chapter 2. For simplification of interpretation, **SM** will be used in this chapter to draw focus to the PEG linkage.

Table 3-1. *Polyacridine Peptide and PEG Linker Series Purified Yields and Masses*

Peptide Designation	**Peptide Sequence**	**% Yield**	**Mass (calc/obs)**
1	$(Acr\text{-}Lys_4)_3$-Acr-Lys-Cys	20	3008.9 / 3008.8[a]
2	$(Acr\text{-}Lys_4)_3$-Acr-Lys-Pen	22	3036.9 / 3036.8[a]
SM	$(Acr\text{-}Lys_4)_3$-Acr-Lys-Cys-Mal-PEG_{5kDa}	77	8909 / 8697[b]
SS	$(Acr\text{-}Lys_4)_3$-Acr-Lys-Cys-SS-PEG_{5kDa}	58	8797 / 8726[b]
PM	$(Acr\text{-}Lys_4)_3$-Acr-Lys-Pen-Mal-PEG_{5kDa}	75	8937 / 8775[b]
PS	$(Acr\text{-}Lys_4)_3$-Acr-Lys-Pen-SS-PEG_{5kDa}	79	8825 / 8749[b]
SV	$(Acr\text{-}Lys_4)_3$-Acr-Lys-Cys-SV-PEG_{5kDa}	26	8709 / 8322[b]
SA	$(Acr\text{-}Lys_4)_3$-Acr-Lys-Cys-Acet-PEG_{5kDa}	86	8409 / 8239[b]
$\mathbf{S_{alk}}$	$(Acr\text{-}Lys_4)_3$-Acr-Lys-Cys-Alk	44	3066.7 / 3066.8[a]

Masses determined by [a]ESI-MS and [b]MALDI-TOF.

SS was anticipated to be an unstable because of the disulfide bond as it has extensively been demonstrated to be readily reduced both *in vitro* and *in vivo*. **SA** and **SV** are thioether bonds that were expected to be as or more stable than the original **SM**, while **PS** and **PM** were expected to be more stable than their respective Cys counterparts, **SS** and **SM**, because of the steric hindrance of the thiol conjugation provided by the geminal dimethyl substitution at the β-carbon [52].

The PEG peptides investigated in this study are described in Figure 3-1 and Table 3-1. Monofunctionalized PEGs with a terminal maleimide, S-2-sulfanylpyridine, vinyl sulfone, or amine were selected based on their commercial availability. A maleimide-PEG_{5kDa} was reacted with the C-terminal Cys or Pen on peptides **1** and **2** to produce PEG-peptides **SM** and **PM,** respectively. An S-2-sulfanylpyridine-PEG_{5kDa} was reacted with a C-terminal Cys or Pen to produce PEG peptides **SS** and **PS**. A vinyl sulfone PEG_{5kDa} was reacted with the C-terminal of Cys to produce **SV**. Conversion of an amino-PEG_{5kDa} to an iodoacetamide, followed by reaction with a C-terminal Cys produced **SA**. In addition, a control non-PEGylated polyacridine peptide was prepared by alkylating the Cys on peptide **1** to form $\mathbf{S_{alk}}$ using iodoacetate.

PEG-peptides **SM**, **PM**, **SS**, **PS**, **SV**, **SA** and $\mathbf{S_{alk}}$ were isolated using preparative RP-HPLC in yields ranging from 26-79 % based on peptides **1** and **2**. MALDI-TOF MS analysis of PEGylated polyacridine peptides resulted in observed masses ranging from 8239-8775 Da. The difference between the calculated and observed mass is related to PEG polydispersity in the commercially available functionalized PEGs as was mentioned in chapter 2. The ability of PEGylated polyacridine peptides to bind pGL3 was evaluated using a thiazole orange dye exclusion assay [18]. The results established that each PEG-peptide completely displaced the fluorophore at a stoichiometry of 0.15 nmol μg^{-1} of pGL3, suggesting that the identity of the linker joining PEG to the peptide did not influence DNA binding affinity (Figure 3-2).

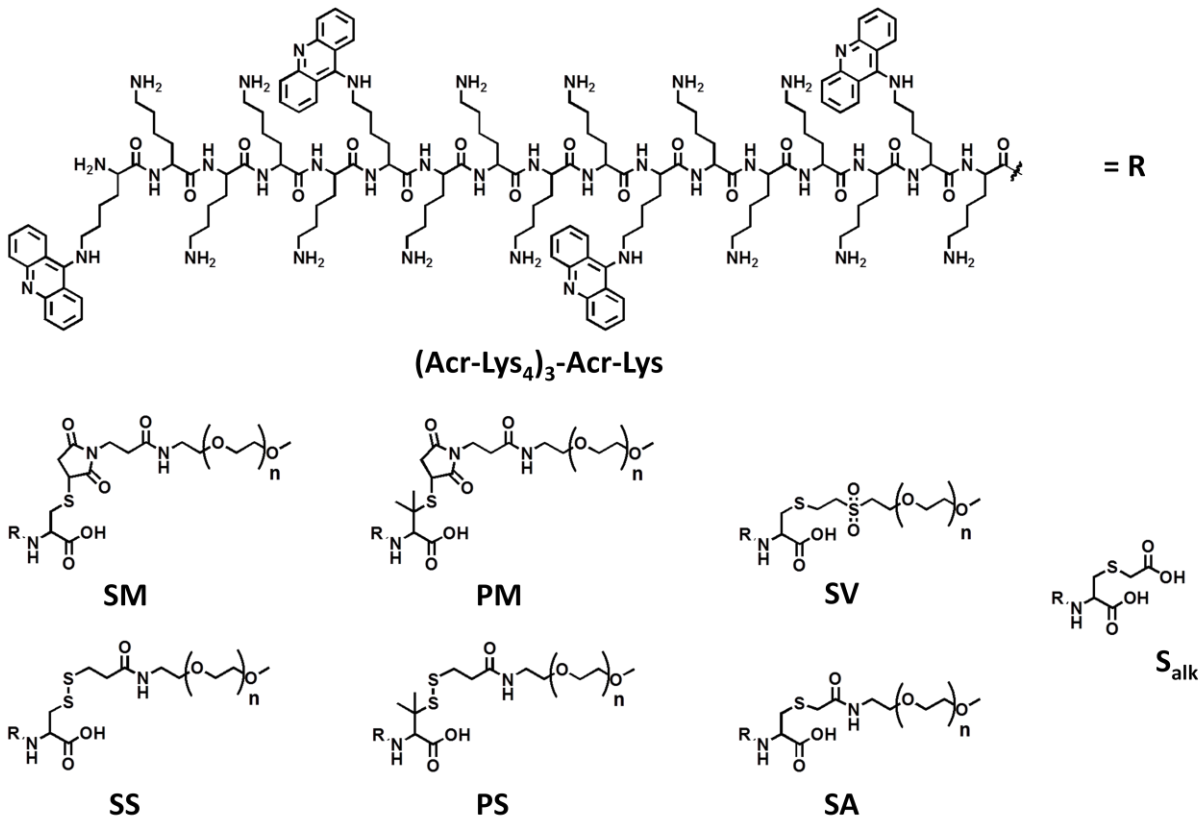

Figure 3-1. *The Structures of the PEG Linker Series of Polyacridine Peptides*. The thiols of peptides **1** and **2** were reacted with various 5 kDa PEGs to generate thiol-maleimide (**SM**), thiol-thiol (**SS**), penicillamine-maleimide (**PM**), penicillamine-thiol (**PS**), thiol-vinyl sulfone (**SV**), and thiol-acetamide (**SA**). $\mathbf{S_{alk}}$ was synthesized by alkylation of peptide **1** with iodoacetic acid. *R* is the sequence $(Acr\text{-}Lys_4)_3$-Acr-Lys bound at the C-terminus of Lys.

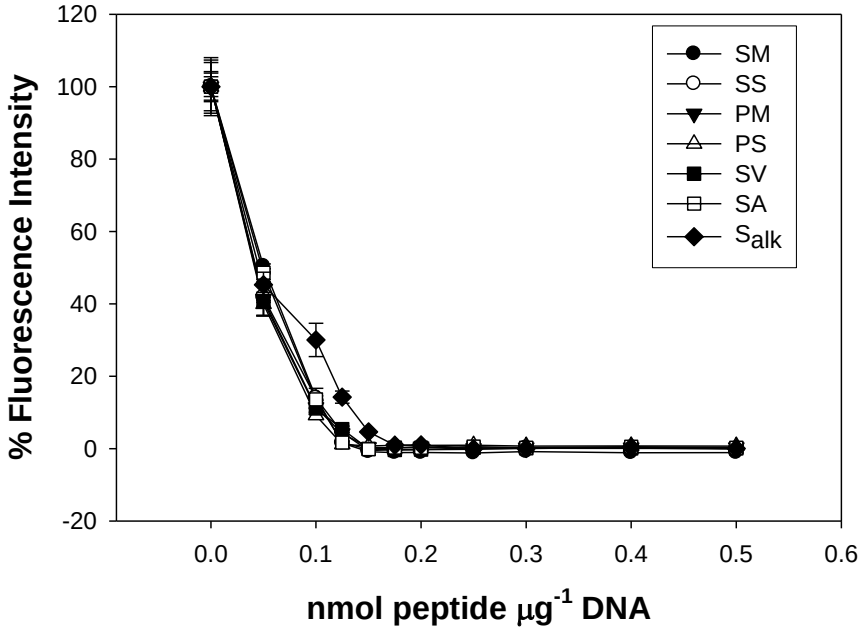

Figure 3-2. *Relative Binding Affinity of PEG Linker Series of Polyacridine Peptides.* Peptides **SM, SS, PM, PS, SV, SA,** and **S_{alk}** were evaluated for their relative binding affinities for pGL3 by thiazole orange displacement assay. The results indicate that PEG linker changes do not affect the affinity of the peptide for DNA. Results are the mean and standard deviation of triplicate determinations.

As was previously shown in chapter 2, PEGylated polyacridine peptides form DNase stable electronegative polyplexes at a stoichiometry of 0.2 nmol μg^{-1} of pGL3, but that further addition of PEG-peptide results in more fully condensed electropositive DNase stable polyplexes at 0.8 nmols of peptide μg^{-1} of pGL3 (Figure 2-1) [9]. While both electronegative and electropositive polyplexes are able to mediate gene expression *in vivo* following hydrodynamic stimulation, electropositive polyplexes are more tightly condensed and protect pGL3 from DNAse in the circulation for a longer time [15].

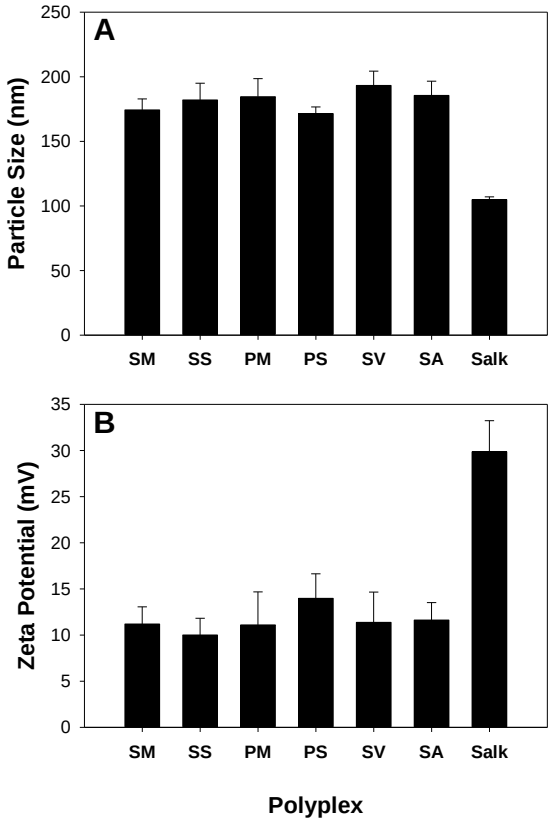

Figure 3-3. *Size and Surface Charge of the PEG Linker Series of Polyacridine Peptide Polyplexes*. QELS was used to determine the particle size and zeta potential of PEG peptide polyplexes prepared at 0.8 nmol μg^{-1} pGL3 at a concentration of 30 $\mu g\ ml^{-1}$. All PEG peptides (**SM, SS, PM, PS, SV,** and **SA**) produce polyplexes with similar size (170-200 nm) and charge (+10-15 mV). $\mathbf{S_{alk}}$ (peptide without PEG) produces smaller particles (105 nm) with a zeta potential of +30 mV. The results are the mean and standard deviation of multiple determinations.

For this reason, the relative particle size and zeta potential were compared for polyplexes prepared at a standard stoichiometry 0.8 nmols of peptide μg^{-1} of pGL3 (Figure 3-3). This stoichiometry was also used for all pharmacokinetics, biodistribution and *in vivo* expression experiments. Polyplexes prepared with **PM**, **SM**, **PS**, **SS**, **SV** and **SA** possessed a mean diameter of 170-200 nm whereas polyplexes prepared with $\mathbf{S_{alk}}$ were determined to be smaller, with a diameter of 105 nm (Figure 3-3A). The zeta potential of polyplexes prepared with **PM**, **SM**, **PS**, **SS**, **SV** and **SA** ranged from +10-14

mV and was independent of PEG-linkage (Fig. 3-3B). In contrast, polyplexes prepared with $\mathbf{S_{alk}}$ produced zeta potentials of +30 mV.

The ability of **PM**, **SM**, **PS**, **SS**, **SV**, and **SA** polyplexes to mediate stimulated gene expression as a function of circulation time was compared (Figure 3-4). The results revealed that **PM**, **SM** and **PS** each produced maximal gene expression of $\geq 10^8$ photons $sec^{-1}cm^{-2}sr^{-1}$ when applying HS at times up to 4-5 h post DNA polyplex delivery (Figure 3-4). The stimulated expression profiles from time zero to 4-5 h were stable suggesting the polyplexes were stable in the circulation, followed by a steady decay in expression to background when applying HS at times ranging from 5-9 h. The loss of gene expression at stimulation times greater than 5 h is most likely the result of peptide shedding and exposing polyplexes to DNAse in the circulation as described in chapter 2 [15]. The **SS** PEG-peptide polyplex demonstrated maximal expression of 10^8 photons $sec^{-1}cm^{-2}ser^{-1}$ at stimulation times up to 2 h, followed by a decay to zero at stimulation times of 2-5 h (Figure 3-4). Surprisingly, **SA** and **SV** each produced ten-fold lower expression at 1 h relative to **PM**, **SM**, **PS** and **SS**, suggesting a decreased stability. The expression profile for **SA** revealed expression of 10^7 photons $sec^{-1}cm^{-2}sr^{-1}$ when applying HS at times ranging from 1 to 3 h post-polyplex delivery, followed by a decay to background at 3-5 h (Figure 3-4). By comparison, **SV** PEG-peptide polyplexes only achieved 10^7 photons $sec^{-1}cm^{-2}ser^{-1}$ after stimulation times of 1 hr followed by a decay in expression to background at stimulation times of 2 h (Fig. 3-4).

The unexpected rapid loss of HS gene expression for **SV** and **SA** PEG-peptide polyplexes was in part explained by the rapid loss of pGL3 polyplexes from the blood. PK analysis revealed a much shorter α half-life for **SA** and **SV** polyplexes relative to **PM**, **PS** and **SS** (Figure 3-5, Table 3-2). The short α half-life is similar to that determined for naked pGL3 which is rapidly acted upon by DNase in the circulation (Figure 3-5) [9, 15]. In contrast, the longer α half-life of **PM**, **PS** and **SS** polyplexes correlated with their greater stability in the circulation and their extended stimulated expression (Figure 3-4

and 3-5). Gel electrophoretic and autoradiographic analysis of blood time points confirmed that **SV** and **SA** polyplexes were also rapidly degraded (Figure 3-6C and D).

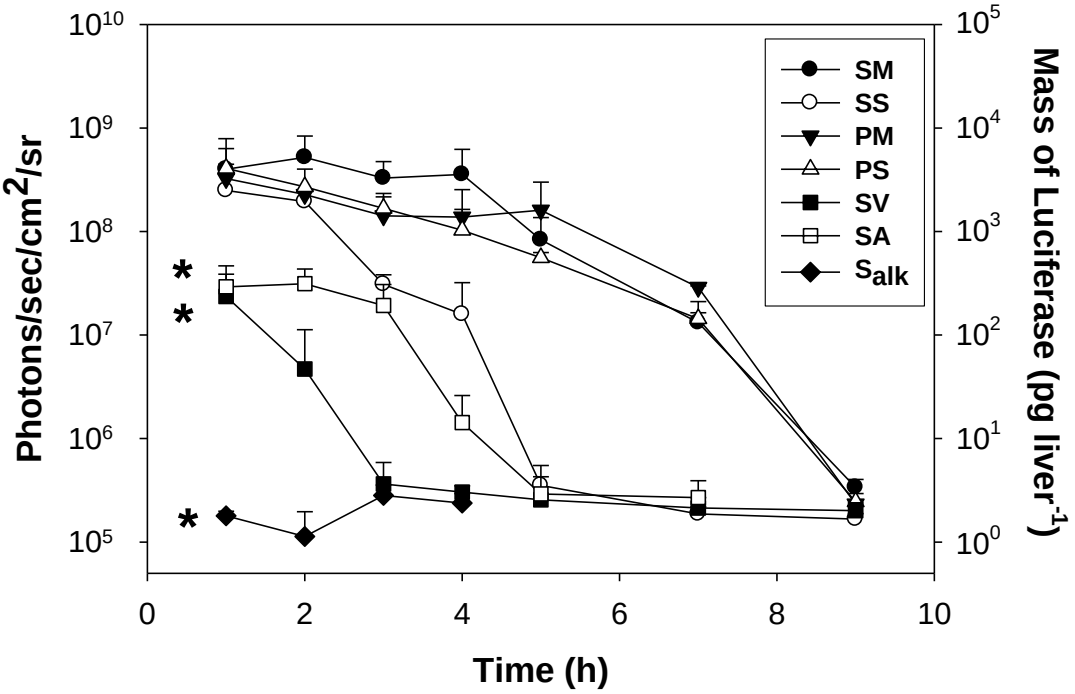

Figure 3-4. *Hydrodynamically-Stimulated (HS) Gene Expression of PEG Linker Series Polyacridine Peptide Polyplexes. In vivo* gene expression in mice was determined using HS at times of 1 to 9 h using 1 µg pGL3 polyplexed with 0.8 nmol of **SM, SS, PM, PS, SV, SA,** or $\mathbf{S_{alk}}$. Luciferase expression was determined 24 h after stimulation. **SV** and **SA** exhibit low expression at early time points followed by a rapid decline to background. Without PEG, $\mathbf{S_{alk}}$ is unable to stimulate any expression as early as 1 h. Results are the mean and standard deviation of triplicate determinations. Asterisks indicate statistical significance of $p \leq 0.05$ when compared to **SM** at 1 h.

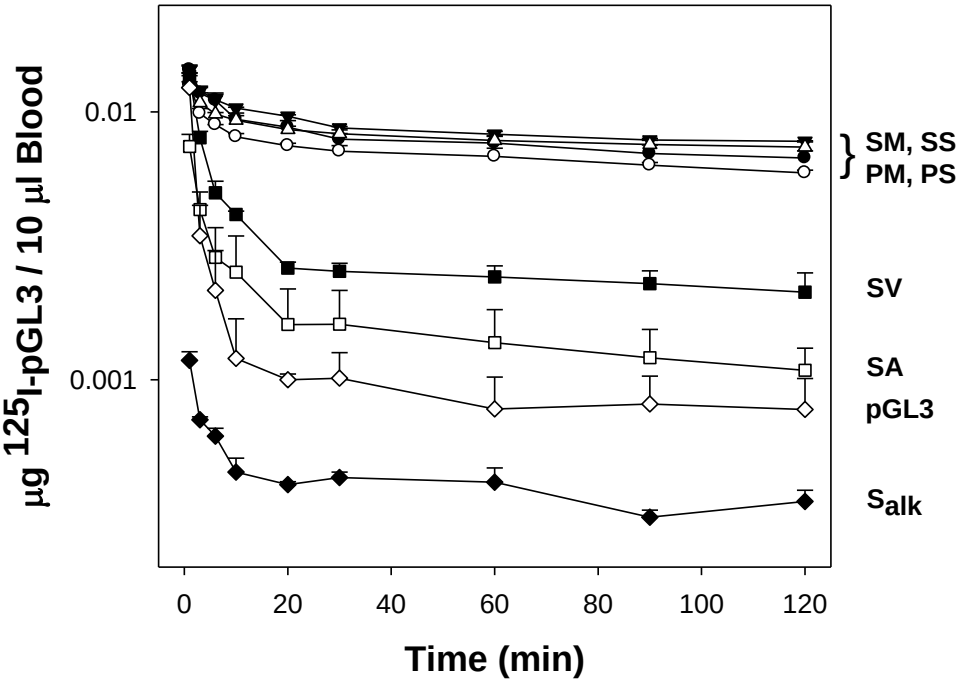

Figure 3-5. *Pharmacokinetic Analysis of PEG Linker Polyacridine Peptide Polyplexes.* ^{125}I-pGL3 was polyplexed and dosed with peptides at 0.8 nmol µg^{-1} pGL3 or dosed without peptide in mice. The concentration in the blood is reported as a function of time. Without PEG (**S$_{alk}$**), polyplexes are rapidly cleared from the blood to a greater extent than pGL3 alone. **SV** and **SA** exhibit greater clearance than all other PEGylated formulations. The results are the mean and standard deviation of triplicate determinations.

The stability of PEG-peptides was examined via incubation in whole mouse blood or liver and spleen homogenates and extraction at low pH. No detectable metabolism of PEGylated peptides **PM, SM, SV** and **SA** was observed when analyzing blood or tissue homogenate digests of polyplexes *in vitro* by RP-HPLC (data not shown). The only metabolically sensitive PEG-peptides were **SS** and **PS** which underwent partial reduction of the disulfide in liver (Figure 3-7) and spleen homogenate, presumably due to reduction by glutathione. One of the byproducts of **SS** incubation in liver homogenate identified by LC-ESI/MS possessed a mass consistent with glutathione conjugation to peptide **1** (Figure 3-7D).

Table 3-2. *Pharmacokinetics of PEG Linker Polyacridine Peptide Polyplexes*[a]

Polyplex	$t_{1/2}\alpha$[b] (min^{-1})	$t_{1/2}\beta$[c] (min^{-1})	V_d[d] (ml)	Cl[e] (ml min^{-1})	MRT[f] (min)	AUC[g] (µg*min ml^{-1})
SM/^{125}I-DNA	4.1 ± 2.2	374 ± 44	159 ± 9	0.3 ± 0.0	540 ± 62	507 ± 43
SS/^{125}I-DNA	2.9 ± 0.2	311 ± 21	193 ± 8	0.4 ± 0.1	446 ± 31	349 ± 9
PM/^{125}I-DNA	4.2 ± 0.3	365 ± 46	154 ± 4	0.3 ± 0.0	527 ± 66	513 ± 53
PS/^{125}I-DNA	3.5 ± 0.3	410 ± 24	170 ± 5	0.3 ± 0.1	589 ± 35	522 ± 30
SV/^{125}I-DNA	2.8 ± 0.4	254 ± 46	494 ± 73	1.4 ± 0.3	352 ± 67	112 ± 19
SA/^{125}I-DNA	2.7 ± 0.4	180 ± 50	694 ± 87	3.2 ± 0.1	245 ± 70	47 ± 2

[a]Calculated using blood cpm values over 120 min and assuming complete DNA stability.

[b]Calculated α-half-life.

[c]Calculated β-half-life.

[d]Volume of distribution.

[e]Total body clearance rate.

[f]Mean residence time.

[g]Area under the curve.

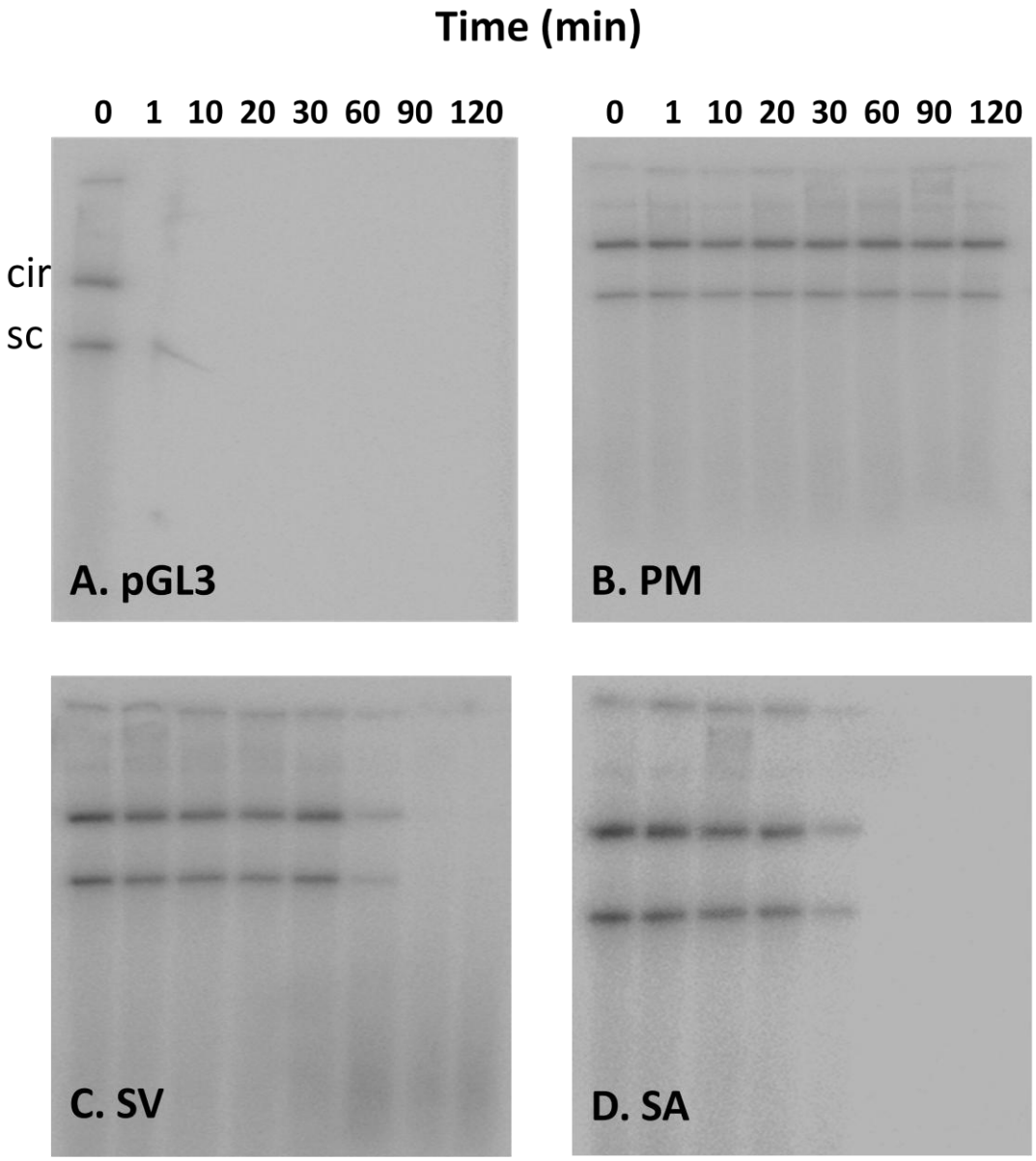

Figure 3-6. *Circulatory Stability of DNA and Polyacridine Polyplexes.* Blood samples of the pharmacokinetic analysis (Figure 3-5) are illustrated here after extraction of ^{125}I-pGL3, agarose gel electrophoresis, and imaging by autoradiography. Unmetabolized pGL3 is indicated by the presence of supercoiled (sc) and circular (cir) bands corresponding with the control at 0 min. Panel A shows pGL3, which is rapidly degraded as early as 1 min. Panel B shows pGL3 extracted from a fully stable polyplex, **PM**. Panels C and D confirm instability of pGL3 in polyplexes with **SV** and **SA** exhibiting degradation as early as 60 min and 30 min, respectively.

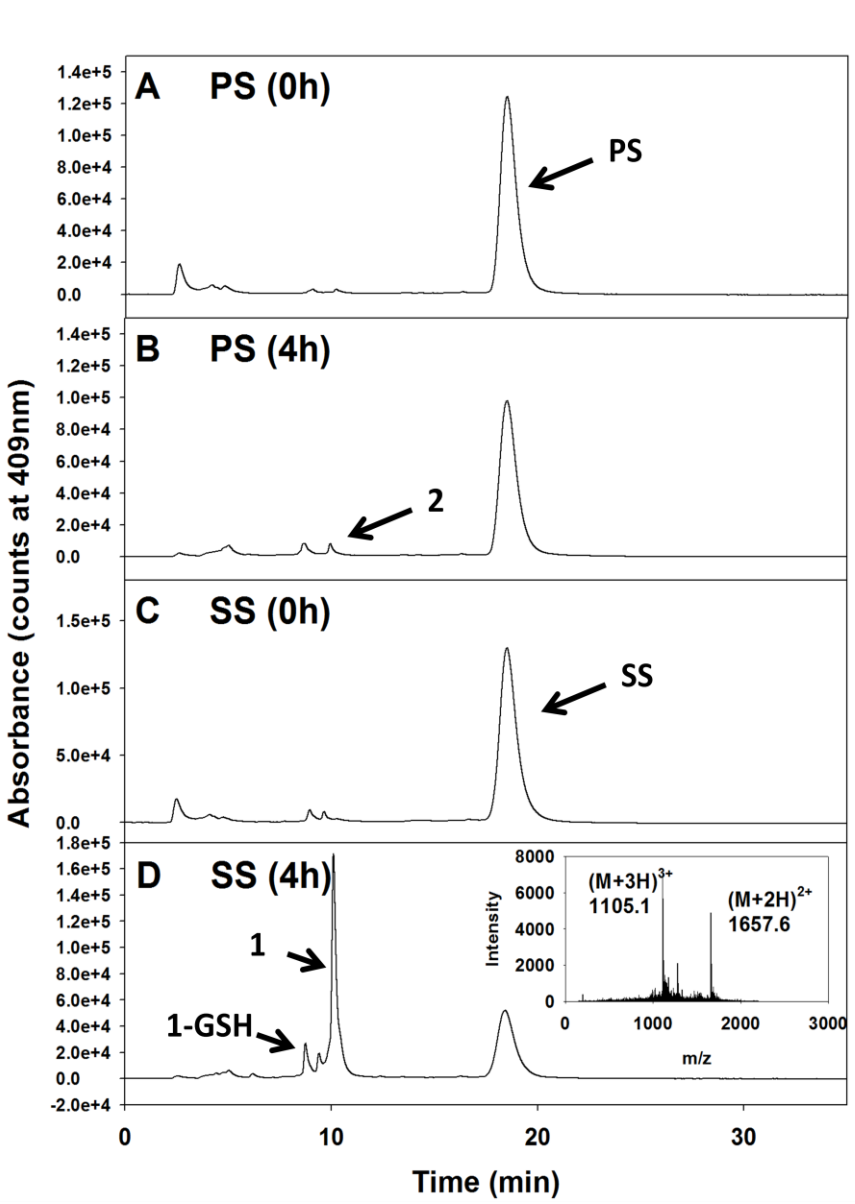

Figure 3-7. *Liver Stability of PEG Linker Polyacridine Peptide Series.* PEG Linker peptides were incubated in mouse liver homogenate for 4 h at 37 ˚C to determine if linkers were unstable. Samples were extracted via addition of 20 v/v % TFA and centrifugation at 4 ˚C, and the supernatant was analyzed by RP-HPLC with 0.1 v/v % TFA and acetonitrile gradient of 15-60 v/v % while detecting 409 nm absorbance. Labeled peaks in chromatograms B and D were confirmed by LC-ESI/MS. **PS** exhibited minor PEG release indicated by the detection of peptide **2** in chromatogram B (4 h incubation) versus A (liver homogenate extraction, no incubation). **SS** released a substantial amount of PEG (~60%) as a result of reducibility in the presence of glutathione (GSH) as indicated in chromatograms C and D, extractions of 0 h and 4 h incubations respectively. Peptide **1** bound to GSH (**1-GSH,** Chromatogram D Inset) was identified by m/z's consistent with the conjugate's mass (3314.2 Da).

In order to confirm the processing of spleen and liver homogenates did not affect enzyme activity, an esterase activity assay was performed using *p*-nitrophenyl acetate (p-NPA) assay. Bicinchoninic acid assay (BCA) was used to determine protein concentration of homogenates. Both spleen and liver homogenate exhibited esterase activity as demonstrated by the increase in the rate of hydrolysis of p-NPA to p-nitrophenol monitored by absorbance at 405 nm compared to blank and heat-treated homogenates (Figure 3-8) [137].

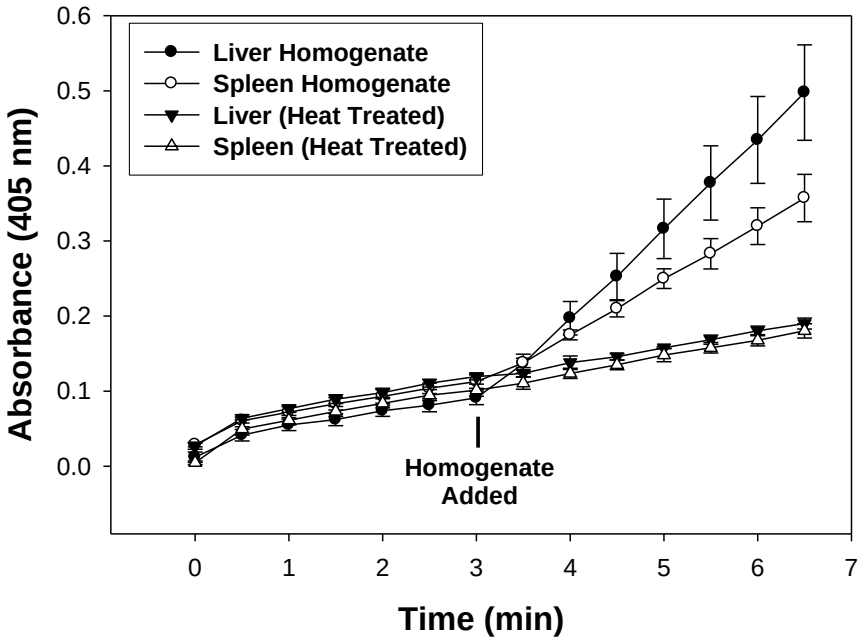

Figure 3-8. *Esterase Activity of Liver and Spleen Homogenates.* Liver and spleen homogenate were tested using *p*-nitrophenyl acetate assay (pNPA) and monitoring its hydrolysis to *p*-nitrophenol via absorbance at 405 nm [137]. BCA assay was used to determine protein concentration of homogenates. The first 3 min the hydrolytic rate of pNPA in assay media was monitored followed by the addition of homogenate and monitoring an additional 3.5 min. Heat-treated homogenate exhibited no increase in hydrolysis rate of pNPA upon addition.

The fundamental importance of PEG to protect polyplexes from protein binding, Kupffer cell recognition in the liver, uptake in the spleen, or entrapment in the lung *in vivo* can be ascertained by analysis of the pharmacokinetics, biodistribution and stimulated expression for $\mathbf{S_{alk}}$ polyplexes. The complete loss of stimulated gene expression (Figure 3-4) is directly correlated with rapid and nearly complete loss of $\mathbf{S_{alk}}$ polyplexes from the blood as revealed by PK analysis (Figure 3-5). The biodistribution properties of $\mathbf{S_{alk}}$ polyplexes are distinctive in their immediate uptake by the liver and lung (Figure 3-9A and B, Table 3-3), with a high percentage of the dose (30%) in lung that remains constant over time (Figure 3-9B). This biodistribution profile is characteristic of a stable cationic non-PEGylated polyplex that ionically attracts albumin, resulting in embolisms that become entrapped in the capillary beds of the lung [138-140]. **SM, SS, PM, PS, SV,** and **SA** all showed comparable liver and lung biodistribution (Figure 3-9A and B, Table 3-3).

Discussion

Optimization of the PK and biodistribution properties of non-viral gene delivery systems administered systemically is key to their successful improvement in mediating gene transfer *in vivo*. Until now, there have been few, if any, delivery platforms that allowed systematic manipulation of PK and biodistribution properties to improve the level of gene expression *in vivo*. The PEGylated polyacridine peptide polyplex delivery platform with delayed HS is unique in its ability to match the efficiency of HD-mediated expression of plasmid DNA [26, 117]. In Chapter 2, polyacridine peptides were systematically improved by increasing the spacing of four Acr residues with four Lys residues to arrive at $(\text{Acr-Lys}_4)_3$-Acr-Lys-Cys-$\text{PEG}_{5\text{kDa}}$ (**SM**) [15]. pGL3 polyplexes prepared with **SM** mediated maximal expression when applying HD-stimulation at up to 4-5 h post-polyplex administration [15].

Table 3-3. *Biodistribution of PEG Linker Polyacridine Peptide Polyplexes.*

	Time (Min)	Blood	Liver	Lung	Spleen	Stomach	Kidney	Heart	SI	LI	Total
S_{alk}	5	4.5 ± 0.7	54.2 ± 4.3	27.9 ± 6.9	3.4 ± 1.3	0.3 ± 0.0	0.5 ± 0.2	0.2 ± 0.1	0.4 ± 0.1	0.2 ± 0.1	91.7 ± 13.7
	120	2.3 ± 0.3	41.1 ± 1.3	25.0 ± 4.6	2.7 ± 1.8	5.6 ± 1.7	0.7 ± 0.2	0.1 ± 0.1	1.5 ± 0.4	0.9 ± 0.7	80.0 ± 12.2
	360	nd	16.5 ± 1.1	30.6 ± 5.7	2.7 ± 0.5	5.5 ± 1.2	0.6 ± 0.1	0.0± 0.0	1.3 ± 0.3	0.8 ± 0.4	58.3 ± 9.3
SA	5	25.6 ± 5.7	66.2 ± 2.1	0.5 ± 0.1	3.7 ± 0.9	0.3 ± 0.1	0.6 ± 0.1	0.1 ± 0.0	0.3 ± 0.0	0.2 ± 0.1	97.4 ± 9.1
	120	13.3 ± 3.4	41.0 ± 2.4	1.0 ± 0.4	3.1 ± 0.9	4.8 ± 0.1	0.7 ± 0.1	0.2 ± 0.0	1.1 ± 0.1	1.1 ± 0.3	66.4 ± 7.8
	360	nd	6.6 ± 0.5	0.7 ± 0.1	2.9 ± 0.1	9.6 ± 2.7	1.7 ± 0.1	0.2 ± 0.1	3.2 ± 0.2	1.5 ± 0.1	26.6 ± 3.7
SV	5	33.1 ± 3.5	65.2 ± 2.0	0.9 ± 0.2	2.8 ± 0.6	0.3 ± 0.1	1.2 ± 0.1	0.2 ± 0.1	0.4 ± 0.1	0.2 ± 0.1	104.2 ± 6.6
	120	15.3 ± 2.1	43.9 ± 4.3	0.4 ± 0.1	4.1 ± 1.6	10.4 ± 3.3	0.9 ± 0.3	0.1 ± 0.0	1.9 ± 0.4	0.8 ± 0.2	77.8 ± 12.3
	360	nd	8.2 ± 0.9	0.5 ± 0.1	4.5 ± 0.7	11.0 ± 2.6	1.1 ± 0.1	0.2 ± 0.1	3.5 ± 0.7	2.4 ± 0.6	31.5 ± 5.8
PM	5	58.2 ± 7.7	50.2 ± 6.3	1.0 ± 0.0	3.5 ± 0.2	0.4 ± 0.2	0.9 ± 0.3	0.3 ± 0.0	0.5 ± 0.2	0.4 ± 0.1	115.4 ± 14.8
	120	42.2 ± 5.3	31.3 ± 1.1	0.6 ± 0.1	4.7 ± 1.6	9.1 ± 1.8	1.1 ± 0.0	0.2 ± 0.0	2.3 ± 0.1	0.8 ± 0.0	92.3 ± 10.0
	360	nd	7.7 ± 1.7	0.8 ± 0.1	4.5 ± 1.6	11.8 ± 2.0	1.4 ± 0.1	0.2 ± 0.0	2.6 ± 0.7	1.4 ± 0.1	30.4 ± 6.3
SS	5	43.5 ± 2.4	54.6 ± 4.2	1.4 ± 0.7	5.0 ± 2.2	0.4 ± 0.2	1.0 ± 0.5	0.3 ± 0.1	0.9 ± 0.4	0.4 ± 0.2	107.5 ± 9.4
	120	28.6 ± 1.0	42.9 ± 9.2	0.7 ± 0.2	4.1 ± 1.7	4.0 ± 2.6	1.3 ± 0.2	0.2 ± 0.1	1.4 ± 0.3	0.6 ± 0.1	83.8 ± 15.4
	360	nd	8.8 ± 2.1	0.4 ± 0.1	2.1 ± 0.3	11.8 ± 2.6	1.0 ± 0.3	0.1 ± 0.0	3.4 ± 0.9	2.0 ± 0.5	29.6 ± 6.8
SM	5	47.9±5.3	51.8±7.5	2.6±1.8	4.3±0.8	0.4±0.2	1.0±0.5	0.3±0.1	0.4±0.1	0.2±0.1	108.3±16.6
	120	32.0±2.8	29.6±4.8	0.8±0.1	6.5±0.6	4.3±0.8	1.7±0.6	0.2±0.1	1.6±0.6	0.9±0.1	77.5±10.5
	360	nd	10.0 ± 3.4	0.7 ± 0.2	4.7 ± 2.9	9.4 ± 3.6	1.0 ± 0.3	0.2 ± 0.1	2.2 ± 0.4	1.2 ± 0.1	29.4 ± 11.0

Values presented are % of dose determined by cpm in pharmacokinetic and biodistribution samples (n.d. is not determined).

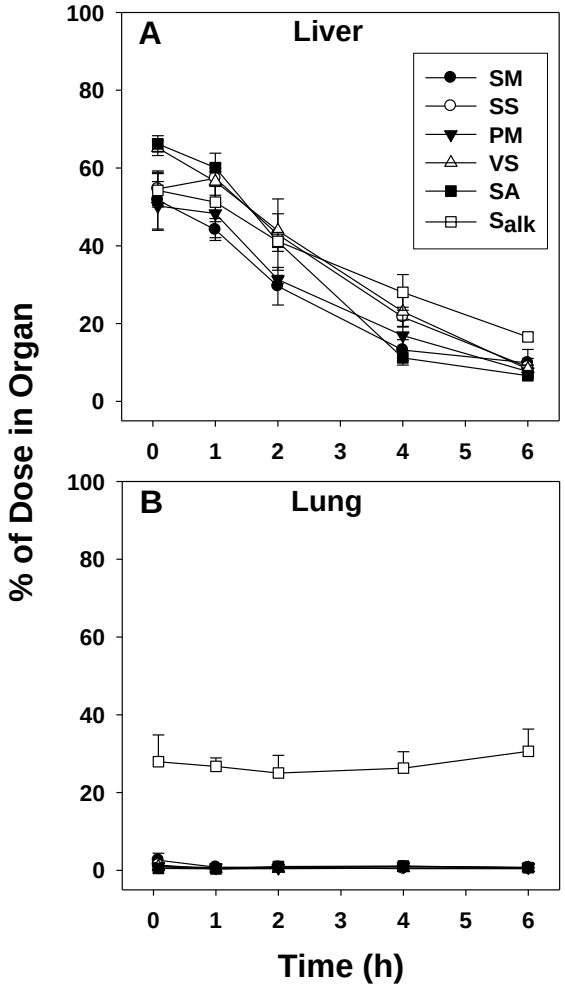

Figure 3-9. *Biodistribution of PEG Linker Polyacridine Peptide Polyplexes*. Peptides were polyplexed with ^{125}I-pGL3 at a stoichiometry of 0.8 nmol μg^{-1} DNA and dosed i.v. in mice. Panels A and B display the % of ^{125}I-pGL3 detected in the liver and lung, respectively, from 5 min to 6 h. **S_{alk}** polyplex exhibits a sustained accumulation in the lung. The results are the mean and standard deviation of triplicate determinations.

In the present study, the influence of PEG linkage on polyacridine peptide mediated gene delivery was examined. Notably, polyplexes prepared with **S_{alk}**, which lacks PEG, were completely inactive in mediating *in vivo* gene expression (Figure 3-4).

The rapid removal of **S_{alk}** polyplexes from the blood is likely the result of serum protein binding to these polyplexes with a +30 mV surface charge, resulting in very rapid and complete loss from the blood, and combined accumulation of 83% of the dose in the liver and lung. It is clear that even though a large percentage (50%) of the dose is associated with liver for up to 60 min following systemic delivery, HS fails to mediate any luciferase expression, suggesting that entrapment of cationic polyplexes by liver Kupffer cells inhibits HS gene expression.

With the exception of linkers designed to undergo reductive or pH sensitive cleavage [141, 142], few studies have considered the ramification of linker metabolic stability when attaching PEG to peptides or polymers used for *in vivo* gene delivery. It is stunning to realize that such subtle changes can have a dramatic influence on the efficiency of *in vivo* gene transfer. The PEG linker is sterically inaccessible to metabolic enzymes and was originally presumed to have little influence over gene transfer efficiency. It is most likely that the mechanism involves dissociation of the PEG-peptide, followed by metabolism to release PEG from the peptide. Deactivation could result from DNase digestion of partially uncondensed polyplex. For **SV** and **SA** the metabolic deactivation is surprisingly fast, especially considering that a thiol-vinyl sulfone and thiol-acetamide linkage are significantly more chemically stable to reduction and elimination compared to **SS**, **PS**, **PM** and **SM**. However, the PK and HS results establish **SV** and **SA** polyplexes have both a short half-life in the circulation and are much less active in mediating gene expression.

Through deduction, it appears that **SV** and **SA** PEG-peptide metabolism is not occurring in the blood, since the de-shielded polyplex products would most likely accumulate in the lung, as was observed for **S_{alk}**. It is hypothesized that **SV** and **SA** polyplexes are metabolized in liver Kupffer cells, where both removal of PEG and digestion of pGL3 by DNase could occur. This hypothesis is supported by biodistribution

results that establish that **SV** and **SA** polyplexes highly accumulate in the liver (66%) and are eliminated at a similar rapid rate compared to other polyplexes.

The comparative metabolic stability of **SS** polyplexes established that disulfide bond reduction occurs more slowly than metabolism of **SV** and **SA**. However, it also leads to a shortened PK half-life and HS expression profile. The magnitude of gene expression mediated by **SS** polyplexes at 1 and 2 h HS time was nearly coincident with that determined for **SM**, indicating PEG is likely not removed by intracellular reduction under the rapid delivery mediated by HS. However, the loss of HS expression for **SS** polyplexes at circulation times of longer than 2 h may be overcome by incorporation of a more reductively stable **PS** bond [52, 143]. The results clearly establish that both **SM** and **PM** are the most metabolically stable chemical linkages resulting in long PK half-lives and an extended HD-stimulation profile.

In conclusion, these results establish a maleimide linkage as the most optimal choice of the thiol-reactive PEGs studied. Thus, no improvement was observed in polyplex pharmacokinetic properties, biodistribution properties, or maximal HD-stimulation, which remains stable when applied at up to 4-5 h following post-DNA administration. However, the poor performance of other chemically stable thioethers indicates the importance of PEG linker moiety on *in vivo* properties and cautions the use of presumably stable moieties without careful optimization for use in systemically-delivered, non-viral gene delivery carriers.

CHAPTER 4: PEG SIZE AND POSITION AFFECTS IN VIVO STABILITY OF DNA POLYPLEXED WITH PEGYLATED POLYACRIDINE PEPTIDES

Abstract

Chapter 4 presents a continuation of the investigation of parameters concerning the polyethylene glycol (PEG) moiety of PEGylated polyacridine peptides. Chapter 3 presented a structure-activity relationship study in which 5 kDa PEG was conjugated to $(Acr\text{-}Lys_4)_3$-Acr-Lys-Cys/Pen using a variety of thiol-reactive groups. Penicillamine-thiol, penicillamine-maleimide, and thiol-maleimide were found to be the most stable and produced polyplexes with equivalent high levels of hydrodynamically-stimulated (HS) expression, but presumably stable linkages (thiol-acetamide and thiol-vinyl sulfone) failed to produce adequate circulation and expression. Based on these results, other PEG attributes of size, linkage position, and loading density and their effects on polyplex pharmacokinetics (PK), biodistribution (BD), and HS expression were investigated using a stable thiol-maleimide linkage and will be discussed herein. Linear PEGs of molecular weight 2, 5, 10, 20, and 30 kDa were used to determine the effect of PEG size. PEG position was examined by attachment to an N-terminal, C-terminal, or central Cys residue, and PEG loading density was addressed by attachment of maleimide-PEG_{5kDa} to Cys residues at both the N- and C-termini. Liver BD of polyplexes was substantially reduced by increases in PEG size with 30 kDa PEG leading to only 13% of liver accumulation, but these polyplexes still exhibited sustained HS expression. While PEG position was not found to greatly influence circulatory stability of polyplexes, the increased PEG density of the bis-substituted peptide resulted in measurable levels of HS expression at 9 h. These results demonstrate important relationships of PEG optimization of polyacridine peptides to effects on polyplex PK, BD, and HS gene expression *in vivo*.

Introduction

The development of an optimal non-viral gene delivery carrier requires a careful balance of characteristics that provide high affinity for DNA, allow management of polyplex characteristics, and release DNA at the site of expression. Polyacridine peptides conjugated to polyethylene glycol (PEG) have unique properties that allow for extended circulation and hydrodynamically stimulated (HS) expression through reversible binding to DNA. Although the aspect of PEG linkage was addressed in Chapter 3, many other parameters of PEGylation of polyacridine peptides remain to be investigated.

Several prior studies have examined the influence of PEG length and loading density on nanoparticle biodistribution *in vivo* [144-148]. In general, increasing the PEG length and loading density decreases serum protein binding and biodistribution to the lung. However, even with a stealth layer of PEG, nanoparticles are still primarily recognized by Kupffer cells, accounting for the majority of biodistribution to liver immediately after i.v. administration [107]. Although these relationships are well understood, to date no studies have reported the development of long-circulating DNA nanoparticles that avoid liver uptake and maintain the ability to mediate gene transfer *in vivo*.

A major difficulty in PEGylating DNA polyplexes is that increasing the PEG loading density can also compromise polyplex stability. This is because PEGylation of PEI [45, 80], polylysine, chitosan [36] or dendrimers simultaneously leads to a proportional decrease in the number of primary amines, which decreases the binding affinity of PEGylated polymers for DNA and results in their dissociation in the circulation [44]. In an effort to overcome this limitation, PEGylated adamantane was incorporated through binding to cationic cyclodextrin polyplexes [149]. While this approach preserved amines to maintain binding affinity for DNA, it failed to achieve a high PEG loading density.

Investigations of PEGylated polyacridine peptides have culminated in an *in vivo* stealthing agent that effectively polyplexes DNA and maintains its ability to express for extended periods post-i.v. administration as demonstrated by HS and bioluminescence imaging (BLI) of pGL3, a 5.3 kbp plasmid that expresses luciferase via an SV40 promoter. Previous studies established a relationship that identified Lys as a high-affinity spacing residue that provides cationic interaction with DNA and that increasing n to 6 in the motif $(Acr\text{-}Lys)_n$-Cys, where Acr is a Lys residue bound to C9 of acridine via the ε-amine, resulted in PEGylated polyplexes that stably circulate and provide maximal HS expression at 1 h [9]. As demonstrated in Chapter 2, polyacridine peptides were modified through increases in Lys spacing of the Acr residues and formulation investigations that produced $(Acr\text{-}Lys_4)_3$-Acr-Lys-Cys-PEG, where $mPEG_{5kDa}$ was conjugated via maleimide to the Cys thiol. Polyplexes with this peptide at 0.8 nmol μg^{-1} pGL3 produced maximal HS luciferase expression for 5 h post-i.v. administration. The influence of PEG parameters was then investigated by changing the thiol-reactive linker to modify polyacridine peptides as described in Chapter 3. While improvement over the use of maleimide conjugation on $(Acr\text{-}Lys_4)_3$-Acr-Lys-Cys/Pen-PEG was not observed, the method of PEG conjugation was shown to be vital to the performance of the resulting polyplex [134].

The influence of PEG length, linkage, and loading density on DNA polyplex pharmacokinetics (PK), biodistribution, and HS gene expression *in vivo* are examined herein. The identified relationships were found using high-affinity, DNA-binding polyacridine peptides. Knowing that a thiol conjugation to maleimide provided the greatest maintenance of maximal expression of polyplexed pGL3 with PEGylated $(Acr\text{-}Lys_4)_3$-Acr-Lys-Cys [134], this peptide and its conjugation to PEG via maleimide were maintained in the following study.

Several PEG lengths corresponding to molecular weights of 2, 5, 10, 20, and 30 kDa were examined using commercially available maleimide-PEG. Location of PEG

conjugation to $(Acr\text{-}Lys_4)_3$-Acr-Lys-Cys was addressed by synthesis of similar motifs containing Cys at the center or N-terminus followed by conjugation to maleimide-PEG_{5kDa}, and, finally, to increase PEG density, Cys-$(Acr\text{-}Lys_4)_3$-Acr-Cys was synthesized to allow disubstituion of maleimide-PEG_{5kDa} at the N- and C-termini. The results indicate increased polyplex stability as determined by pharmacokinetics and decreased liver distribution as the PEG size is increased from 2 to 30 kDa. Increased PEG density was found to improve HS luciferase expression of polyplexes at 9 h. The observations reported herein stress the importance of addressing improvements to the *in vivo* utility of i.v.-dosed non-viral gene delivery carriers through careful adjustment of PEG parameters. The contents of this chapter are reported by Khargharia et al [134].

Materials and Methods

Unsubstituted Wang resin, 9-hydroxybenzotriazole, Fmoc-protected amino acids, O-(7-Azabenzo-triazol-1-yl)-*N,N,N′,N′*-tetramethyluronium hexafluorophosphate (HATU), Fmoc-Lysine-OH, and *N*-methyl-2-pyrrolidone (NMP) were obtained from AAPPTec (Louisville, KY, USA). *N*,*N*-dimethylformamide (DMF), trifluoroacetic acid (TFA) and acetonitrile were purchased from Fisher Scientific (Pittsburgh, PA, USA). Diisopropylethylamine, piperidine, acetic anhydride, Tris(2-carboxyethyl)-phosphine hydrochloride (TCEP), 9-chloroacridine, thiazole orange, *N*-hydroxysuccinimide (NHS), iodoacetic acid and dicyclocarbodiimide (DCC) were obtained from Sigma Chemical Co. (St Louis, MO, USA). Agarose was obtained from Gibco-BRL (Carlsbad, CA, USA). Linear PEG-maleimides of molecular weights 2, 5, 10, 20, and 30 kDa were purchased from Laysan Bio (Arab, AL, USA). D-Luciferin and luciferase from *Photinus pyralis* were obtained from Roche Applied Science (Indianapolis, IN, USA). pGL3 control vector, a 5.3-kbp luciferase plasmid containing a SV40 promoter and enhancer, was obtained from Promega (Madison, WI, USA). pGL3 was amplified in a DH5α strain of *Escherichia coli* and purified according to the manufacturer's instructions.

Synthesis and Characterization of Polyacridine Peptides (In collaboration with Nicholas J. Baumhover and Mark D. Ericson)

9-Phenoxyacridine and Fmoc-Lysine(Acr)-OH were prepared as recently reported [114, 115]. Polyacridine peptides were prepared by solid phase peptide synthesis on a 30 μmol scale using an APEX 396 synthesizer (Advanced ChemTech, Louisville, KY, USA) with standard Fmoc procedures. The reaction yields were improved by activating amino acids with 9-hydroxybenzotriazole and HATU while using double coupling of Fmoc-Lys(Acr)-OH and triple coupling for the spacing amino acid, using a five-fold excess of amino acid over resin. Peptides were removed from resin and deprotected using a cleavage cocktail of TFA/ethanedithiol/water (93:4:3 v/v/v) for 3 h followed by precipitation in cold ether. Precipitates were centrifuged at 5000 × *g* and 4 °C for 10 min and the supernatant decanted. Peptides were then reconstituted with 0.1 v/v % TFA and purified to homogeneity on reversed phase-high pressure liquid chromatography (RP-HPLC) by injecting 0.5–2 μmol onto a Vydac C18 (Grace Davison Discovery Sciences, Deerfield, IL, USA) semi-preparative column (2 × 25 cm) eluted at 10 ml min^{-1} with 0.1 v/v % TFA with an acetonitrile gradient of 15–25 v/v % over 30 min while monitoring acridine at 409 nm. The major peak was collected and pooled from multiple runs, concentrated by rotary evaporation, lyophilized and stored at −20 °C. Purified peptides were reconstituted in 0.1 v/v % TFA and quantified by absorbance (acridine $\varepsilon_{409\,nm}$=9266 M^{-1} cm^{-1} assuming additivity of ε for multiple acridines) to determine isolated yield. Purified peptides were characterized by LC-MS by injecting 2 nmol onto a Vydac C18 analytical column (0.47 × 25 cm) eluted at 1 ml min^{-1} with 0.1 v/v % TFA and an acetonitrile gradient of 15–45 v/v % over 30 min while acquiring electrospray ionization mass spectrometry (ESI-MS) in the positive mode.

Synthesis and Characterization of PEGylated Polyacridine Peptides (In collaboration with Nicholas J. Baumhover and Mark D. Ericson)

PEGylation of the Cys residue on (Acr-Lys_4)$_3$-Acr-Lys-Cys was achieved by reacting 1 μmol of peptide with 1.1 μmol of mPEG-maleimide (2, 5, 10, 20, or 30 kDa) in 4 ml of 100 mM 4-(2-hydroxyethyl)-1-piperazineethanesulfonic acid (HEPES) buffer pH 7 for 12 h at room temperature. The same conditions were used to conjugate PEG_{5kDa}-maleimide to Cys-(Acr-Lys_4)$_3$-Acr-Lys or Acr-Lys_4-Acr-Lys_2-Cys-Lys_2-Acr-Lys_4-Acr-Lys. PEGylation of both available thiols on 1 μmol Cys-(Acr-Lys_4)$_3$-Cys was accomplished using the same conditions in the presence of 3 μmol PEG_{5kDa}-maleimide.

PEGylated peptides were purified by semi-preparative RP-HPLC eluted with 0.1% v/v TFA with an acetonitrile gradient of 20–60% v/v acetonitrile while monitoring acridine at 409 nm. The major peak was collected and pooled from multiple runs, concentrated by rotary evaporation, lyophilized and stored at −20 °C. The counter ion was exchanged by chromatography on a G-25 column (2.5 × 50 cm) equilibrated with 0.1 v/v % acetic acid to obtain the peptide in an acetate salt form. The major peak corresponding to the PEG peptide eluted in the void volume (100 ml) was pooled, concentrated by rotary evaporation and lyophilized. PEG peptides were reconstituted in water and quantified by Abs_{409nm} (each acridine $\varepsilon_{409\,nm}$=9266 M^{-1} cm^{-1}) to determine isolated yield. PEG peptides were characterized by matrix-assisted laser desorption/ionization-time of flight mass (MALDI-TOF) spectrometry by combining 1 nmol with 10 μl of 2 mg ml^{-1} α-cyano-4-hydroxycinnamic acid in 50% v/v acetonitrile and 0.1% v/v TFA. Samples were spotted onto the target and ionized on a Bruker Biflex III Mass Spectrometer (Bruker Daltonics Inc., Billerica, MA, USA) operated in the positive ion mode.

Formulation and Characterization of PEGylated Polyacridine Peptide Polyplexes

The relative binding affinity of PEGylated polyacridine peptides for pGL3 was determined by a fluorophore exclusion assay [18]. pGL3 (200 µl of 5 µg ml^{-1} in 5 mM HEPES pH 7.5 containing 0.1 µM thiazole orange) was combined with 0, 0.05, 0.1, 0.13, 0.15, 0.18, 0.2, 0.25, 0.3, 0.4, or 0.5 nmol of PEGylated polyacridine peptide in 300 µl of HEPES and allowed to bind at room temperature for 30 min. Thiazole orange fluorescence was measured using an LS50B fluorometer (Perkin-Elmer, Cambridge, UK) by exciting at 498 nm while monitoring emission at 546 nm with the slit widths set at 10 nm. A fluorescence blank of thiazole orange in the absence of pGL3 was subtracted from all values before data analysis.

The particle size and zeta potential were determined by preparing 2 ml of polyplex in 5 mM HEPES pH 7.5 at a pGL3 concentration of 30 µg ml^{-1} and a PEGylated polyacridine peptide stoichiometry of 0.8 nmol μg^{-1} of pGL3. The particle size was measured by quasi-elastic light scattering at a scatter angle of 90° on a Brookhaven ZetaPlus Particle Sizer (Brookhaven Instruments Corporation, Holtsville, NY, USA). The zeta potential was determined as the mean of 10 measurements immediately following acquisition of the particle size.

Pharmacokinetic Analysis of PEGylated Polyacridine Polyplexes (In collaboration with Sanjib Khargharia)

Radioiodinated pGL3 was prepared as previously described [116]. Triplicate mice were anesthetized by intraperitoneal injection of ketamine hydrochloride (100 mg kg^{-1}) and xylazine hydrochloride (10 mg kg^{-1}) and underwent a dual cannulation of the right and left jugular veins. An i.v. dose of ^{125}I-pGL3 (3 µg, 1.2 µCi in 50 µl of HEPES-buffered mannitol (5 mM HEPES, 0.27 M mannitol pH 7.4)) or ^{125}I-pGL3 polyplex (3 µg) was administered via the left catheter. Blood samples (10 µl) were drawn from the right

catheter at 1, 3, 6, 10, 20, 30, 60, 90 and 120 min and immediately frozen. The volumes withdrawn were replaced with 10 µl of normal saline. The amount of radioactivity in each blood sample was quantified by direct γ-counting. Blood samples were digested with proteinase K for 12 h and polyplexes were extracted with 500 µl of phenol/chloroform/isoamyl alcohol (24:25:1) to remove PEGylated peptides followed by precipitation of DNA with the addition of 1 ml of ethanol [8, 9]. The precipitate was collected by centrifugation at 13 000 × *g* for 10 min, and the DNA pellet was dried and dissolved in 5 mM HEPES buffer pH 7.4. DNA samples were combined with 2 µl of loading buffer and applied to a 1% agarose gel (50 ml) and electrophoresed in Tris-borate-EDTA buffer at 70 V for 60 min [51]. The gel was dried on a zeta probe membrane and autoradiographed on a Phosphor Imager (Molecular Devices, Sunnyvale, CA, USA) following a 15 h exposure.

Biodistribution Analysis of PEGylated Polyacridine Polyplexes (In collaboration with Sanjib Khargharia)

^{125}I-pGL3 (1.5 µg in 50 µl of HEPES-buffered mannitol, 0.6 µCi) or ^{125}I-pGL3 polyplexes (1.5 µg) were dosed in triplicate mice via tail vein injection. At times ranging from 5 min to 6 h, mice were anesthetized by intraperitoneal injection of ketamine (100 mg kg^{-1}) and xylazine (10 mg kg^{-1}) and then killed by cervical dislocation. The major organs (liver, lung, spleen, stomach, kidney, heart, large intestine and small intestine) were harvested, rinsed with saline, and the radioactivity in each organ was determined by direct γ-counting and expressed as the percentage of the dose in the organ.

Hydrodynamically Stimulated Expression (In collaboration with Sanjib Khargharia)

Hydrodynamically stimulated (HS) expression was performed by tail vein injection in three mice with 1 µg of pGL3 polyplexes, prepared with 0.8 nmol PEG-peptide per µg pGL3, in 50 µl of HBM. At times ranging from 5 min to 9 h, a HD-

stimulatory dose of normal saline (9 w/v % of the body weight) was administered over 5 sec. At 24 h post-HD stimulation, mice were anesthetized by 3 % isofluorane, and an intraperitoneal dose of 80 µl (2.4 mg) of D-luciferin (30 µg μl^{-1} in phosphate-buffered saline) was administered. At 5 min following the d-luciferin dose, bioluminescence imaging (BLI) was conducted on mice using an IVIS Imaging 200 Series (Xenogen, Hopkins, MA, USA). BLI was performed in a light-tight chamber on a temperature-controlled, adjustable stage while isofluorane was administered by a gas manifold at a flow rate of 3%. Images were acquired at a 'medium' binning level and a 24.6-cm field of view with 10 sec acquisition time. The Xenogen system reported bioluminescence as photons sec^{-1} cm^{-2} sr^{-1} in a 2.86-cm diameter region of interest covering the liver. The integration area was transformed to pmols of luciferase in the liver using a previously reported standard curve [38]. Results were determined to be statistically significant ($p \leq 0.05$) based on a two-tailed unpaired t-test (Dunnett T3 using SPSS 19.0 analysis of variance software).

Results

The influence of PEG length on polyplex PK and *in vivo* gene transfer was evaluated by modification of peptide **1** with maleimide modified $PEG_{2, 5, 10, 20, or 30kDa}$ to prepare **2k, 5k, 10k, 20k,** and **30k** (Figure 4-1, Table 4-1). In addition, peptides **2** and **3** were designed as geometric isomers of peptide **1** with either an N-terminal or middle Cys residue, respectively. Peptides **2** and **3** were reacted with maleimide-PEG_{5kDa} to prepare **N5k** and **Mid5k**, respectively. These PEG peptides were developed to test the influence of PEG location on the ability of PEGylated polyacridine peptides to mediate gene expression *in vivo* (Figure 4-1 and Table 4-1). Finally, peptide **4** was synthesized and conjugated with $mPEG_{5kDa}$-maleimide at both the N- and C-termini to develop **Bis5k**, which was developed to investigate increased loading density of PEG per peptide.

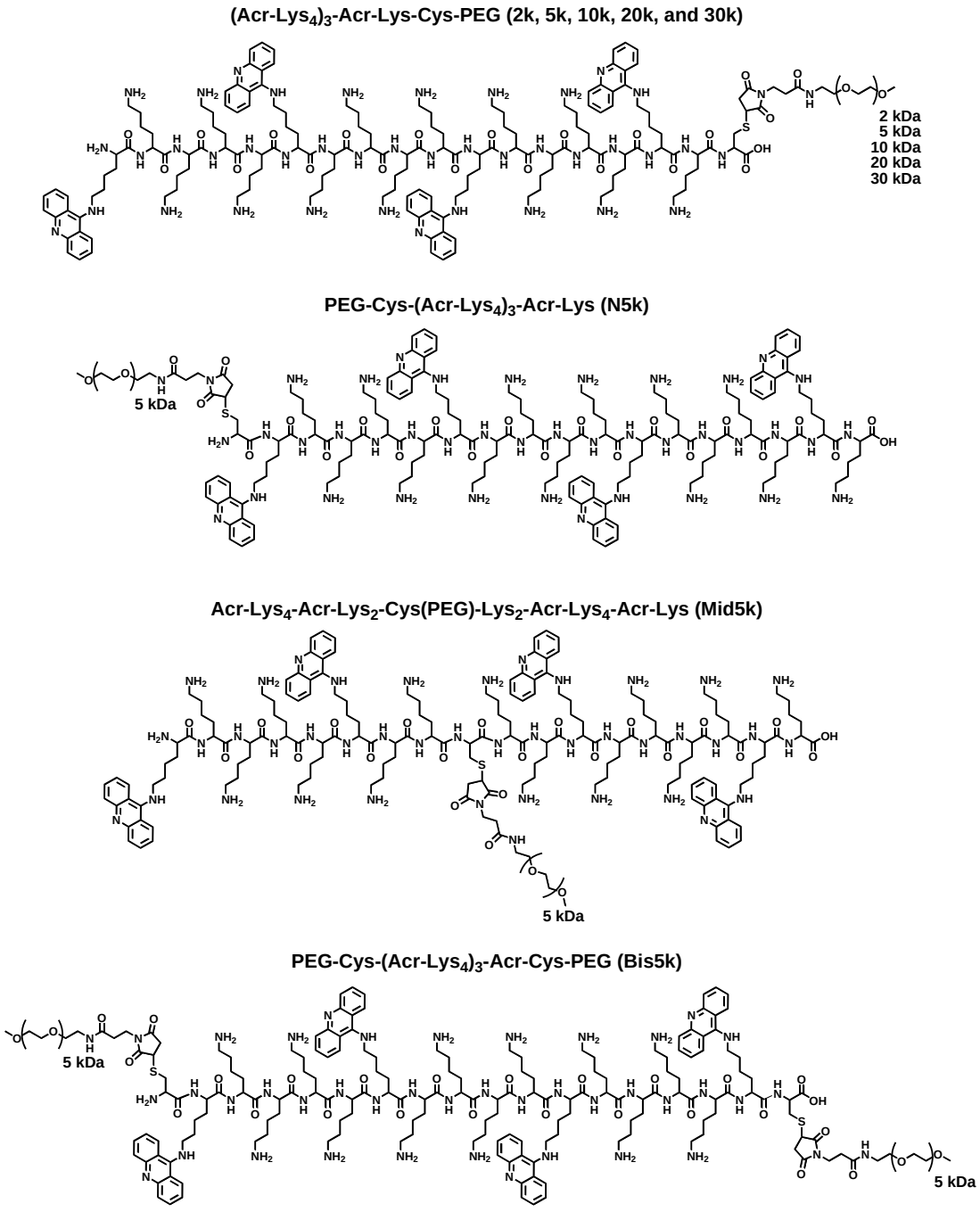

Figure 4-1. *Structure of PEGylated Polyacridine Peptides Varying PEG Length, Position, and Loading Density.* Peptide structures are presented varying PEG length by variation the molecular weight of linear maleimide-PEG conjugated to peptide **1** (Table 4-1) from 2-30 kDa (peptides **2k, 5k, 10k, 20k,** and **30k**). Conjugation of maleimide-PEG_{5kDa} to the Cys residues of peptides **2** and **3** varied the position of PEG within the binding motif producing peptides **N5k** and **Mid5k,** respectively. Peptide **Bis5k** was made via conjugation of maleimide-5kDa to the N- and C-terminal Cys residues of peptide **4**.

Table 4-1. *Polyacridine Peptide Sequences, Yields, and Masses Varying PEG Size and Location.*

Name	Peptide Sequence	% Yield	Mass (calc/obs)
1	$(Acr\text{-}Lys_4)_3$-Acr-Lys-Cys	20	3008.9 / 3008.8[a]
2	Cys-$(Acr\text{-}Lys_4)_3$-Acr-Lys	16	3008.9 / 3009.0[a]
3	Acr-Lys_4-Acr-Lys_2-Cys-Lys_2-Acr-Lys_4-Acr-Lys	16	3008.9 / 3009.0[a]
4	Cys-$(Acr\text{-}Lys_4)_3$-Acr-Cys	16	2983.9 / 2983.6[a]
S_{alk}	$(Acr\text{-}Lys_4)_3$-Acr-Lys-Cys-Alk	44	3066.7 / 3066.8[a]
2k	$Acr\text{-}Lys_4)_3$-Acr-Lys-Cys-Mal-PEG_{2kDa}	81	5109 / 5174[b]
5k	$(Acr\text{-}Lys_4)_3$-Acr-Lys-Cys-Mal-$PEG_{5kDa\backslash}$	77	8909 / 8697[b]
10k	$(Acr\text{-}Lys_4)_3$-Acr-Lys-Cys-Mal-PEG_{10kDa}	65	13909 / 13801[b]
20k	$(Acr\text{-}Lys_4)_3$-Acr-Lys-Cys-Mal-PEG_{20kDa}	61	24460 / 24635[b]
30k	$(Acr\text{-}Lys_4)_3$-Acr-Lys-Cys-Mal-PEG_{30kDa}	80	36840 / 36459[b]
N5k	PEG_{5kDa}-Mal-Cys-$(Acr\text{-}Lys_4)_3$-Acr-Lys	70	8909 / 8811[b]
Mid5k	Acr-Lys_4-Acr-Lys_2-Cys(Mal-PEG_{5kDa})-Lys_2-Acr-Lys_4-Acr-Lys	72	8909 / 8645[b]

Masses determined by [a]ESI-MS and [b]MALDI-TOF.

PEG-peptides **2k**, **5k, 10k, 20k, 30k, N5k**, **Mid5k**, and **Bis5k** were isolated using preparative RP-HPLC in yields ranging from 61-81 % based on peptides **1**-**4**. MALDI-TOF MS analysis of PEGylated polyacridine peptides resulted in observed average masses ranging from 5174-36459 Da. The difference between the calculated and observed mass is related to PEG polydispersity in the commercially available functionalized PEGs as described in Chapter 2. The ability of PEGylated polyacridine peptides to bind pGL3 was evaluated using a thiazole orange dye exclusion assay [18]. The results established that each PEG-peptide completely displaced the fluorophore at a stoichiometry of 0.15 nmol μg^{-1} of pGL3 indicating that length had negligible influence on binding affinity of peptide **1** for DNA. In addition, the location of PEG exerted no

detectable influence on the ability of PEG-peptides to displace thiazole orange (Figure 4-2B).

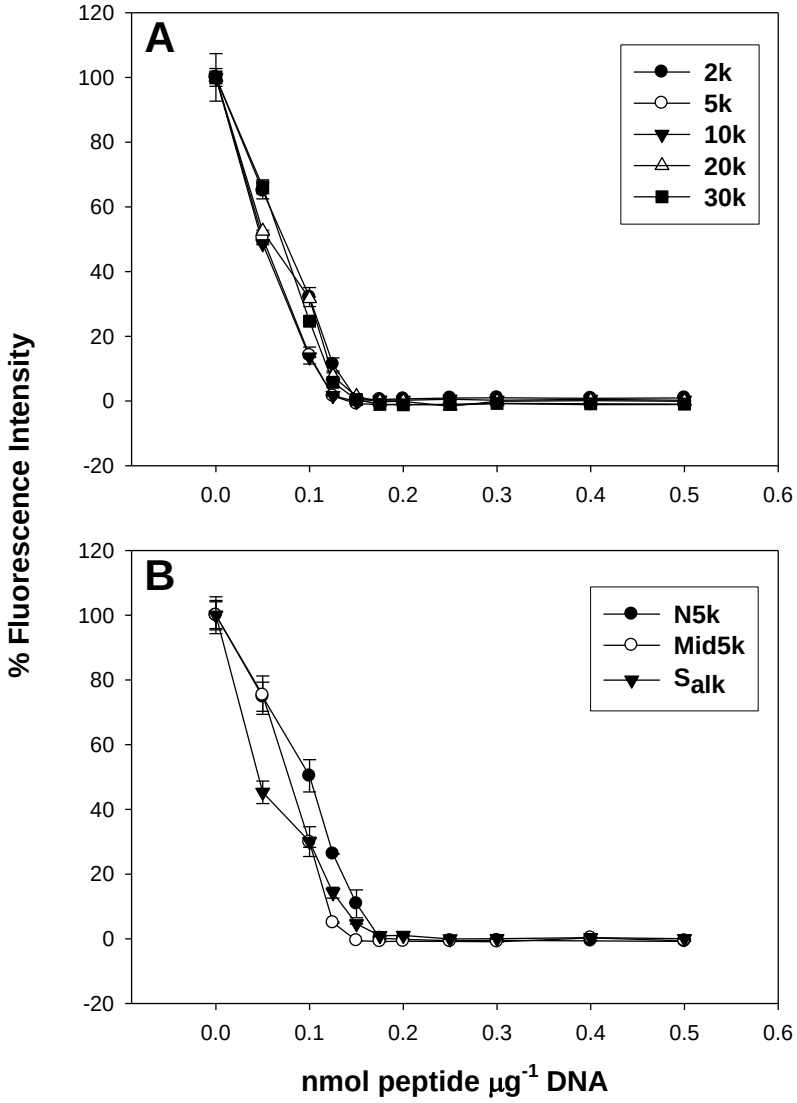

Figure 4-2. *Binding Affinity of PEGylated Polyacridine Peptides Varying PEG Length, Position.* The binding of PEGylated polyacridine peptides for pGL3 (DNA) was determined at varying stoichiometries via thiazole orange dye displacement assay. Panel A displays the relative affinities of peptides **2k, 5k, 10k, 20k,** and **30k** which vary by PEG size. Panel B illustrates dye displacement by PEGs of differing position (**N5k** and **Mid5k**) and $\mathbf{S_{alk}}$**.** Results are the mean and standard deviation of triplicate samples.

To maintain consistency of comparison of the current series of peptides with those discussed in Chapters 2 and 3, the particle size and zeta potential were compared for polyplexes prepared at a standard stoichiometry 0.8 nmols of peptide μg^{-1} of pGL3 (Figure 4-3), and this stoichiometry was also used for all PK, biodistribution and *in vivo* expression experiments. As previously mentioned, this stoichiometry is well above the full displacement observed in the dye exclusion assay, but it was observed that this stoichiometry produces fully-condensed, closed polyplexes that are more stable in the circulation [9, 15]. Polyplexes prepared with **2k**, **5k**, and **10k** were approximately 170 nm in diameter, whereas **20k** and **30k** produced polyplexes that were 200 and 250 nm in diameter, respectively (Figure 4-3A). $\mathbf{S_{alk}}$ is included in this study as a non-PEGylated control (Table 4-1) and possesses a much smaller diameter of 105 nm. Polyplexes prepared with either $\mathbf{S_{alk}}$ or **2k** both produced zeta potentials of +28-30 mV, establishing that a 2kDa PEG was unable to mask polyplex charge relative (Figure 4-3B). In contrast, a substantially lower zeta potential of +10 mV was achieved using 5 and 10 kDa PEG on **5k** and **10k** (Figure 4-3B). Increasing the PEG size further to 20 or 30kDa using **20k** and **30k** to form polyplexes resulted in a progressive decrease in zeta potential to +5 and 0 mV, respectively (Figure 4-3B).

Polyplexes (1 µg pGL3) were tested for their ability to mediate hydrodynamically stimulated (HS) expression using a high volume of saline (9 % w/v of mouse) at various circulation times post-i.v. administration of a low volume (50 µl) polyplex dose. Comparison of **10k**, **20k** and **30k** polyplexes established that each mediated a five-fold lower HS gene expression relative to **5k** polyplexes at a delay time of 1hr (Figure 4-4A). Delay times of up to 4 hrs post-polyplex delivery resulted in a stable level of expression for **5k** polyplexes, which then declined to background over 5 h. Alternatively, **2k** polyplexes mediated nearly 500-fold lower gene expression compared to **5k** polyplexes. The HS expression profile was stable for 3 hrs and then rapidly declined to background (Figure 4-4A). The differences in the magnitude of HS gene expression when varying

PEG length were partially explained by analysis of the polyplex PK and biodistribution. **2k** polyplexes possessed the shortest α half-life, whereas **5k**, **10k**, **20k** and **30k** polyplexes possessed a coincident PK profile indicative of greater circulatory stability (Figure 4-5A, Table 4-2).

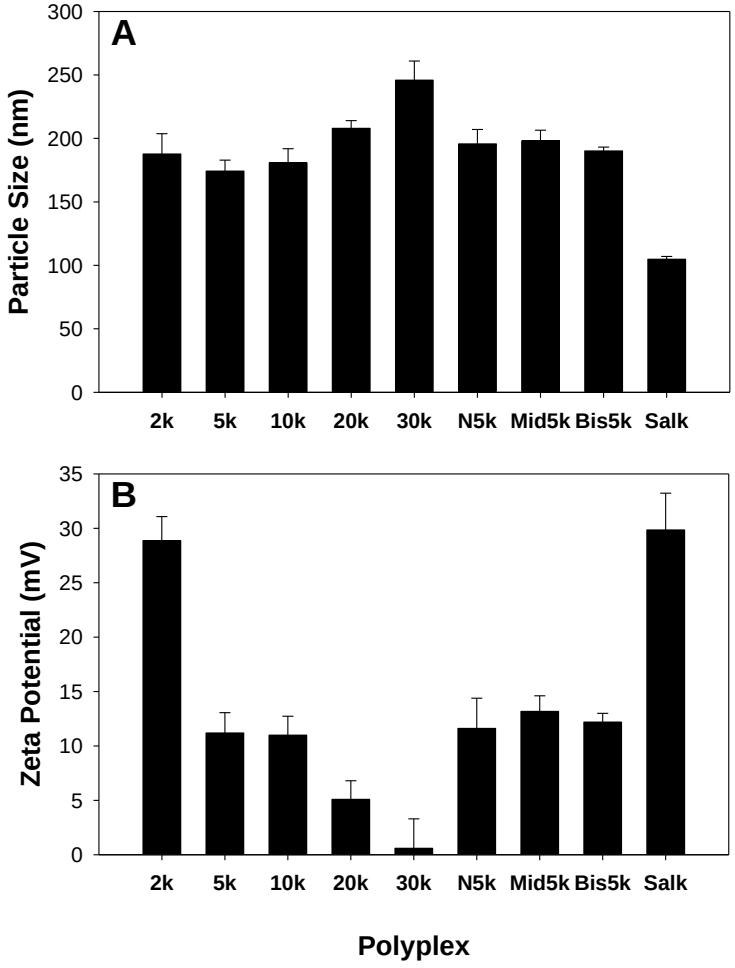

Figure 4-3. *Size and Charge of PEGylated Polyacridine Peptide Polyplexes with varied PEG Length, Position, and Density*. PEGylated polyacridine peptides (**2k, 5k, 10k, 20k, 30k, N5k, Mid5k,** and **Bis5k**) and $\mathbf{S_{alk}}$ were used to polyplex pGL3 (30 μg ml^{-1}) at a stoichiometry of 0.8 nmol μg^{-1} pGL3. Polyplexes were analyzed by QELS to determine particle size (panel A) and zeta potential (panel B). The results indicate decreasing zeta potential as PEG size is increased. Each mean and standard deviation is the result of multiple determinations.

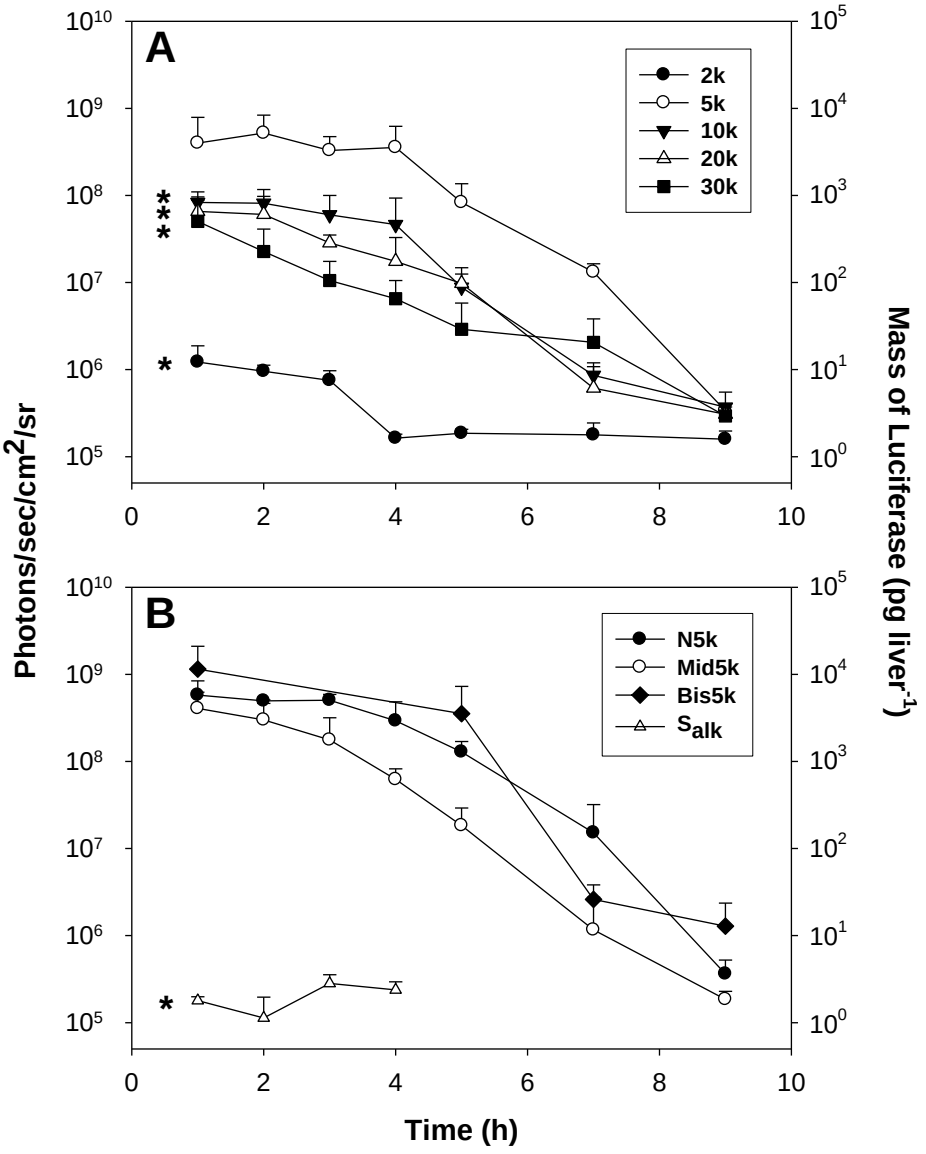

Figure 4-4. *Hydrodynamically-Stimulated (HS) Gene Expression of PEGylated Polyacridine Peptide Polyplexes with varied PEG Length, Postion, and Density.* pGL3 (1 µg) was polyplexed with 0.8 nmol of each polyacridine peptide and administered using HS at 1-9 h followed by BLI at 24 h post-stimulation. Panel A illustrates the effect of PEG length on HS gene expression using **2k, 5k, 10k, 20k,** and **30k** polyplexes. Panel B illustrates the effect of PEG position (**N5k** and **Mid5k**), loading density (**Bis5k**), and peptide without PEG ($\mathbf{S_{alk}}$) on HS gene expression. Less efficient gene transfer is observed for polyplexes with 10, 20, and 30 kDa PEG versus 5 kDa PEG. **2k** and $\mathbf{S_{alk}}$ (little or no PEG present) produce greatly reduced HS gene expression. The results are the mean and standard deviation of triplicate determinations. Asterisks indicate statistical significance of $p \leq 0.05$ when compared with **5k** at 1h.

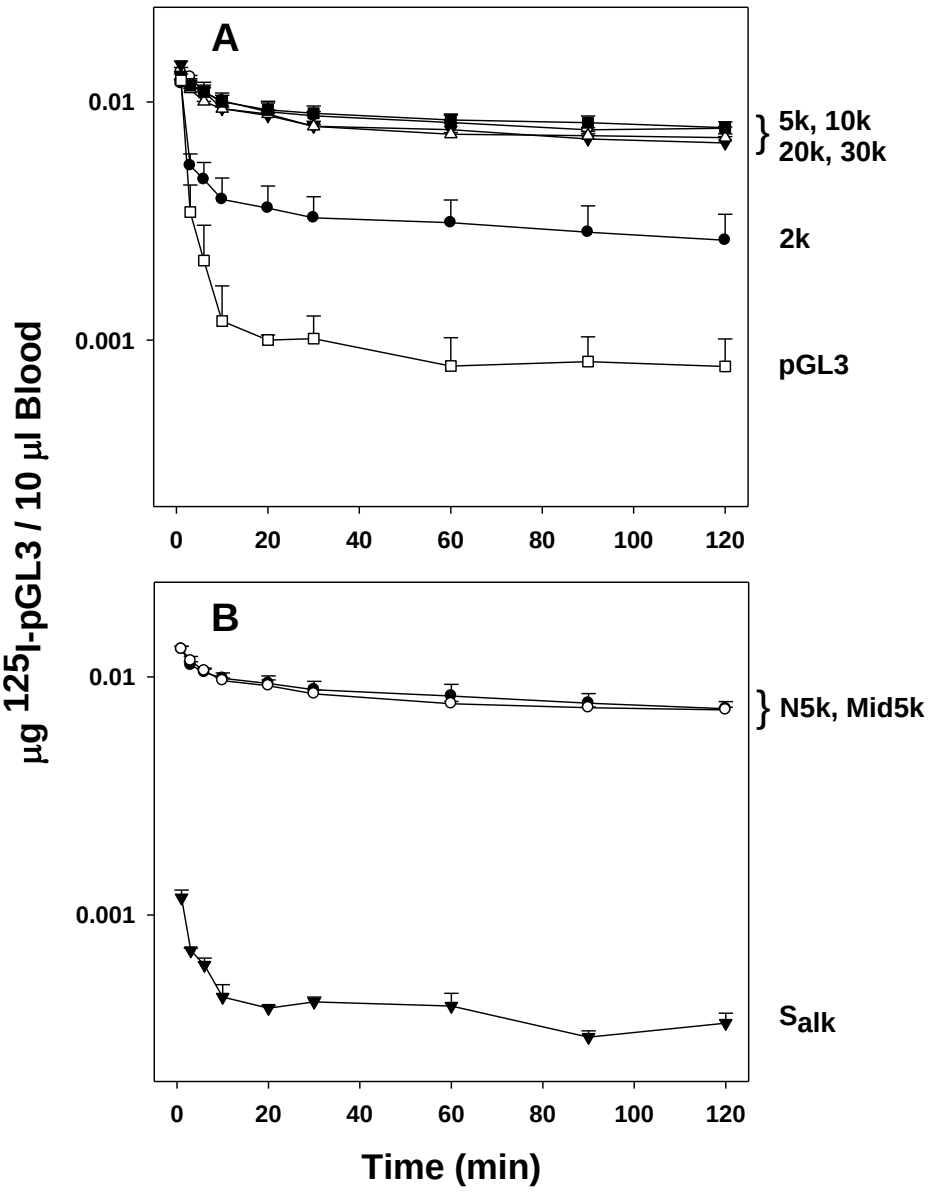

Figure 4-5. *Pharmacokinetic (PK) Analysis of PEGylated Polyacridine Peptide Polyplexes with varied PEG Length and Position.* PK was conducted in mice using polyplexed ^{125}I-pGL3 at a stoichiometry of 0.8 nmol peptide µg^{-1} DNA. Data are presented as concentration of ^{125}I-pGL3 in blood samples as a function of time. The results of circulating naked pGL3 and **2k, 5k, 10k, 20k,** and **30k** polyplexes are presented in panel A. Panel B demonstrates the PK of **N5k, Mid5k,** and $\mathbf{S_{alk}}$ polyplexes. Lack of PEG ($\mathbf{S_{alk}}$) or smaller PEG length (**2k**) results in rapid removal from the bloodstream to a similar or greater extent than naked pGL3. The results are the mean and standard deviation of triplicate determinations.

Table 4-2. *Pharmacokinetics of PEGylated Polyacridine Peptide Polyplexes Varying PEG Size and Location.*[a]

^{125}I-pGL3 Polyplex	$t_{1/2}\alpha$ [b] (min)	$t_{1/2}\beta$[c] (min)	V_d[d] (ml)	Cl[e] (ml min^{-1})	MRT[f] (min)	AUC[g] (µg*min ml^{-1})
2k	2.1 ± 0.4	242 ± 56	409 ± 89	1.3 ± 0.6	342 ± 82	135 ± 4
5k	4.1 ± 2.2	374 ± 44	159 ± 9	0.3 ± 0.0	540 ± 62	507 ± 43
10k	3.3 ± 0.2	302 ± 51	167 ± 10	0.4 ± 0.1	435 ± 72	392 ± 65
20k	4.6 ± 0.9	369 ± 37	120 ± 25	0.2 ± 0.0	484 ± 98	424 ± 89
30k	4.7 ± 0.9	426 ± 28	117 ± 15	0.3 ± 0.0	579 ± 40	576 ± 61
N5k	4.1 ± 0.7	343 ± 35	155 ± 14	0.4 ± 0.1	485 ± 59	467 ± 18
Mid5k	3.6 ± 0.5	329 ± 41	160 ± 10	0.4 ± 0.1	466 ± 71	436 ± 42

[a]Calculated using blood cpm values over 120 min and assuming complete DNA stability.

[b]Calculated α-half-life.

[c]Calculated β-half-life.

[d]Volume of distribution.

[e]Total body clearance rate.

[f]Mean residence time.

[g]Area under the curve.

The short α half-life of **2k** polyplexes is likely the result of the higher (+30 mV) surface charge revealed by zeta potential analysis (Figure 4-3B) which correlates with greater liver uptake (70% of dose) compared to 50% of dose for **5k** (Figure 4-6A). Presumably, this is due to Kupffer cell recognition of the electropositive polyplex. Interestingly, as the PEG length was increased from 10 to 30 kDa, the percent of dose captured by the liver decreased, resulting in only 13% of dose associated with liver following administration of **30k** polyplexes, which is nearly the blood volume of the liver in mice (Figure 4-6A) [147, 150]. The biodistribution of **20k** polyplexes resulted in an increase in spleen uptake, which reached a maximum of 18% of dose at biodistribution

time of 2 hr (Figure 4-6C, Table 4-3). As previously stated, lack of any PEG ($\mathbf{S_{alk}}$) for peptide **1** results in complete loss of circulating polyplex in the bloodstream as evidenced by PK (Figure 4-5B) and a complete lack of HS expression (Figure 4-4B), and 30% of polyplex dose becomes entrapped in the lung (Figure 4-6B) as a result of fully-exposed cationic surface charge [138-140].

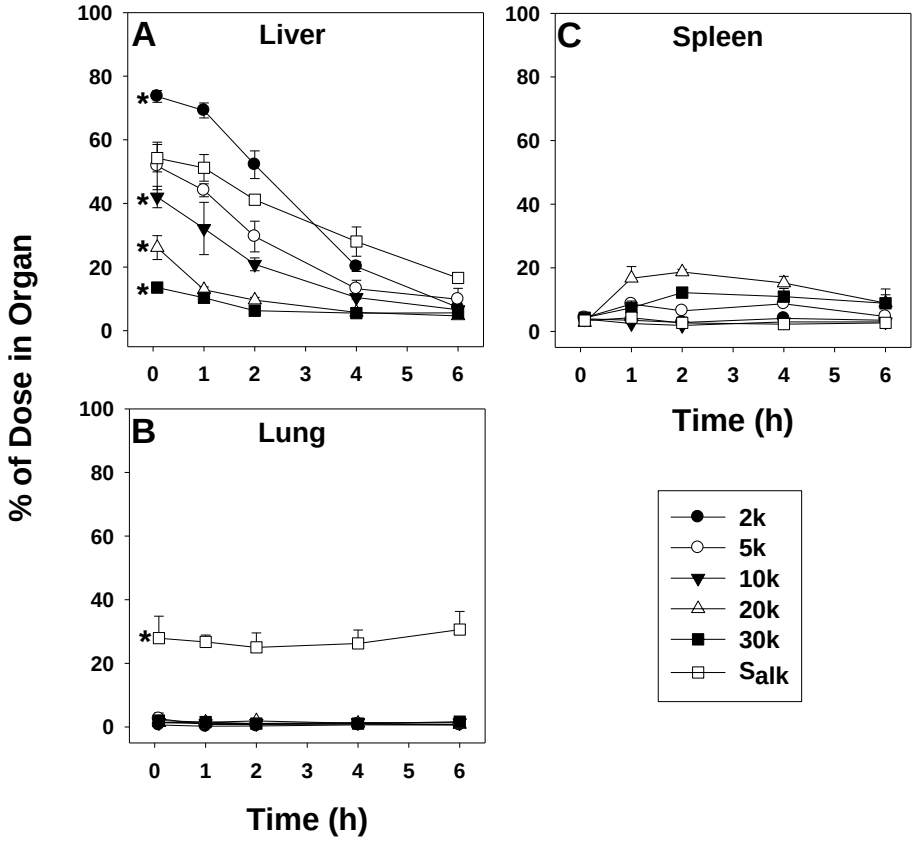

Figure 4-6: *Biodistribution (BD) Analysis of PEGylated Polyacridine Peptide Polyplexes with varied PEG Length.* BD was performed in mice with ^{125}I-pGL3 polyplexes at a stoichiometry of 0.8 nmol peptide μg^{-1} DNA. Results of $\mathbf{S_{alk}}$**, 2k, 5k, 10k, 20k,** and **30k** polyplexes in liver (panel A), lung (panel B), and spleen (panel C) are presented. The results show sustained presence of $\mathbf{S_{alk}}$ polyplexes in the lung and decrease in liver uptake as PEG length is increased from 2 to 30 kDa. Results are the mean and standard deviation of triplicate mice. Asterisks indicate statistical significance ($p \leq 0.05$) at 5 min when compared with **5k**.

Attaching PEG via a maleimide linkage to either the C-terminal (**5k**) or N - terminal (**N5k**) Cys residue resulted in only small differences in DNA binding affinity (Figure 4-2B), and no significant change in particle size, zeta potential (Figure 4-3A and B), PKs (Figure 4-5B) or HS gene expression profiles (Figure 4-4B). While attachment of PEG to a Cys placed in the center of the polyacridine peptide (**Mid5k**) resulted in a slight decrease in the apparent DNA binding affinity (Figure 4-2B), this did not did influence the particle size, zeta potential (Figure 4-3A and B) or PKs (Figure 4-5B). **Mid5k** polyplexes did mediate five-fold less expression versus **5k** and **Mid5k** polyplexes at HS expression at delay times of 4, 5, and 7 hrs (Figure 4-4B). Therefore, it can be concluded that PEG attachment at the C or N-terminus has a negligible effect on polyplex performance in HD-stimulated gene expression whereas placement of the PEG in the middle of polyacridine peptide results in decreased gene transfer efficiency.

PEG density was increased by polyplexing pGL3 with **Bis5k**. Increasing PEG density in this manner is attractive for combating changes in surface charge as the peptide sheds in the circulation [15]. Although no apparent difference in particle size or zeta potential was observed when compared with **5k** (Figure 4-3A and B), these polyplexes showed greater HS expression at extended time points with ~10-fold expression above background at 9 h, which is an increase over the background expression observed for **5k** at the same time point (Figure 4-4A versus B).

Increasing the PEG density via **Bis5k** led to an improvement in the duration of expression at extended times (9 h). If the peptide moiety of **Bis5k** sheds at the same rate as **5k**, twice the amount of PEG remains to better stealth the dynamic polyplex surface charge against Kupffer cell uptake or DNase metabolism. This result is favorable as high levels of expression were also observed at early time points demonstrating intracellular release.

Discussion

It is well established that PEG is of great importance in making therapeutic agents, such as proteins, compatible with conditions in the circulatory system [75]. In Chapter 3, the stability of PEGylated polyacridine polyplexes *in vivo* as it relates to parameters of the PEG moiety were found to be greatly influenced by the choice of linker. Length, site of attachment, and loading density of PEG were investigated in this study to determine their respective influences on PK, biodistribution, and HS expression.

The PEG length is known to influence the PK of liposomal formulations [151]; however this relationship is less defined for DNA polyplexes. The results establish that **2k** mediates a significantly shortened PK half-life, increased liver uptake (70%) and 100-fold loss in HS gene expression relative to **5k**. However, it is evident that **2k** provides some stealthing to the polyplex surface because it is not sequestered in the lung as is the case without PEG (**S_{alk}**). The reason why **10k, 20k,** and **30k** mediate five-fold lower HS gene expression relative to **5k** at delay times of 1 hr is not clear, but is most likely due to less efficient delivery to hepatocytes and release of pGL3 in the nucleus, and not related to biodistribution. Premature shedding of these PEG-peptides in the circulation is also unlikely given the high affinity and stable HS luciferase expression profiles they provide (Figure 4-4A).

Although diameter increases were not detected as PEG molecular weight was increased, it is possible that fully hydrated PEG that is not associated with the polyplex core is not scattering light in a detectable manner. Size measurements are not possible for naked dsDNA because the light scattering of conventional instruments using a 90˚ angle is not enough to be detected by QELS [152]. Studies with PEGylated proteins using size exclusion chromatography have reported substantial linear increases in hydrodynamic volume coinciding with increases in PEG molecular weight [75]. By inference, the actual hydrodynamic volume of PEGylated polyplexes using a 30 kDa PEG will be much larger than polyplexes relying on 2, 5, 10, or 20 kDa PEG for stealthing when using the same

peptide. This concept is further supported by the **Bis5k** result, which possesses two PEGs with length equivalent to 5 kDa. This peptide has 10 kDa PEG mass total but exhibits expression equivalent to **5k** at 1-5 h HS (Figure 4-4A and B).

Although the polyplexes are likely too large to pass through liver fenestrae, the finding that a 30 kDa PEG is able to stealth DNA polyplexes to nearly completely avoid liver uptake (13 % of dose) is of fundamental importance for the development of targeted delivery systems [153]. Kupffer cells have access to the bloodstream [20], but a clear systematic progression of decreasing liver uptake as PEG length increases suggests that stable polyplexes with a stealth layer of 30 kDa PEG can avoid Kupffer cell recognition in the liver (Figure 4-6A).

The influence of PEG location on a peptide in relationship to polyplex PK and *in vivo* gene expression has not been previously reported. Installing PEG_{5kDa} on the C-terminal or N-terminal Cys residue of a polyacridine peptide results in no detectable change in PK or the level of HS gene expression (Figures 4-4B and 4-5B). Conversely, locating the PEG in the middle of the peptide does not influence the level of gene expression at HS times of 1-3 h but does decrease expression five-fold at HD-stimulation times of 4-7 h. The reason for the observed decrease in expression is likely due to a weaker binding affinity of the peptide for DNA caused by a steric interruption of PEG in the binding sequence of four Acr residues spaced by four Lys residues.

It is likely that the underlying mechanism of HS gene expression is the same as HD dosing [31, 33, 34, 154], both of which transfect liver hepatocytes following a rapid delivery of a large volume of saline. The primary difference is that HS utilizes PEGylated polyplexes that are stable in the circulation for hours, whereas HD dosing uses naked plasmid DNA which has a metabolic half-life of minutes in the circulation.

Table 4-3. *Biodistribution of PEGylated Polyacridine Peptide Polyplexes Varying PEG Size.*

	Time (Min)	Blood	Liver	Lung	Spleen	Stomach	Kidney	Heart	SI	LI	Total
^{125}I-pGL3	5	14.4 ± 5.8	65.7 ± 2.5	6.1 ± 2.2	2.8 ± 0.3	0.2 ± 0.0	0.9 ± 0.2	0.1 ± 0.0	0.2 ± 0.1	0.4 ± 0.1	84.7 ± 11.2
	60	5.2 ± 1.6	12.7 ± 2.0	0.9 ± 0.2	1.3 ± 0.2	4.5 ± 1.0	3.5 ± 0.6	0.2 ± 0.0	1.1 ± 0.2	2.1 ± 0.3	31.5 ± 6.4
	120	5.2 ± 1.5	6.1 ± 1.5	0.5 ± 0.2	0.8 ± 0.2	9.4 ± 3.2	1.6 ± 0.9	0.1 ± 0.1	0.3 ± 0.2	0.4 ± 0.1	28.2 ± 8.9
S_{alk}	5	4.5 ± 0.7	54.2 ± 4.3	27.9 ± 6.9	3.4 ± 1.3	0.3 ± 0.0	0.5 ± 0.2	0.2 ± 0.1	0.4 ± 0.1	0.2 ± 0.1	91.7 ± 13.7
	120	2.3 ± 0.3	41.1 ± 1.3	25.0 ± 4.6	2.7 ± 1.8	5.6 ± 1.7	0.7 ± 0.2	0.1 ± 0.1	1.5 ± 0.4	0.9 ± 0.7	80.0 ± 12.2
	360	nd	16.5 ± 1.1	30.6 ± 5.7	2.7 ± 0.5	5.5 ± 1.2	0.6 ± 0.1	0.0± 0.0	1.3 ± 0.3	0.8 ± 0.4	58.3 ± 9.3
2k	5	26.4 ± 3.2	73.7 ± 1.9	0.7 ± 0.1	4.0 ± 0.8	0.2 ± 0.1	0.5 ± 0.1	0.2 ± 0.1	0.3 ± 0.1	0.1 ± 0.0	106.0 ± 6.3
	120	14.8 ± 1.7	52.2 ± 4.3	0.3 ± 0.1	2.8 ± 0.3	5.3 ± 0.8	0.8 ± 0.1	0.1 ± 0.0	1.3 ± 0.2	0.8 ± 0.2	78.5 ± 7.7
	360	nd	7.3 ± 0.8	0.6 ± 0.1	3.5 ± 0.9	10.4 ± 1.9	1.3 ± 0.1	0.1 ± 0.0	3.0 ± 0.6	1.7 ± 0.7	28.0 ± 5.1
5k	5	47.9^{+}5.3	51.8^{+}7.5	2.6^{+}1.8	4.3^{+}0.8	0.4^{+}0.2	1.0^{+}0.5	0.3^{+}0.1	0.4^{+}0.1	0.2^{+}0.1	108.3±16.6
	120	32.0^{+}2.8	29.6^{+}4.8	0.8^{+}0.1	6.5^{+}0.6	4.3^{+}0.8	1.7^{+}0.6	0.2^{+}0.1	1.6^{+}0.6	0.9^{+}0.1	77.5±10.5
	360	nd	10.0 ± 3.4	0.7 ± 0.2	4.7 ± 2.9	9.4 ± 3.6	1.0 ± 0.3	0.2 ± 0.1	2.2 ± 0.4	1.2 ± 0.1	29.4 ± 11.0
10k	5	58.8± 2.3	42.1 ± 3.3	1.4 ± 0.3	3.9 ± 0.1	0.3 ± 0.1	0.7 ± 0.1	0.3 ± 0.0	0.8 ± 0.3	0.3 ± 0.0	108.6 ± 6.5
	120	35.3 ± 1.7	20.9 ± 2.1	1.2 ± 0.4	1.9 ± 0.5	1.9 ± 0.6	1.0 ± 0.2	0.3 ± 0.0	1.2 ± 0.1	0.7 ± 0.1	64.4 ± 5.7
	360	nd	6.6 ± 1.2	1.4 ± 0.1	3.0 ± 0.9	7.9 ± 1.0	2.6 ± 0.1	0.3 ± 0.1	2.3 ± 0.1	1.3 ± 0.2	25.4 ± 3.7
20k	5	66.5 ± 2.2	26.1 ± 3.8	1.4 ± 0.1	2.8 ± 0.2	0.4 ± 0.1	2.0 ± 0.1	0.6 ± 0.2	1.0 ± 0.1	0.6 ± 0.1	85.7 ± 7.4
	120	41.3 ± 4.4	9.6 ± 0.9	1.9 ± 0.6	18.7 ± 0.8	2.7 ± 0.5	1.6 ± 0.2	0.2 ± 0.1	2.3 ± 0.2	1.0 ± 0.1	78.4 ± 9.2
	360	nd	4.7 ± 0.7	0.8 ± 0.1	8.9 ± 2.6	6.5 ± 0.8	2.0 ± 0.1	0.4 ± 0.1	2.4 ± 0.3	1.2 ± 0.1	28.2 ± 3.5
30k	5	68 ± 4.0	13.6 ± 0.7	2.0 ± 0.5	4.3 ± 1.0	0.4 ± 0.1	1.9 ± 0.3	0.3 ± 0.1	1.1 ± 0.3	0.8 ± 0.3	92.4 ± 7.3
	120	43.1 ± 3.7	6.3 ± 0.4	1.1 ± 0.2	12.2 ± 1.5	3.0 ± 0.8	1.2 ± 0.4	0.2 ± 0.0	1.4 ± 0.9	1.0 ± 0.3	69.5 ± 8.2
	360	nd	5.6 ± 0.4	1.7 ± 0.3	8.8 ± 4.5	5.2 ± 2.3	2.3 ± 0.1	0.3 ± 0.0	2.4 ± 0.2	0.9 ± 0.1	27.2 ± 7.9

Values are reported as % of dose and were determined by cpm of pharmacokinetic and biodistribution samples.

In conclusion, an optimal PEG length of 5 kDa linked to a C- or N-terminal Cys of polyacridine peptides through a maleimide linkage (**5k** or **N5k**, respectively) results in PK and biodistribution properties that translate to maximal HS gene expression when applied at up to 4-5 h post-DNA delivery. Disruption of the binding motif by central placement of PEG causes some loss in HS expression at extended times (≥ 4 h). Increasing the PEG length leads to corresponding reductions in liver biodistribution with 30 kDa blocking most of the polyplex uptake by the liver, but the majority of stimulated gene expression in the liver is retained. From these observations, it is apparent that PEG plays a major role in polyplex circulation and expression, and changes to this moiety have a substantial effect on polyplex use *in vivo*. The reported relationships of PK, biodistribution, and HS gene expression should be considered in the optimization of future PEGylated non-viral gene delivery carriers.

CHAPTER 5: RESEARCH SUMMARY

Although progress has been made in gene delivery with the first application slated for release later this year in the Europe, it is still evident that development of a safe, circulating, and generally applicable carrier system for gene delivery will require further research. This is especially the case in non-viral gene delivery where numerous barriers require a finely tuned molecule to interact strongly and reversibly with DNA and maintain polyplex characteristics (size and charge) that allow for circulatory stability, tissue absorption through vascular endothelium, and uptake and expression by cells (Figure 5-1). Polyacridine peptides were developed as an amendable platform for addressing gene delivery barriers systematically. The goal of this thesis was to address the development of a non-viral gene delivery carrier in a ground-up approach, which was pursued via the improvement of circulatory stability of polyplexes made with polyacridine peptides.

Because *in vitro* development leads to creation of polyplexes that do not meet the challenges presented *in vivo*, it was necessary to have a calibrated assay that provides feedback in an *in vivo* model. Previous work by the Rice group led to the development of hydrodynamic stimulation (HS) and detection of polyplexed pGL3 (luciferase) gene expression via bioluminescence imaging (BLI) in mouse liver [38, 40]. HS is a powerful investigative tool that allows the expression of circulating DNA polyplexes with reversibly-bound carriers.

Using HS and corresponding data from pharmacokinetic (PK), biodistribution (BD), and particle characterization assays, it was possible to refine PEGylated polyacridine peptides to provide increasing circulatory stability to polyplexes. Initial studies addressed the amount of Acr, a Lys residue with acridine bound at the ε-amine, incorporation using the motif $(Acr\text{-}Lys)_n$-Cys-mal-PEG_{5kDa}, where n = 2, 4, or 6, and found six acridines to be optimal in providing complete HS expression for 1 h. Variation

of the spacing residue was also examined in $(Acr\text{-}X)_4$-Cys, where X was Glu, Leu, Lys, or Arg, and was found to affect affinity such that Lys > Arg > Leu > Glu [9].

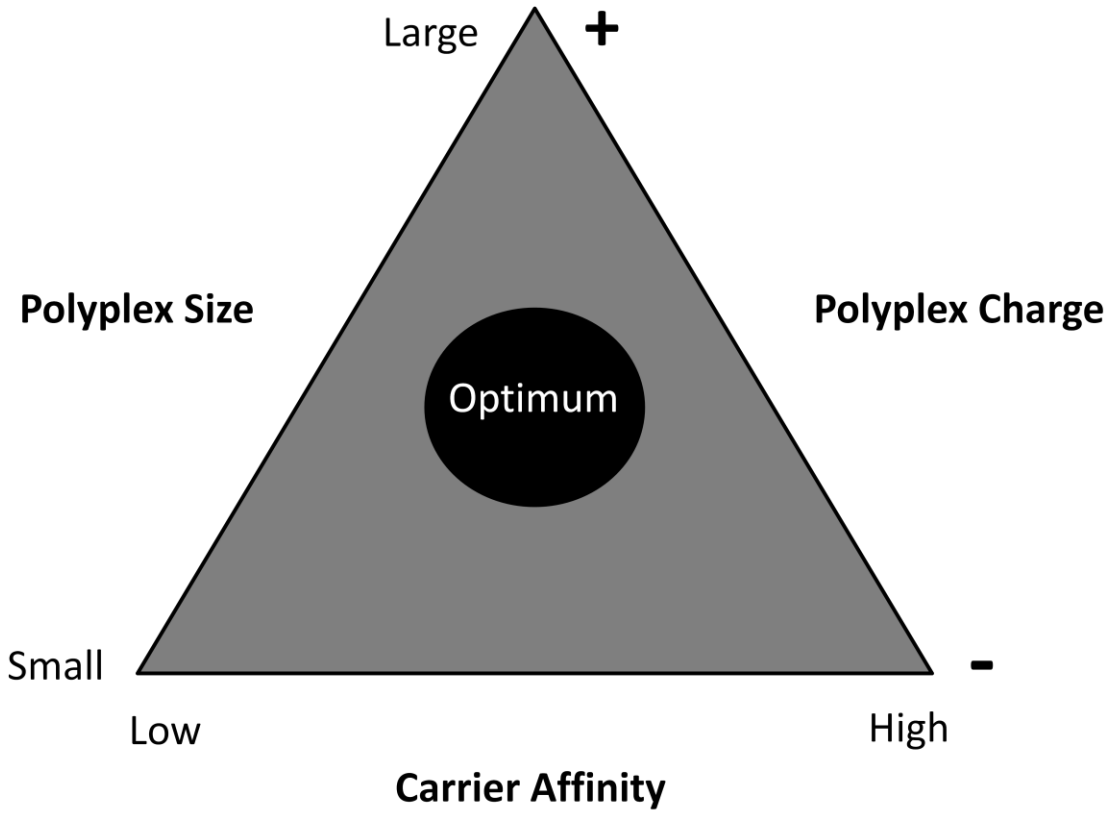

Figure 5-1. *Optimal Characteristics of a Non-Viral Gene Delivery Carrier*. The diagram illustrates the design criteria a non-viral gene delivery carrier needs to meet in order to create expressible, circulating polyplexes with the black circle representing the optimal region for balancing these attributes. The carrier must have high enough affinity for DNA to prevent rapid dissociation in the bloodstream but low enough to allow expression of the desired gene. Polyplex size must be large enough to avoid renal filtration (>10 nm) but small enough to allow escape from the vasculature to the site of action (<100 nm depending on type of normal tissue). Finally, if polyplex charge is too extreme (+ or -), Kupffer cell uptake will prevail. High positive charge also causes albumin binding, aggregation, and aberrant biodistribution.

Although these advances provided insight into the requirements needed to address stability of systemically administered polyplexes, many other aspects of the polyacridine

peptides presented still remained to be explored. As addressed in Chapter 2, one possible route for improvement was a structure-activity relationship study of the spacing Lys residues and their effect on HS gene expression. The nearest-neighbor exclusion principle states that the distance between polyintercalators on either end of a linear molecule must be $\geq$ 10.2 Å, which stems from the observation that most calculations of intercalator studies exhibit binding that would only occupy half of the available sites on a given DNA molecule [92]. The distance between side chain branching points of Acr residues on the original motif, $(Acr\text{-}Lys)_n$-Cys where n is 2 or greater, is 6.8 Å. Additionally, observations by Ueyama *et al*. indicated that inclusion of at least two Lys between Acr residues in a similar peptide allowed for complete intercalation of all intercalators simultaneously [59, 60].

Based on these premises and previous work by our group [9], spacing of Acr by Lys residues in PEGylated polyacridine peptides were investigated using the four Acr peptide, $(Acr\text{-}Lys_n)_3$-Acr-Lys-Cys, where n=1-6. The use of polyplexes *in vivo* formed with this peptide series (modified at the C-terminus with maleimide-PEG_{5kDa}) uncovered many important clues to the requirements of circulatory stability. As n was increased, corresponding increases in the stability of polyplexes were observed in pharmacokinetics and HS gene expression, where expression equivalent to HD of naked pGL3 was observed for 5 h when n=4 or 5. Stable HS expression was observed for n=6 but at a reduced level. Though inadequate intracellular release was initially suspected as the reason for result, the most likely cause was Kupffer cell uptake triggered by the high surface charge (+21 mV) of these particles. This was supported by the observation that liver biodistribution showed increases corresponding with the increasing surface charge of the polyplexes as n is increased and that peptide **6** produces expression equivalent to naked pGL3 under HD (Figure 2-7A). Comparisons of peptides **4, 4Ac,** and **R1** established a need for multiple modes of binding to DNA via intercalation and ionic

interaction to achieve stable, circulating polyacridine peptide polyplexes (Figure 2-7 and 2-9).

Chapter 2 also addressed other parameters such as stoichiometry, use of D-Lys residues for proteolytic stability, and dose dependency as demonstrated by 'decoy' dosing. Increased stoichiometry of peptides to form polyplexes was previously found to lead to tighter 'closed' polyplexes (0.8 nmol peptide μg^{-1} DNA) versus 'open' polyplexes at lower stoichiometries (0.2 nmol peptide μg^{-1} DNA) (Figure 2-4) [9], and use of a higher stoichiometry to allow for consistent comparison of all peptides was found to provide much greater stability to polyplexes in the bloodstream (Figure 2-9A). Peptides with D-Lys spacing residues were found to hinder both HD and 5 min HS gene expression in the case of peptides **4D** and **6D** (Figure 2-7), which correlated with less favorable affinity and particle characteristics (Figures 2-5 and 2-6). Acr residues used in **4D** and **6D** were still synthesized from L-Lys, and it is suspected that the new configuration as influenced by the D-Lys side chains may cause an unfavorable presentation of the acridine moieties for intercalation.

After establishing that peptide **4** could provide maximal expression to about 5 h under HS at 0.8 nmol peptide μg^{-1} DNA, the issue of shedding of the peptide from the polyplex in the circulation was investigated (Figure 2-10). Co-administration of 1 µg pGL3 polyplex with varying amounts of pSEAP polyplex (decoy) up to 9 µg established a dose dependent relationship of polyplex amount with HS expression, and the use of 9 µg pSEAP (10 µg DNA polyplex total) allowed full expression to be observed after 9 h. One µg doses of pGL3 polyplex were used for many reasons the most important of which were consistency for the sake of comparison and the dose being more relevant to use in humans. However, as indicated by the decoy experiments in Chapter 2, the 1 µg of effective polyplex (pGL3) must experience altered biodistribution or be degraded at a slower rate due to the occupancy of nucleases as a result of added polyplex. PK and BD

studies of the dose dependency of peptide **4** polyplex could provide some interesting clues about the 'decoy' effect.

Prior investigations of PEGylated polyacridine peptides focused on changes to the peptide moiety. Some evidence of the reversal of maleimide bonds in the presence of glutathione was recently reported [132]. In Chapter 3, the linkage that bound PEG to the peptide was investigated as premature release of PEG from polyplexes would lead to decreased circulatory stability. Using 5 kDa PEG, six linkages were examined: the original Cys-maleimide (**SM**), Cys-disulfide (**SS**), Cys-vinyl sulfone (**SV**), and Cys-acetamide (**SA**) and the penicillamine derivatives, Pen-maleimide (**PM**) and Pen-disulfide (**PS**). While it was discovered that **SM** was one of the most stable linkages along with **PS** and **PM**, other linkages known to be chemically stable, **SV** and **SA**, showed a reduced ability to allow pGL3 polyplexes to be expressed by HS. This was accompanied by a notable reduction in circulatory stability as evidenced by PK studies in which **SV** and **SA** polyplexes were shown to be less stable than polyplexes with the reducible **SS** linker. It is evident that use of PEG without careful optimization of the type of linker used could have dramatic effects on the stability of a PEGylated polyplex *in vivo*.

Because of the dramatic results in from the PEG linker study, other parameters of the PEG moiety were addressed and reported in Chapter 4. The length of linear PEG was altered by use of maleimide-PEGs of average molecular weight 2, 5, 10, 20, and 30 kDa which were conjugated to $(Acr\text{-}Lys_4)_3$-Acr-Lys-Cys to obtain **2k, 5k, 10k, 20k,** and **30k**, respectively. As polyplex PEG size was increased, liver biodistribution decreased indicating an avoidance of Kupffer cell uptake. This could be a result of better charge masking as indicated by zeta potential analysis. The hydrodynamic volume of PEG is known to increase with molecular weight as has previously been demonstrated in PEGylated proteins by size exclusion chromatography [155]. It is possible that a size increase, undetected by QELS, is inhibiting Kupffer cell uptake and filtration from the

vasculature. **2k** polyplex had a high surface charge as a result of inadequate charge masking, which resulted in a substantial loss of HS gene expression. While higher PEG sizes provided sustained HS expression at extended times (up to 7 h), **10k, 20k,** and **30k** polyplexes showed reduced ability to mediate HS expression when compared to **5k**.

Position of a maleimide-PEG_{5kDa} was also examined in Chapter 4 by conjugation to the N-terminus (**N5k**) and center (**Mid5k**) of the polyacridine peptide, and PEG density was increased by conjugating two PEGs to the N- and C-termini of the peptide (**Bis5k**). Changing the site of conjugation to the polyacridine peptide only caused a slight loss of HS expression in the case of **Mid5k**. **Bis5k** polyplexes mediated high levels of HS gene expression at early time points and were able to mediate measurable levels of expression at 9 h, an improvement over the use of one 5 kDa PEG at the N- or C-terminus on the same peptide. Increasing the density versus the length of PEG bound to polyacridine peptides appears to have a better ability to stabilize polyplexes in the circulation. This may also indicate the use of branched PEGs might be favored over linear PEGs to increase PEG substitution when considering molecular weight.

The purpose of this thesis was extension of the stability of circulating polyplexes through systematic modification of PEGylated polyacridine peptides, and this was achieved through modification of the polyacridine peptide sequence. While investigation of the PEG moiety resulted in no further optimization over the use of the maleimide-PEG_{5kDa}, the selection of this particular PEG was serendipitous as issues of linkage and size can have dramatic effects on the properties of PEGylated polyacridine peptides. The work presented also demonstrates the utility of HS expression to assist the development of gene delivery carrier structure *in vivo*.

Although polyacridine peptides show some promise to allow development for overcoming the next gene delivery barrier of tissue targeting, the issue of size will have to be addressed before this becomes feasible. Size is likely preventing PEGylated polyacridine polyplexes from exiting the circulation and allowing them to avoid first-pass

metabolism for a time. As was stated before, tumors exhibit the enhanced permeability and retention (EPR) effect by which it has been observed that larger particles (≤ 400 nm) are permitted to pass through the vasculature [21]. PEGylated polyacridine peptide polyplexes could provide a viable option for *in vivo* gene delivery to tumors.

While 9-aminoacridine or the polyacridine peptides presented may not possess high toxicity, use of unnatural intercalators as gene delivery agents would be met with resistance if clinical approval was sought. However, acridine has proved a useful tool in examining the need for multiple modes of binding for *in vivo* delivery. It is possible that substitution of this moiety for another intercalator may prove just as efficient at providing circulatory stability for polyplexed DNA *in vivo*. For example, while much weaker in intercalative interaction than acridine, the side chains of Tyr, Trp, and Phe possess some ability to intercalate DNA and would provide natural substitutes for Acr [102-106]. Although it is evident that multiple modes of reversible binding are required, it may not be necessary for ionic interaction and intercalation to be the sole combination to achieve circulatory stability. One may also envision the incorporation of hydrophobic residues to provide this additional interaction with DNA in concert with these modes or as a replacement for one of them. It might also be possible to use hydrophobic interaction as a way to balance the resultant zeta potential by replacement of some cationic residues as it is evident that high zeta potentials in either direction appear to lead to Kupffer cell uptake. Polyacridine peptides have proven a versatile and useful tool for probing the requirements of polyplex stability and expression *in vivo*. Further optimization to address issues of polyplex size and charge as well as the proper incorporation of targeting and fusogenic moieties could lead to a non-viral carrier that permits expression after systemic dosing without the aid of physical methods.

REFERENCES

1. Park, T. G., J. H. Jeong, and S. W. Kim. 2006. Current status of polymeric gene delivery systems. *Adv. Drug. Deliv. Rev.* 58(4):467-486.

2. Fernandez, C. A., and K. G. Rice. 2009. Engineered Nanoscaled Polyplex Gene Delivery Systems. *Molecular Pharmaceutics* 6(5):1277-1289.

3. Glover, D. J., H. J. Lipps, and D. A. Jans. 2005. Towards safe, non-viral therapeutic gene expression in humans. *Nat Rev Genet* 6(4):299-310.

4. Friedman, T., and R. Roblin. 1972. Gene therapy for human genetic disease. *Science* 175:949-955.

5. Yla-Herttuala, S. 2012. Endgame: Glybera finally recommended for approval as the first gene therapy drug in the European Union. *Mol. Ther.* 20(10):1831-1832.

6. Davis, M. E., J. E. Zuckerman, C. H. J. Choi, D. Seligson, A. Tolcher, C. A. Alabi, Y. Yen, J. D. Heidel, and A. Ribas. 2010. Evidence of RNAi in humans from systemically administered siRNA via targeted nanoparticles. *Nature* 464:1067-1070.

7. Tabernero, J., G. I. Shapiro, P. M. LoRusso, A. Cervantes, G. K. Schwartz, G. J. Weiss, L. Paz-Ares, D. C. Cho, J. R. Infante, M. Alsina, M. M. Gounder, R. Flazone, J. Harrop, A. C. S. White, I. Toudjarska, D. Bumcrot, R. E. Meyers, G. Hinkle, N. Svrzikapa, R. M. Hutabarat, V. A. Clausen, J. Cehelsky, S. V. Nochur, C. Gamba-Vitalo, A. K. Vaishnaw, D. W. Y. Sah, J. A. Gollob, and H. A. Burris III. 2013. First-in-man trial of an RNA interference therapeutic targeting VEGF and KSP in cancer patients with liver involvement. *Cancer Discovery* 3(4):406-417.

8. Collard, W. T., Y. Yang, K. Y. Kwok, Y. Park, and K. G. Rice. 2000. Biodistribution, metabolism, and *in vivo* gene expression of low molecular weight glycopeptide polyethylene glycol peptide DNA co-condensates. *Journal of Pharmaceutical Sciences* 89(4):499-512.

9. Fernandez, C. A., N. J. Baumhover, J. T. Duskey, S. Khargharia, K. Kizzire, M. D. Ericson, and K. G. Rice. 2011. Metabolically stabilized long-circulating PEGylated polyacridine peptide polyplexes mediate hydrodynamically stimulated gene expression in liver. *Gene Therapy* 18:23-37.

10. Dash, P. R., M. L. Read, L. B. Barrett, M. A. Wolfert, and L. W. Seymour. 1999. Factors affecting blood clearance and in vivo distribution of polyelectrolyte complexes for gene delivery. *Gene Therapy* 6:643-650.

11. Oupicky, D., C. Konak, P. R. Dash, L. W. Seymour, and K. Ulbrich. 1999. Effect of albumin and polyanion on the structure of DNA complexes with polycation containing hydrophilic nonionic block. *Bioconjug Chem* 10(5):764-72.

12. Yu, W., N. Zhang, and C. Li. 2009. Saccharide modified pharmaceutical nanocarriers for targeted drug and gene delivery. *Curr. Pharm. Des.* 15:3826-3836.

13. Edinger, D., and E. Wagner. 2011. Bioresponsive polymers for the delivery of therapeutic nucleic acids. *Wiley Interdisciplinary Reviews Nanomedicine and Nanobiotechnology* 3(1):33-46.

14. Samal, S. K., M. Dash, S. V. Vlierberghe, D. L. Kaplan, E. Chiellini, C. V. Blitterswijk, L. Moroni, and P. Dubruel. 2012. Cationic polymers and their therapeutic potential. *Chem. Soc. Rev.* 41:7147-7194.

15. Kizzire, K., S. Khargharia, and K. G. Rice. 2013. High-Affinity PEGylated polyacridine peptide polyplexes mediate potent *in vivo* gene expression. *Gene Therapy* 20:407-416.

16. Adami, R. C., W. T. Collard, S. A. Gupta, K. Y. Kwok, J. Bonadio, and K. G. Rice. 1998. Stability of peptide-condensed plasmid DNA formulations. *J. Pharm. Sci.* 87(6):678-683.

17. McKenzie, D. L., E. Smiley, K. Y. Kwok, and K. G. Rice. 2000. Low molecular weight disulfide cross-linking peptides as nonviral gene delivey carriers. *Bioconjugate Chemistry* 11:901-909.

18. Wadhwa, M. S., W. T. Collard, R. C. Adami, D. L. McKenzie, and K. G. Rice. 1997. Peptide-mediated gene delivery: influence of peptide structure on gene expression. *Bioconjugate Chemistry* 8(1):81-8.

19. Jacobs, F., E. Wisse, and B. De Geest. 2010. The role of liver sinusoidal cells in hepatocyte-directed gene transfer. *Am J Pathology* 176(1):14-21.

20. McCuskey, R. S. 2008. The hepatic microvascular system in health and its response to toxicants. *The Anatomical Record* 291:661-671.

21. Yuan, F., M. Dellian, D. Fukumura, M. Leunig, D. Berk, V. Torchilin, and R. Jain. 1995. Vascular permeability in a human tumor xenograft: molecular size dependence and cutoff size. *Cancer Research* 55:3752-3756.

22. Fang, J., H. Nakamura, and H. Maeda. 2011. The EPR effect: unique features of tumor blood vessels for drug delivery, factors involved, and limitations and augmentation of the effect. *Adv. Drug. Deliv. Rev.* 63:136-151.

23. Rettig, G. R., and K. G. Rice. 2007. Non-viral gene delivery: from the needle to the nucleus. *Expert Opin Biol Ther* 7(6):799-808.

24. Dean, D. A., D. D. Strong, and W. E. Zimmer. 2005. Nuclear entry of nonviral vectors. *Gene Therapy* 12:881-890.

25. Liang, K. W., M. Nishikawa, F. Liu, B. Sun, Q. Ye, and L. Huang. 2004. Restoration of dystrophin expression in mdx mice by intravascular injection of naked DNA containing full-length dystrophin cDNA. *Gene Therapy* 11:901-908.

26. Liu, F., Y. Song, and D. Liu. 1999. Hydrodynamics-based transfection in animals by systemic administration of plasmid DNA. *Gene Ther* 6(7):1258-66.

27. Sato, Y., T. Ajiki, S. Inoue, Y. Hakamata, T. Murakami, T. Kaneko, M. Takahashi, and E. Kobayashi. 2003. A novel gene therapy to the graft organ by rapid injection of naked DNA I: long-lasting gene expression in a rat model of limb transplantation. *Transplantation* 76:1294-1298.

28. Song, J., J. C. Chappell, M. Qi, E. J. Van Gieson, S. Kaul, and R. J. Price. 2002. Influence of injection site, microvascular pressure and ultrasound variables on microbubble-mediated delivery of microspheres to muscle. *J Am Coll Cardiol* 39:726-731.

29. Suzuki, T., B. C. Shin, K. Fujikura, T. Matsuzaki, and K. Takata. 1998. Direct gene transfer into rat liver cells by *in vivo* electroporation. *FEBS Lett* 425:436-440.

30. Weecharangsan, W., P. Opanasopit, and R. J. Lee. 2007. *In vitro* gene transfer using cationic vectors, electroporation and their combination. *Anticancer Research* 27:309-313.

31. Lecocq, M., F. Andrianaivo, S. Wattiaux-De Coninck, R. Wattiaux, and M. Jadot. 2004. Hydrodynamics-based transfection of the liver: entrance into hepatocytes of DNA that causes expression takes place very early after injection. *Journal of Gene Medicine* 6(8):877-83.

32. Suda, T., K. Suda, and D. Liu. 2008. Computer-assisted hydrodynamic gene delivery. *Mol. Ther.* 16(6):1098-1104.

33. Zhang, G., X. Gao, Y. K. Song, R. Vollmer, S. D.B., J. Z. Gaskowski, D. A. Dean, and D. Liu. 2004. Hydroporation as the mechanism of hydrodynamic delivery. *Gene Ther.* 11:675-682.

34. Budker, V. G., V. M. Subbotin, T. Budker, M. G. Sebestyen, G. Zhang, and J. A. Wolff. 2006. Mechanism of plasmid delivery by hydrodynamic tail vein injection. II. Morphological studies. *J Gene Med* 8(7):874-888.

35. Kamimura, K., T. Suda, W. Xu, G. Zhang, and D. Liu. 2009. Image-guided, lobe-specific hydrodynamic gene delivery to swine liver. *Molecular Therapy* 17(3):491-499.

36. Jaing, X., H. Dai, K. Leong, S. Goh, H. Q. Mao, and Y. Y. Yang. 2006. Chitosan-g-PEG/DNA complexes deliver gene to the rat liver via intrabiliary and intraportal infusions. *J Gene Med* 8:477-487.

37. Tada, Y., T. Kitahara, T. Yoshioka, T. Nakamura, N. Ichikawa, M. Nakashima, K. Nishida, J. Nakamura, and H. Sasaki. 2006. Partial hepatectomy enhances polyethylenimine-mediated plasmid DNA delivery. *Biol Pharm Bull* 29(8):1712-1716.

38. Rettig, G., M. McAnuff, J. Kim, D. Liu, and K. G. Rice. 2006. Quantitative Bioluminscence Imaging of Transgene Expression In Vivo. *Analytical Biochemistry* 335:90-94.

39. Liu, F., and L. Huang. 2002. Noninvasive gene delivery to the liver by mechanical massage. *Hepatology* 35:1314-1319.

40. Chen, C. P., J. S. Kim, D. Liu, G. R. Rettig, M. A. McAnuff, M. E. Martin, and K. G. Rice. 2007. Synthetic PEGylated Glycoproteins and Their Utility in Gene Delivery. *Bioconjugate Chemistry* 18(2):371-378.

41. Akinc, A., M. Thomas, A. M. Klibanov, and R. Langer. 2005. Exploring polyethylenimine-mediated DNA transfection and the proton sponge hypothesis. *J Gene Med* 7:657-663.

42. Kichler, A., C. Lebrogne, and O. Danos. 2005. Dilution of reporter gene with stuffer DNA does not alter the transfection efficiency of polyethylenimines. *J Gene Med* 7:1459-1467.

43. Zintchenko, A., A. Philipp, A. Dehshahri, and E. Wagner. 2008. Simple modifications of branched PEI lead to highly efficient siRNA carriers with low toxicity. *Bioconjugate Chemistry* 19:1448-1455.

44. Fitzsimmons, R. E., and H. Uludag. 2012. Specific effects of PEGylation on gene delivery efficacy of polyethylenimine: Interplay between PEG substitution and N/P ratio. *Acta Biomater* 8(11):3941-3955.

45. Mao, S., M. Neu, O. Germershaus, O. Merkel, J. Sitterberg, U. Bakowsky, and T. Kissel. 2006. Influence of polyethylene glycol chain length on the physiochemical and biological properties of poly(ethylene imine)-graft-poly(ethylene glycol) block copolymer/siRNA polyplexes. *Bioconjugate Chemistry* 17(5):1209-1218.

46. Wu, G. Y., and C. H. Wu. 1987. Receptor-mediated *in vitro* gene transformation by a soluble DNA carrier system. *J Biol Chem* 262:4429-4432.

47. Wu, G. Y., and C. H. Wu. 1988. Evidence for targeted gene delivery to Hep G2 hepatoma cells *in vitro*. *Biochemistry* 27:887-892.

48. McKenzie, D. L., K. Y. Kwok, and K. G. Rice. 2000. A potent new class of reductively activated peptide gene delivery agents. *J Biol Chem* 275:9970-9977.

49. Midoux, P., and M. Monsigny. 1999. Efficient gene transfer by histidylated polylysine/pDNA complexes. *Bioconjugate Chemistry* 10:406-411.

50. McKenzie, D. L., W. T. Collard, and K. G. Rice. 1999. Comparative gene transfer efficiency of low molecular weight polylysine DNA-condensing peptides. *J Peptide Res* 54:311-318.

51. Adami, R. C., and K. G. Rice. 1999. Metabolic stability of glutaraldehyde cross-linked peptide DNA condensates. *Journal of Pharmaceutical Sciences* 88:739-746.

52. Parker, A. J., and N. Kharasch. 1959. The scission of the sufur-sulfur bond. *Chem Rev* 59(583-628).

53. Oupicky, D., R. C. Carlisle, and L. W. Seymour. 2001. Triggered intracellular activation of disulfide crosslinked polyelectrolyte gene delivery complexes with extended systemic circulation *in vivo*. *Gene Therapy* 8:713-724.

54. Trubetskoy, V. S., V. G. Budker, L. J. Hanson, P. M. Slattum, J. A. Wolff, and J. E. Hagstrom. 1998. Self-assembly of DNA-polymer complexes using template polymerization. *Nucleic Acids Res* 26:4178-4185.

55. Trubetskoy, V. S., A. Loomis, P. M. Slattum, J. E. Hagstrom, V. G. Budker, and J. A. Wolff. 1999. Caged DNA does not aggregate in high ionic strength solutions. *Bioconjugate Chemistry* 10:624-628.

56. Kwok, K. Y., D. L. McKenzie, D. L. Evers, and K. G. Rice. 1999. Formulation of highly soluble poly(ethylene glycol)-peptide DNA condensates. *J Pharm Sci* 88:996-1003.

57. Haensler, J., and J. F. C. Szoka. 1993. Synthesis and characterization of a trigalactosylated bisacridine compound to target DNA to hepatocytes. *Bioconjug. Chem.* 4(1):85-93.

58. Shiraishi, T., R. Hamzavi, and P. E. Nielsen. 2005. Targeted Delivery of Plasmid DNA into the Nucleus of Cells via Nuclear Localization Signal Peptide Conjugated to DNA Intercalating Bis- and Trisacridines *Bioconjugate Chemistry* 16(5):1112-1116.

59. Ueyama, H., M. Takagi, and S. Takenaka. 2002. Tetrakis-acridinyl peptide: a novel fluorometric reagent for nucleic acid analysis based on the fluorescence dequenching upon DNA binding. *Analyst* 127(7):886-8.

60. Ueyama, H., M. Takagi, M. Waki, and S. Takenaka. 2001. DNA binding behavior of peptides carrying acridinyl units: First example of effective poly-intercalation. *NUCLEIC ACIDS SYMP SER (OXF)* 1(1):163-164.

61. Ueyama, H., M. Waki, M. Takagi, and S. Takenaka. 2000. Novel synthesis of a tetra-acridinyl peptide as a new DNA polyintercalator. *Nucleic Acids Symp Ser*(44):133-4.

62. Chiu, F. C. K., R. T. C. Brownlee, and D. R. Phillips. 1993. Cupric ion chelation assisted synthesis of Nα–protected Nω–acridin-9-yl αω-diamino carboxylic acids. *Australian Journal of Chemistry* 46:1207-1212.

63. Tung, C., T. Zhu, H. Lackland, and S. Stein. 1992. An acridine amino acid derivative for use in Fmoc peptide synthesis. *Peptide Research* 5(2):115-8.

64. Prevette, L. E., M. L. Lynch, K. Kizjakina, and T. M. Reineke. 2008. Correlation of amine number and pDNA binding mechanism for trehalose-based polycations. *Langmuir* 24(15):8090-8101.

65. Yu, H., X. Chen, T. Lu, J. Sun, H. Tian, J. Hu, Y. Wang, P. Zhang, and X. Jing. 2007. Poly(L-lysine)-graft-chitosan copolymers: synthesis, characterization, and gene transfection effect. *Biomacromolecules* 8:1425-1435.

66. Morgan, A. R., D. H. Evans, J. S. Lee, and D. E. Pulleyblank. 1979. Review: ethidium bromide assay. Part II. Enzymatic studies and DNA-protein interactions. *Nucleic Acids Res* 7:571-594.

67. Wadhwa, M., D. L. Knoell, A. P. Young, and K. G. Rice. 1995. Targeted gene delivery with a low molecular weight glycopeptide. *Bioconjugate Chemistry* 6:283-291.

68. Urban, C., and P. Schurtenberger. 1998. Characterization of turbid colloidal suspensions using light scattering techniques combined with cross-correlation methods. *J Colloid and Interface Science* 207(1):150-158.

69. Zhang, L. S., E. G. Saravolac, J. J. Wheeler, P. Tardi, K. Clow, E. Leng, R. Sun, P. R. Cullis, and P. Scheerer. 1999. Stabilized plasmid-lipid particles for regional gene therapy: formulation and transfection properties. *Gene Therapy* 6:1438-1447.

70. Delgado, A. V., F. Gonzalez-Caballero, R. J. Hunter, L. K. Koopal, and J. Lyklema. 2005. Measurement and interpretation of electrokinetic phenomena (IUPAC technical report). *Pure Appl Chem* 77(10):1753-1805.

71. Zhou, X., B. Liu, X. Yu, X. Zha, X. Zhang, Y. Chen, X. Wang, Y. Jin, Y. Wu, Y. Chen, Y. Shan, Y. Chen, J. Liu, W. Kong, and J. Shen. 2007. Controlled release of PEI/DNA complexes from mannose-bearing chitosan microspheres as a potent delivery system to enhance immune response to HBV DNA vaccine. *J Control Release* 121(3):200-207.

72. Liu, G., D. Li, M. K. Pasumarthy, T. H. Kowalczyk, C. R. Gedeon, S. L. Hyatt, J. M. Payne, T. J. Miller, P. Brunovskis, T. L. Fink, O. Muhammad, R. C. Moen, R. W. Hanson, and M. J. Cooper. 2003. Nanoparticles of Compacted DNA Transfect Postmitotic Cells. *J. Biol. Chem* 278(35):32578-32586.

73. Abuchowski, A., J. R. McCoy, N. C. Palczuk, E. van Es, and F. F. Davis. 1977. Effect of covalent attachment of polyethylene glycol on immunogenicity and circulating life of bovine liver catalase. *J Biol Chem* 252:3582-3586.

74. Isrealachvili, J. 1997. The different faces of poly(ethylene glycol). *Proc Natl Acad Sci* 94:8378-8379.

75. Pasut, G., and F. M. Veronese. 2012. State of the art in PEGylation: The great versatility achieved after forty years of research. *J Controlled Release* 161:461-472.

76. Ogris, M., S. Brunner, S. Schuller, R. Kircheis, and E. Wagner. 1999. PEGylated DNA/transferrin-PEI complexes: reduced interaction with blood components, extended circulation in blood and potential for systemic gene delivery. *Gene Ther* 6(4):595-605.

77. Read, M. L., A. Logan, and L. W. Seymour. 2005. Barriers to Gene Delivery Using Synthetic Vectors. *In* J. C. Hall, J. C. Dunlap, T. Friedmann and V. van Heyningen, editors. Advances in Genetics, 2nd ed. Academic Press. 19-46.

78. Kawabata, K., Y. Takakura, and M. Hashida. 1995. The Fate of Plasmid DNA After Intravenous Injection in Mice: Involvement of Scavenger Receptors in Its Hepatic Uptake. *Pharm. Res.* 12(6):825-830.

79. Woodle, M. C., and D. D. Lasic. 1992. Sterically stabilized liposomes. *Biochim Biophys Acta* 1113(2):171-99.

80. Burke, R. S., and S. H. Pun. 2008. Extracellular barriers to *in vivo* PEI and PEGylated PEI polyplex-mediated gene delivery to the liver. *Bioconjugate Chemistry* 19(3):693-704.

81. Acheson, R. M. 1973. The Chemistry of Heterocyclic Compounds: A Series of Monographs. *In* A. Weissberger and E. C. Taylor, editors. The Acridines, Second ed. John Wiley and Sons, New York.

82. Albert, A., and B. Ritchies. 1955. 9-Aminoacridine. *Organic Syntheses* 3:53.

83. Graebe, C., and K. Lagodzinski. 1893. Ueber Oxyderivative des Anthracholinchinons. *Justus Liebigs Annalen der Chemie* 276:35.

84. Wakelin, L. P. G. 1986. Polyfunctional DNA intercalating agents. *Medicinal Research Reviews* 6(3):275-340.

85. Neidle, S., and Z. Abraham. 1984. Structural and sequence-dependent aspects of drug intercalation into nucleic acids. *CRC Crit Rev Biochem* 17:73-121.

86. Ghosh, A., and M. Bansal. 2003. A glossary of DNA structures from A to Z. *Acta Cryst* D59:620-626.

87. Dupre, D. J., and F. A. Robinson. 1945. N-substituted 5-aminoacridines. *J Chem Soc*:549-551.

88. Peacocke, A. R., and J. N. H. Skerrett. 1956. The interaction of aminoacridines with nucleic acids. *Trans Faraday Soc* 52:261-279.

89. Lerman, L. S. 1961. Structural considerations in the interactions of deoxyribonucleic acid and acridines. *J Mol Biol* 3:18-30.

90. Wilson, W. D., and R. L. Jones. 1981. Intercalating drugs: DNA binding and molecular pharmacology. *Advances in pharmacology and chemotherapy* 18:177-222.

91. Sobell, H. M. 1973. The stereochemistry of actinomycin binding to DNA and its implications in molecular biology. *Prog Nucleic Acid Res Mol Biol* 13:153-190.

92. McGhee, J. D., and P. H. von Hippel. 1974. Theoretical aspects of DNA-protein interactions: Co-operative and non-co-operative binding of large ligands to a one-dimensional homogeneous lattice. *J. Mol. Biol.* 86:469-489.

93. Rocha, M. S. 2010. Revisiting the neighbor exclusion model and its applications. *Biopolymers* 93(1):1-7.

94. Le Pecq, J. B., M. Le Bret, J. Barbet, and B. Roques. 1975. DNA polyintercalating drugs: DNA binding of diacridine derivatives. *Proc Natl Acad Sci* 72(8):2915-2919.

95. Kukowska-Kaszuba, M., and K. Dzierzbicka. 2007. Synthesis and structure-activity studies of peptide-acridine/acridone conjugates. *Curr Med Chem* 14:3079-3104.

96. Wright, R. G. M., L. P. G. Wakelin, A. Fieldes, M. J. Waring, and R. M. Acheson. 1980. Effects of ring substituents and linker chains on the bifunctional intercalation of diacridines into deoxyribonucleic acid. *Biochemistry* 19(25):5825-5836.

97. Nasim, A., and T. Brychcy. 1979. Genetic effects of acridine compounds. *Mutation Research* 65:261-288.

98. Gurova, K. 2009. New hopes from old drugs: revisiting DNA-binding small molecules as anticancer agents. *Future Oncology* 5(10):1685.

99. Auerbach, C., and J. M. Robson. 1947. The production of mutations by chemical substances. *Proc R Soc Edinburgh B* 62:271-283.

100. Ferguson, L. R., and W. A. Denny. 1991. The genetic toxicology of acridines. *Mutation Research* 258:123-160.

101. Ferguson, L. R., and W. A. Denny. 2007. Genotoxicity of non-covalent interactions: DNA intercalators. *Mutation Research* 623:14-23.

102. Anderson, R. A., and J. E. Coleman. 1975. Physicochemical properties of DNA binding proteins: Gene 32 protein of T4 and Escherichia coli unwinding protein. *Biochemistry* 14(25):5485-5491.

103. Rajeswari, M. R., H. S. Bose, S. Kukreti, A. Gupta, V. S. Chauhan, and K. B. Roy. 1992. Binding of oligopeptides to d-AGATCTAGATCT and d-AAGCTTAAGCTT: can tryptophan intercalate in DNA hairpins? *Biochemistry* 31(27):6237-6241.

104. Santella, R. M., and H. J. Li. 1975. Studies on the interaction between poly(L-lysine58, L-phenylalanine42) and deoxyribonucleic acids. *Biochemistry* 14(16):3604-3611.

105. Sheoran, A., A. King, A. Velasco, J. M. Pero, and S. Garneau-Tsodikova. 2008. Characterization of TioF, a tryptophan 2,3-dioxygenase involved in 3-hydroxyquinaldic acid formation during thiocoraline biosynthesis. *Mol. Biosyst.* 4(6):622-628.

106. Werner, M. H., M. Clore, C. L. Fisher, R. J. Fisher, L. Trinh, J. Shiloach, and A. M. Gronenborn. 1995. The solution structure of the human ETS1-DNA complex reveals a novel mode of binding and true side chain intercalation. *Cell* 83(5):761-771.

107. Merdan, T., K. Kunath, H. Petersen, U. Bakowsky, K. H. Voigt, J. Kopecek, and T. Kissel. 2005. PEGylation of poly(ethylene imine) affects stability of complexes with plasmid DNA under *in vivo* conditions in a dose-dependent manner after intravenous injection into mice. *Bioconjugate Chemistry* 16(4):785-792.

108. Cohen, R. N., M. A. van der Aa, N. Macaraeg, A. P. Lee, and F. C. Szoka Jr. 2009. Quantification of plasmid DNA copies in the nucleus after lipoplex and polyplex transfection. *J Controlled Release* 135:166-174.

109. Grigsby, C. L., and K. W. Leong. 2010. Balancing protection and release of DNA: tools to address a bottleneck of non-viral gene delivery. *J R Soc Interface* 7 Suppl 1:S67-82.

110. van der Aa, M. A., G. A. Koning, C. d'Oliveira, R. S. Oosting, K. J. Wilschut, W. E. Hennink, and D. J. A. Crommelin. 2005. An NLS peptide covalently linked to linear DNA does not enhance transfection efficiency of cationic polymer based gene delivery systems. *The Journal of Gene Medicine* 7(2):208-217.

111. Boussif, O., F. Lezoualc'h, M. A. Zanta, M. D. Mergny, D. Scherman, B. Demeneix, and J. P. Behr. 1995. A versatile vector for gene and oligonucleotide transfer into cells in culture and in vivo: polyethylenimine. *Proceedings of the National Academy of Sciences of the United States of America* 92(16):7297-301.

112. Felgner, P. L., T. R. Gadek, M. Holm, R. Roman, H. W. Chan, M. Wenz, J. P. Northrop, G. M. Ringold, and M. Danielsen. 1987. Lipofection: a highly efficient, lipid-mediated DNA-transfection procedure. *Proceedings of the National Academy of Sciences of the United States of America* 84(21):7413-7.

113. Rettig, G. R., and K. G. Rice. 2009. Quantitative In Vivo Imaging of Non-viral-Mediated Gene Expression and RNAi-Mediated Knockdown. *In* P. Rich and C. Douillet, editors. Bioluminescence. Humana Press, New York. 155-171.

114. Anderson, K., C. A. Fernandez, and K. G. Rice. 2010. N-Glycan Targeted Gene Delivery to the Dendritic Cell SIGN Receptor. *Bioconjugate Chemistry* 21:1479-1485.

115. Baumhover, N. J., K. Anderson, C. A. Fernandez, and K. G. Rice. 2010. Synthesis and In Vitro Testing of New Potent Polyacridine-Melittin Gene Delivery Peptides. *Bioconjugate Chemistry* 21:74-86.

116. Terebesi, J., K. Y. Kwok, and K. G. Rice. 1998. Iodinated plasmid DNA as a tool for studying gene delivery. *Analytical Biochemistry* 263:120-123.

117. Zhang, G., V. Budker, and J. A. Wolff. 1999. High levels of foreign gene expression in hepatocytes after tail vein injections of naked plasmid DNA. *Human Gene Therapy* 10(10):1735-1737.

118. Mullen, P. M., C. P. Lollo, Q. C. Phan, A. Amini, M. G. Banaszczyk, M. Fabrycki, D. Wu, A. T. Carlo, P. Pezzoli, C. C. Coffin, and D. J. Carlo. 2000. Strength of conjugate binding to plasmid DNA affects degradation rate and expression level *in vivo*. *Biochim Biophys Acta* 1523(1):103-110.

119. Heyes, J., L. Palmer, K. Chan, C. Giesbrecht, L. Jeffs, and I. MacLachlan. 2007. Lipid encapsulation enables the effective systemic delivery of polyplex plasmid DNA. *Mol Ther* 15(4):713-20.

120. Fortune, J. A., T. I. Novobrantseva, and A. M. Klibanov. 2011. Highly effective gene transfection *in vivo* by alkylated polyethyleneimine. *J Drug Deliv* 2011:204058.

121. Harris, T. J., J. J. Green, P. W. Fung, R. Langer, D. G. Anderson, and S. N. Bhatia. 2010. Tissue-specific gene delivery via nanoparticle coating. *Biomaterials* 31(5):998-1006.

122. Kim, K. S., Y. Lei, D. B. Stolz, and D. Liu. 2007. Bifunctional compounds for targeted hepatic gene delivery. *Gene Therapy* 14:704-708.

123. Kunath, K., A. von Harpe, H. Petersen, D. Fischer, K. Voigt, T. Kissel, and U. Bickel. 2002. The Structure of PEG-Modified Poly(Ethylene Imines) Influences Biodistribution and Pharmacokinetics of Their Complexes with NF-κB Decoy in Mice. *Pharmaceutical Research* 19(6):810-817.

124. Li, S.-D., Y.-C. Chen, M. J. Hackett, and L. Huang. 2007. Tumor-targeted Delivery of siRNA by Self-assembled Nanoparticles. *Mol Ther* 16(1):163-169.

125. Mahato, R. I., K. Kawabata, T. Nomura, Y. Takakura, and M. Hashida. 1995. Physicochemical and pharmacokinetic characteristics of plasmid DNA/cationic liposome complexes. *Journal of Pharmaceutical Sciences* 84(11):1267-71.

126. Mahato, R. I., K. Kawabata, Y. Takakura, and M. Hashida. 1995. In vivo disposition characteristics of plasmid DNA complexed with cationic liposomes. *Journal of Drug Targeting* 3(2):149-57.

127. Morille, M., T. Montier, P. Legras, N. Carmoy, P. Brodin, B. Pitard, J.-P. Benoît, and C. Passirani. 2010. Long-circulating DNA lipid nanocapsules as new vector for passive tumor targeting. *Biomaterials* 31(2):321-329.

128. Fernandez, C. A., N. J. Baumhover, K. Anderson, and K. G. Rice. 2010. Discovery of metabolically stabilized electronegative polyacridine-PEG peptide DNA open polyplexes. *Bioconjugate Chemistry* 21(4):723-30.

129. Oupicky, D., M. Ogris, K. A. Howard, P. R. Dash, L. Ulbrich, and L. W. Seymour. 2002. Importance of Lateral an Steric Stabilization of Polyelectrolyte Gene Delivery Vectors for Extended Systemic Circulation. *Molecular Therapy* 5:463-472.

130. Yang, Y., Y. Park, S. Man, Y. Liu, and K. G. Rice. 2001. Cross-linked low molecular weight glycopeptide-mediated gene delivery: relationship between DNA metabolic stability and the level of transient gene expression in vivo. *J Pharm Sci* 90(12):2010-22.

131. Zhou, Q. H., D. L. Miller, R. C. Carlisle, L. W. Seymour, and D. Oupicky. 2005. Ultrasound-enhanced transfection activity of HPMA-stabilized DNA polyplexes with prolonged plasma circulation. *J Controlled Release* 106(3):416-427.

132. Baldwin, A. D., and K. L. Kiick. 2011. Tunable degradation of maleimide-thiol adducts in reducing environments. *Bioconjugate Chemistry* 22:1946-1953.

133. Stohs, S. J., J. M. Hassing, W. A. Al-Turk, and A. N. Masoud. 1980. Glutathione levels in hepatic and extrahepatic tissues of mice as a function of age. *Age* 3(1):11-14.

134. Khargharia, S., K. Kizzire, M. D. Ericson, N. J. Baumhover, and K. G. Rice. 2013. PEG Length and chemical linkage control polyacridine peptide DNA polyplex pharmacokinetics, biodistribution, metabolic stability and *in vivo* gene expression. *J Controlled Release* In Press.

135. Finkle, B. J., and E. L. Smith. 1958. Crystalline papain: Number and reactivity of thiol groups; chromatographic behavior. *J Biol Chem* 230(2):669-690.

136. Ehrenreich, J. H., J. J. Bergeron, P. Siekevitz, and G. E. Palade. 1973. Golgi fractions prepared from rat liver homogenates. I. Isolation procedure and morphological characterization. *J Cell Biol* 59(1):45-72.

137. Krisch, K. 1965. Reaction of a microsomal esterase from hog liver with diethyl *p*-nitrophenyl phosphate. *Biochim Biophys Acta* 122:265-280.

138. Li, S., M. A. Rizzo, S. Bhattacharya, and L. Huang. 1998. Characterization of cationic lipid-protamine-DNA (LPD) complexes for intravenous gene delivery. *Gene Therapy* 5(7):930-7.

139. Mahato, R. I., K. Anwer, F. Tagliaferri, C. Meaney, P. Leonard, M. S. Wadhwa, M. Logan, M. French, and A. Rolland. 1998. Biodistribution and gene expression of lipid/plasmid complexes after systemic administration. *Hum Gene Ther* 9(14):2083-99.

140. Scheule, R. K., J. A. St George, R. G. Bagley, J. Marshall, J. M. Kaplan, G. Y. Akita, K. X. Wang, E. R. Lee, D. J. Harris, C. Jiang, N. S. Yew, A. E. Smith, and S. H. Cheng. 1997. Basis of pulmonary toxicity associated with cationic lipid-mediated gene transfer to the mammalian lung. *Human Gene Therapy* 8(6):689-707.

141. Fella, C., G. F. Walker, M. Ogris, and E. Wagner. 2008. Amine-reactive pyridylhydrazone-based PEG reagents for pH-reversible PEI polyplex shielding. *Eur J Pharm Sci* 34:309-320.

142. Walker, G. F., C. Fella, J. Pelisek, J. Fahrmeir, S. Boeckle, M. Ogris, and E. Wagner. 2005. Toward synthetic viruses: endosomal pH-triggered deshielding of targeted polyplexes greatly enhances gene transfer in vitro and in vivo. *Mol Ther* 11(3):418-25.

143. Drummer, O. H., L. Routley, and N. Christophidis. 1987. Reversibility of disulfide formation. Comparison of chemical and enzyme-mediated reduction of penicillamine and catopril disulfides. *Biochem Pharmacol* 36(8):1197-1201.

144. Choi, H. S., B. I. Ipe, P. Misra, J. H. Lee, M. G. Bawendi, and J. V. Frangioni. 2009. Tissue- and organ-selective biodistribution of NIR fluorescent quantum dots. *Nano Lett.* 9(6):2354-2359.

145. Daou, T. J., L. Li, P. Reiss, V. Josserand, and I. Texier. 2009. Effect of poly(ethylene glycol) length on the *in vivo* behavior of coated quantum dots. *Langmuir* 25(5):3040-3044.

146. Faure, A. C., S. Dufort, V. Josserand, P. Perriat, J. L. Coll, S. Roux, and O. Tillement. 2009. Control of the *in vivo* biodistribution of hybrid nanoparticles with different poly(ethylene glycol) coatings. *Small (Weinheim an der Bergstrasse, Germany)* 5(22):2565-2575.

147. Maldiney, T., C. Richard, J. Seguin, N. Wattier, M. Bessodes, and D. Scherman. 2011. Effect of core diameter, surface coating, and PEG chain length on the biodistribution of persistent luminescence nanoparticles in mice. *ACS Nano* 5(2):854-862.

148. Mosqueira, V. C., P. Legrand, J. L. Morgat, M. Vert, E. Mysiakine, R. Gref, J. P. Devissaguet, and G. Barratt. 2001. Biodistribution of long-circulating PEG-grafted nanocapsules in mice: effects of PEG chain length and density. *Pharm Res* 18(10):1411-1419.

149. Pun, S. H., and M. E. Davis. 2002. Development of a nonviral gene delivery vehicle for systemic application. *Bioconjugate Chemistry* 13(3):630-639.

150. Davies, B., and T. Morris. 1993. Physiological parameters in laboratory animals and humans. *Pharm Res* 10(7):1093-1095.

151. Torchilin, V. P. 1985. Liposomes as Targetable Drug Carriers. *CRC Crit. Rev. Therap. Drug Carrier Sys.* 2(1):65-115.

152. Kaszuba, M., D. McKnight, M. T. Connah, F. K. McNeil-Watson, and U. Nobbmann. 2008. Measuring sub nanometre sizes using dynamic light scattering. *J Nanoparticle Res* 10:823-829.

153. Kursa, M., G. F. Walker, V. Roessler, M. Ogris, W. Roedl, R. Kircheis, and E. Wagner. 2003. Novel shielded transferrin-polyethylene glycol-polyethylenimidne/DNA complexes for systemic tumor-targeted gene transfer. *Bioconjugate Chemistry* 14(1):222-231.

154. Crespo, A., A. Peydro, F. Dasi, M. Benet, J. J. Calvete, F. Revert, and S. F. Alino. 2005. Hydrodynamic liver gene transfer mechanism invovles transient sinusoidal blood stasis and massive hepatocyte endocytotic vesicles. *Gene Therapy* 12(11):927-935.

155. Fee, C. J., and J. M. Van Alstine. 2004. Prediction of the viscosity radius and the size exclusion chromatography behavior of PEGylated proteins. *Bioconjugate Chemistry* 15:1304-1313.